UNCLASSIFIED

CENTRAL RESEARCH LIBRARY
DOCUMENT COLLECTION

MARTIN MARIETTA ENERGY SYSTEMS LIBRARIES
3 4456 0060092 7

ORNL-2049
Progress

cy. 5

HEALTH PHYSICS DIVISION

SEMIANNUAL PROGRESS REPORT

FOR PERIOD ENDING JANUARY 31, 1956

CENTRAL RESEARCH LIBRARY
DOCUMENT COLLECTION

LIBRARY LOAN COPY

DO NOT TRANSFER TO ANOTHER PERSON

If you wish someone else to see this document, send in name with document and the library will arrange a loan.

OAK RIDGE NATIONAL LABORATORY
OPERATED BY
UNION CARBIDE NUCLEAR COMPANY
A Division of Union Carbide and Carbon Corporation
UCC
POST OFFICE BOX P · OAK RIDGE, TENNESSEE

UNCLASSIFIED

UNCLASSIFIED

ORNL-2049
ERRATUM

HEALTH PHYSICS DIVISION SEMIANNUAL PROGRESS REPORT
FOR PERIOD ENDING JANUARY 31, 1956

Page No.	Erratum
40	Last equation should read: $K = \frac{10^{-3}}{Dg} (1 - \alpha) \frac{1}{r} \left(1 + \frac{0.087}{r}\right) \times (2.09\, V^{-0.57} + 22\, V^{-0.78}\, r^3)$

Changed 6.27.56

UNCLASSIFIED

ORNL-2049

Contract No. W-7405-eng-26

HEALTH PHYSICS DIVISION SEMIANNUAL PROGRESS REPORT

For Period Ending January 31, 1956

K. Z. Morgan, Director

DATE ISSUED

APR 12 1956

OAK RIDGE NATIONAL LABORATORY
Operated by
UNION CARBIDE NUCLEAR COMPANY
A Division of Union Carbide and Carbon Corporation
Post Office Box P
Oak Ridge, Tennessee

MARTIN MARIETTA ENERGY SYSTEMS LIBRARIES
3 4456 0060092 7

UNCLASSIFIED

Semiannual reports previously issued by the Health Physics Division are as follows:

ORNL-1596	Period Ending July 31, 1953
ORNL-1684	Period Ending January 31, 1954
ORNL-1763	Period Ending July 31, 1954
ORNL-1860	Period Ending January 31, 1955
ORNL-1942	Period Ending July 31, 1955

ORNL-2049
Progress

INTERNAL DISTRIBUTION

1. C. E. Center
2. Biology Library
3. Health Physics Library
4-6. Central Research Library
7. Reactor Experimental Engineering Library
8-12. Laboratory Records Department
13. Laboratory Records, ORNL R.C.
14. C. E. Larson
15. L. B. Emlet (K-25)
16. J. P. Murray (Y-12)
17. A. M. Weinberg
18. J. A. Swartout
19. E. D. Shipley
20. E. J. Murphy
21. F. C. VonderLage
22. K. Z. Morgan
23. S. C. Lind
24. A. S. Householder
25. C. S. Harrill
26. C. E. Winters
27. A. H. Snell
28. E. H. Taylor
29. W. H. Jordan
30. T. A. Lincoln
31. A. Hollaender
32. F. L. Culler
33. D. W. Cardwell
34. E. M. King
35. M. T. Kelley
36-47. E. E. Anderson
48. R. S. Livingston
49. C. P. Keim
50. G. H. Clewett
51. C. D. Susano
52. L. B. Farabee
53. F. J. Davis
54. R. J. Morton
55. C. E. Haynes
56. Hugh F. Henry (K-25)
57. E. G. Struxness
58. W. E. Cohn
59. H. H. Hubbell
60. D. E. Arthur
61. J. Neufeld
62. D. D. Cowen
63. P. M. Reyling
64. G. C. Williams
65. M. J. Skinner
66. J. C. Hart
67. T. H. J. Burnett
68. W. J. Lacy
69. B. G. Saunders
70. G. S. Hurst
71. T. E. Bortner
72. J. A. Lane
73. R. W. Johnson
74. H. P. Yockey
75. C. E. Clifford
76. J. L. Gabbard
77. R. A. Charpie
78. G. E. Boyd
79. S. J. Cromer
80. L. C. Emerson (Y-12)
81. D. M. Davis
82. P. E. Brown
83. E. D. Gupton
84. J. C. Ledbetter
85. R. L. Clark
86. G. C. Cain
87. L. C. Johnson
88. W. Ogg
89. O. D. Teague
90. E. L. Sharp
91. E. J. Kuna
92. H. H. Abee
93. C. R. Guinn
94. A. D. Warden
95. S. R. Bernard
96. C. C. Sartain
97. J. R. Muir
98. J. A. Auxier
99. C. P. Straub
100. M. F. Fair
101. S. I. Auerbach
102. G. W. Royster, Jr.
103. R. R. Dickison
104. ORNL – Y-12 Technical Library, Document Reference Section

EXTERNAL DISTRIBUTION

105. R. F. Bacher, California Institute of Technology
106. G. E. Thoma, USAF
107. H. J. McAlduff, AEC, Oak Ridge
108. Vanderbilt University (Physics Library)
109. Massachusetts Institute of Technology (Department of Electrical Engineering)
110. University of California (Gerhard Klein)
111. R. M. Richardson, U.S. Geological Survey, 2-C P.O. Building, Knoxville, Tennessee
112. C. V. Theis, U.S. Geological Survey, Box 433, Albuquerque, New Mexico
113. Lola Lyons, Librarian, Olin Industries, Inc., East Alton, Illinois
114. Jack Story, University of Chicago, Argonne Cancer Research Hospital, 950 East 59th Street, Chicago 37, Illinois
115. J. H. Ebersole, USS Nautilus, c/o Fleet Post Office, New York, New York
116. David Smith, Electric Boat Division, Groton, Connecticut
117. Division of Research and Development, AEC, ORO
118. S. C. Sigoloff, USAF, The Radiobiological Laboratory, University of Texas and U.S. Air Force, Austin, Texas
119. Robert Wood, Department of Physics, Memorial Center, 444 E. 68th St., New York 21, New York

120-501. Given distribution as shown in TID 4500 (11th ed.) under Health and Biology Category

DISTRIBUTION PAGE TO BE REMOVED IF REPORT IS GIVEN PUBLIC DISTRIBUTION

CONTENTS

APPLIED RADIOBIOLOGY 1
- Distribution and Excretion of Uranium in Man 1
- Ecology 5
- Urinalysis Research 17
- Distribution of Radioisotopes in Animal Tissue 17
- Isotopic Distribution in Man 18

SANITARY ENGINEERING RESEARCH 27
- Field Investigations 27
- Chemistry and Soils Engineering 36
- Airborne-Radioactivity Studies 38

RADIATION DOSIMETRY 43
- Experimental Physics of Dosimetry 43
- Theoretical Physics of Dosimetry 53
- Dosimetry Applications 54

EDUCATION, TRAINING, AND CONSULTATION 60

PUBLICATIONS 60

PAPERS 62

LECTURES 62

HEALTH PHYSICS DIVISION SEMIANNUAL PROGRESS REPORT

APPLIED RADIOBIOLOGY

E. G. Struxness

DISTRIBUTION AND EXCRETION OF URANIUM IN MAN

S. R. Bernard
D. K. Bowman
G. J. Dodson
M. B. Edwards
B. R. Fish
N. L. Gillum
W. E. Lotz
K. K. McDaniel
J. R. Muir
G. W. Royster, Jr.

In a continuation of the study[1] of the distribution and excretion of uranium in man, all the urine, blood, and feces samples from patients VII and VIII, who were injected with uranium tetrachloride (UCl_4), have been analyzed. In addition, the analyses of autopsy samples taken from patients III and VIII have been completed.

Detailed statistical analyses of the distribution and excretion data on the patients (I through VI) injected with U(VI) were started during this period in order to obtain the best set of parameters to represent the data. One of the statistical methods used is the regression test of linearity[2] applicable to data such as decay curves when several measurements are taken at a given time. The test is simple; the variance within measurements is compared to the variance between the data and the best fitting regression curve by the F ratio test, and, if this variance is significantly different, the data are said to depart significantly from a regression curve. When this procedure was applied to excretion data of patients I, II, III, IV, V, and VI where the linear version of the power function $At^b (b < 0)$ was assumed, it was concluded that the data were not best described by this function. It is interesting to know that when the same test was applied to plutonium urinary excretion data[3] there was no significant departure from linear regression.

The per cent of injection dose per 10^4 g of bone (autopsy samples) for patients I, II, III, V, and VI is plotted in Fig. 1. The graph, which includes all the individual analyses, shows a wide range of concentrations. If a single exponential is assumed to be representative of these data and if the linearity test (*vide supra*) is applied, the data depart significantly from this function. The value of the intercept is $3.8 \times 10^{-4}\%$ of injected dose per gram and the half life is 241 days. Functions other than the single exponential term, for example, $(a + bt)^{-2}$, were similarly tested without success.

It is suggested that these data can be represented by letting λ in the function $\epsilon^{-\lambda t}$ vary with time. The following procedure shows that this is true: (1) assume a single exponential term; (2) calculate the half life from bone biopsy and autopsy values for each patient; and (3) plot this calculated half life vs the time of expiration. The calculated half lives of step 2 are listed in Table 1. Note the significant difference between

[1] S. R. Bernard *et al.*, *HP Semiann. Prog. Rep. July 31, 1955*, ORNL-1942, p 1.

[2] W. J. Dixon and F. J. Massey, *Introduction to Statistical Analysis*, p 160–161, McGraw-Hill, New York, 1951.

[3] W. H. Langham *et al.*, *Distribution and Excretion of Plutonium Administered Intravenously to Man*, LA-1151 (Sept. 20, 1950), p 24–25.

TABLE 1. BIOLOGICAL HALF LIVES OF U(VI) IN BONE – BIOPSY AND AUTOPSY SPECIMENS

	Patient Number				
	I	VI	II	V	III
	Expiration Time (days)				
	2.5	18	74	139	566
Biological half life and standard deviation (days)	2.3 ± 0.56	15.1 ± 6.24	17.1 ± 6.89	44.4 ± 6.83	222.1 ± 68.3

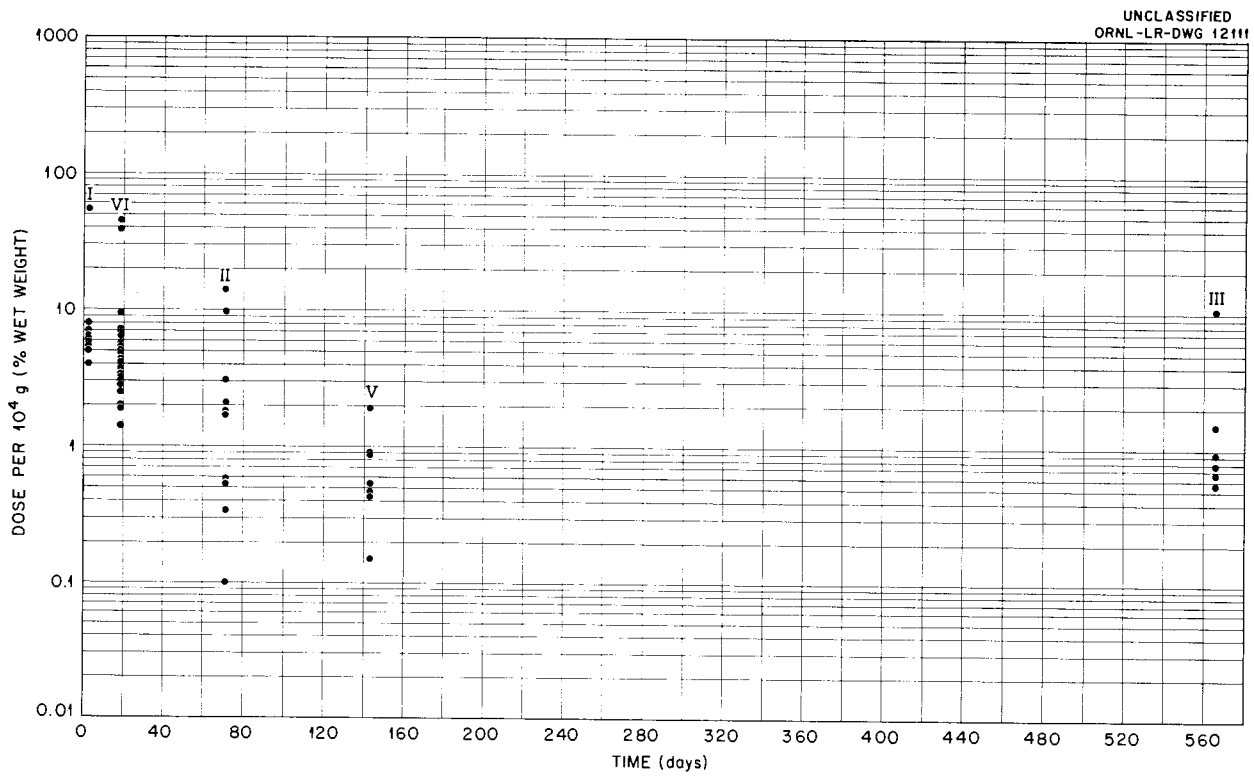

Fig. 1. Plot of Individual Bone Autopsy Results for Five Patients Injected with U(VI).

the patients. The graph of step 3 is shown in Fig. 2, where the half life is seen to increase in proportion to $t^{4/5}$.

Other data which have important application to the calculations of maximum permissible concentrations (MPC) for uranium are those contained in Tables 2 and 3 and Fig. 3. Table 2 shows that (1) the different samples of bone reflect different mean concentrations; (2) the U(IV) autopsy bone concentrations are very similar to U(VI); and (3) the samples of the femur are the lowest in concentration, while the vascular bone, rib, is highest in the early stages after injection and the skull concentration is highest at later stages. Figure 3 is a diagram of the uranium concentrations in a longitudinal plane sectioned from the distal end of the femur. The section, approximately ¼ in. thick, was cut into smaller sections and each section was analyzed for uranium. The numbers in each section are the concentrations in counts per minute per gram of bone. In general, it may be said that the concentrations decrease in the direction of the shaft.

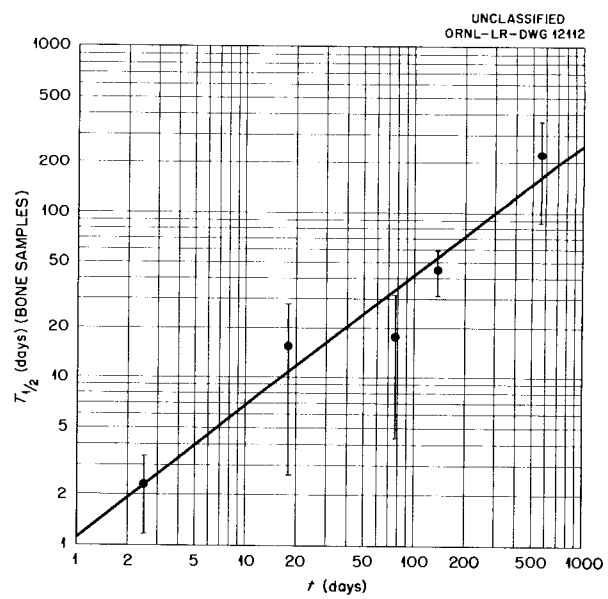

Fig. 2. Plot of Biological Half Life of U(VI) in Bone Determined from Femur Autopsy and Biopsy Samples vs Time of Autopsy.

TABLE 2. BONE AUTOPSY DATA – PER CENT OF INJECTED DOSE PER 7000 g

Patient No.*	Postinjection Time (days)	Sample					Mean
		Femur	Rib	Skull	Sternum	Vertebra	
		Injection: $UO_2(NO_3)_2 \cdot 6H_2O$					
I	2½	4.1	13.8	5.5		37.7	14.0
VI	18	3.3	29.5				16.3
II	74	0.4	1.8	8.3	0.4	1.3	2.4
V	139	0.4	0.6	1.3			0.8
III	566	0.6	0.6	7.4	1.1	0.4	2.0
		Injection: UCl_4					
VIII	21	0.6	27.5			15.1	14.4

*No autopsy data obtained for patients IV and VII.

UNCLASSIFIED
ORNL-LR-DWG 12113

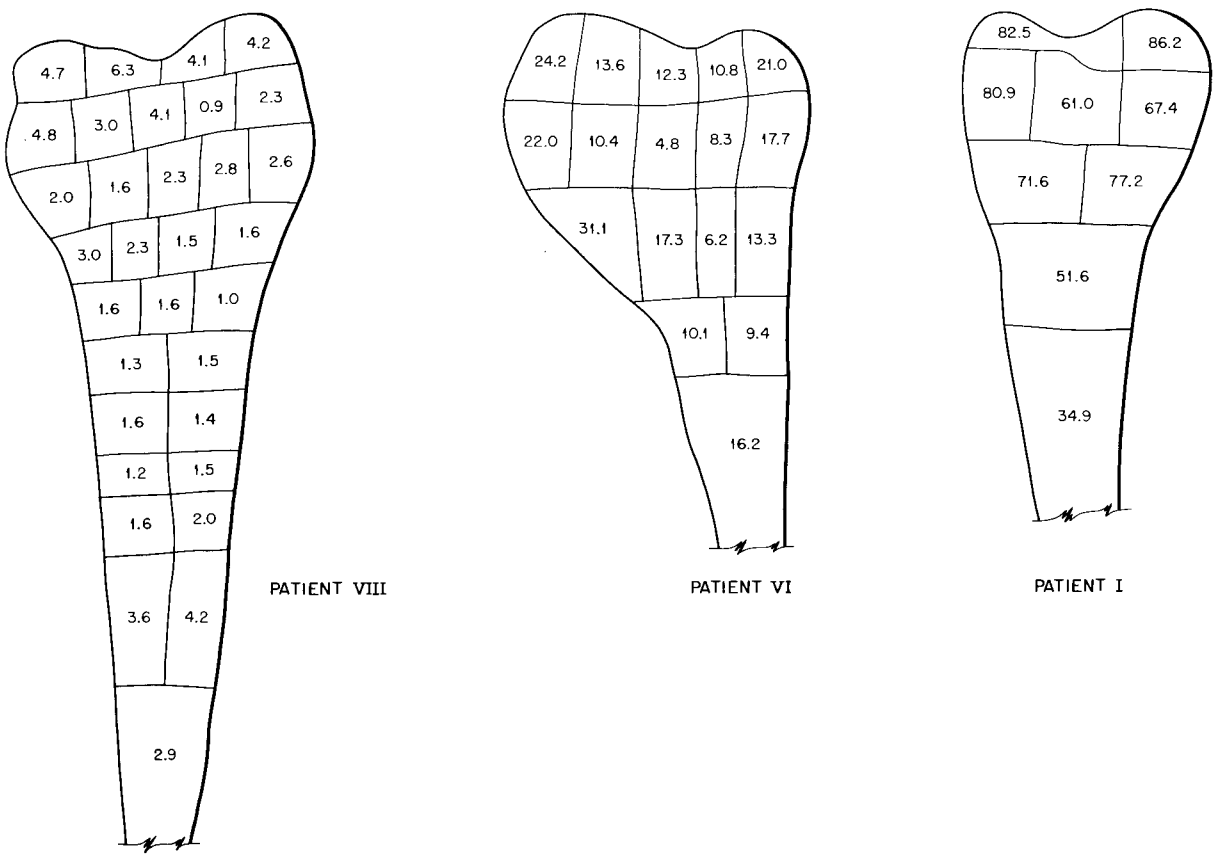

Fig. 3. Diagram of Concentration of Uranium in Longitudinal Section of Distal End of the Femur. Numbers in each section represent counts/min/g.

TABLE 3. PER CENT OF INJECTED DOSE PER STANDARD MEAN ORGAN OR TISSUE FOR SIX TERMINAL BRAIN TUMOR PATIENTS

Patients I, VI, II, V, and III injected with $UO_2(NO_3)_2 \cdot 6H_2O$
Patient VIII injected with UCl_4

Organ or Tissue	Sample Amount (g)	Patient Number					
		I	VI	II	V	III	VIII
		Expiration Time (days)					
		2.5	18	74	139	566	21
Kidney	300	16.6	7.2	0.7	1.2	0.4	1.1
Muscle	30,000	1.2	2.1	0.9	0.3	0.06	0.4
Skin and subcutaneous tissues	6,100	1.8	1.0	0.1	0.06		
Fat	10,000	0.6	0.6			0.04	
Red marrow	1,500			0.02	0.03	0.1	
Yellow marrow	1,500						
Blood	5,400	1.0	0.2	0.005	0.002	0.004	0.08
Lower large intestine	150						
Stomach	250	0.08	0.02	0.003	0.001	0.001	
Small intestine	1,100	0.2	0.2	0.03	0.01	0.006	0.1
Upper large intestine	135						
Liver	1,700	1.8	1.1	0.2	0.2	0.05	9.2
Brain	1,500						
Lungs	1,000	0.5	0.4	0.03	0.02	0.008	0.3
Lymphoid tissue	700						
Heart	300	0.06	0.02	0.003	0.006	0.002	0.004
Spleen	300	0.6	0.2	0.1	0.02	0.006	5.6
Urinary bladder	150	0.03		0.002	0.001	0.0003	0.06
Pancreas	70	0.7	0.008	0.008	0.0006	0.0004	
Salivary glands	50						
Testes	40		0.01	0.008	0.002	0.002	0.008
Spinal cord	30						
Eyes	30						
Thyroid gland	20		0.003	0.0002	0.0001	0.0002	0.0009
Teeth	20						
Prostate gland	20		0.003	0.0004	0.0004	0.0001	0.003
Adrenal gland	20	0.02	0.01	0.003	0.001	0.0004	0.02
Thymus	10						
Miscellaneous tissues (blood vessels, cartilage, nerves, etc.)	390	0.3	0.2	0.04	0.002	0.002	0.04

Some interesting observations can be made of the distribution and excretion of tetravalent uranium. Table 3 shows that U(IV) favors deposition in the reticulo-endothelial tissues of the liver and spleen in direct contrast to U(VI), which concentrates in the kidney. Figures 4, 5, and 6 show the disappearance of U(IV) from blood, feces, and urine, respectively. There appears to be little difference between the urinary excretion of U(VI) and U(IV); however, in excretion via the gastrointestinal tract, the data in Fig. 5 for U(IV) show some time relationship not seen in the data for the fecal excretion of U(VI). Only 0.1% of the injected dose had accumulated in feces of patient VII at 430 hr. The rate of disappearance of U(IV) from the blood is only slightly different from that of U(VI).

ECOLOGY

S. I. Auerbach
C. J. Rohde
H. F. Howden[4]
V. L. Sheldon[4]
M. D. Engelmann[5]
R. J. Davis, Jr.[5]

Soil Fertility and the Uptake of Strontium by Plants

Strontium and calcium have been related chemically in both soils and plants. Variations in the uptake of these elements have been attributed to the amount and kind of clay minerals occurring in soils and to the rate of plant growth.

Since soils may serve for the disposal of nuclear wastes containing strontium, an evaluation is required to determine the degree to which this element may replace calcium on soil colloids.

In the studies reported here the nonradioactive isotope of strontium and the normal plant nutrients have been adsorbed on Conasauga shale, and the amounts of the isotope and the nutrients taken up by bean plants at various stages of maturity have been determined. In addition, each series of soils received equal amounts of radioactive Sr^{90}.

Occurring naturally as the subsoil of Armuchee silt loam, the Conasauga shale was taken from the Four-Acre Site at ORNL. Preliminary studies indicate this material to be 87% silt (0.006 to 0.002 mm) and 12% clay (0.002 mm and less). It has a total exchange capacity of 20 milliequivalents (meq) with 4.26 meq Ca^{++}, 1.08 meq Mg^{++}, 0.19 meq Na^{+}, and 0.47 meq K^{+} per 100 g of soil. It contains 0.009% nitrogen, 0.0055% sulfur, 0.064% carbon, and 0.53% strontium. About 0.82 ppm of phosphorus is extractable with 0.1 *N* HCl. Results from the x-ray powder photographs, electromicrographs, and differential-thermal-analyses patterns of the colloidal fraction indicate that the exchange surface is composed of a mica-type mineral with some quartz and a little halloysite present. Little or no kaolin was detectable. The soil was brought to the laboratory, air-dried, and ground to pass through an 8-mesh screen.

Seven ratios of calcium to strontium were established so that the soils of each series had a cation composition of 5% potassium, 15% magnesium, and 80% calcium and strontium. The latter two elements were varied so that their sum remained constant. For each Ca-Sr ratio, triplicate cultures, consisting of 3 kg of oven-dried soil, were prepared for each of the four stages of bean plant maturity at which the plant will be analyzed for Sr. Each culture received 360 mg of nitrogen, 300 mg of phosphorus, and 240 mg of sulfur.

An aliquot of soil material of particle size less than 175 μ in diameter and representing approximately 5% by weight of the total soil to be contaminated was obtained by mechanical dry sieving. To the aliquot, $Sr^{90}CO_3$ was added to give a 1:1 ratio by weight of soil to water suspension which was maintained by agitation for 30 min and then dried at 70°C. These dried fine fractions and the nutrients to be added were pulverized and incorporated into the soil for each plant series by mechanical batch- or barrel-type mixing. The specific activity was adjusted to about 2.7 μc per 100 g of soil.

The cultures were kept moist for at least five days to allow each soil nutrient complex to reach a possible equilibrium. Five seeds of the garden bush bean *Phaseolus vulgaris*, variety Top Crop, were seeded in each pot and covered with ½ in. of white quartz sand. Plants from each calcium-strontium series were harvested at 12-day intervals.

The upper portions of the plants were removed by cutting the stem 1 in. above the soil. The individual plant parts were separated and weighed and then dried at 70°C for 24 hr. The entire material was digested by the nitric-perchloric acid method of Piper. Aliquots were removed for counting and for making chemical determinations of calcium, strontium, magnesium, and potassium.

One object of this experiment was to determine the effect of high concentrations of calcium and

[4]Research participant.
[5]Temporary summer employee.

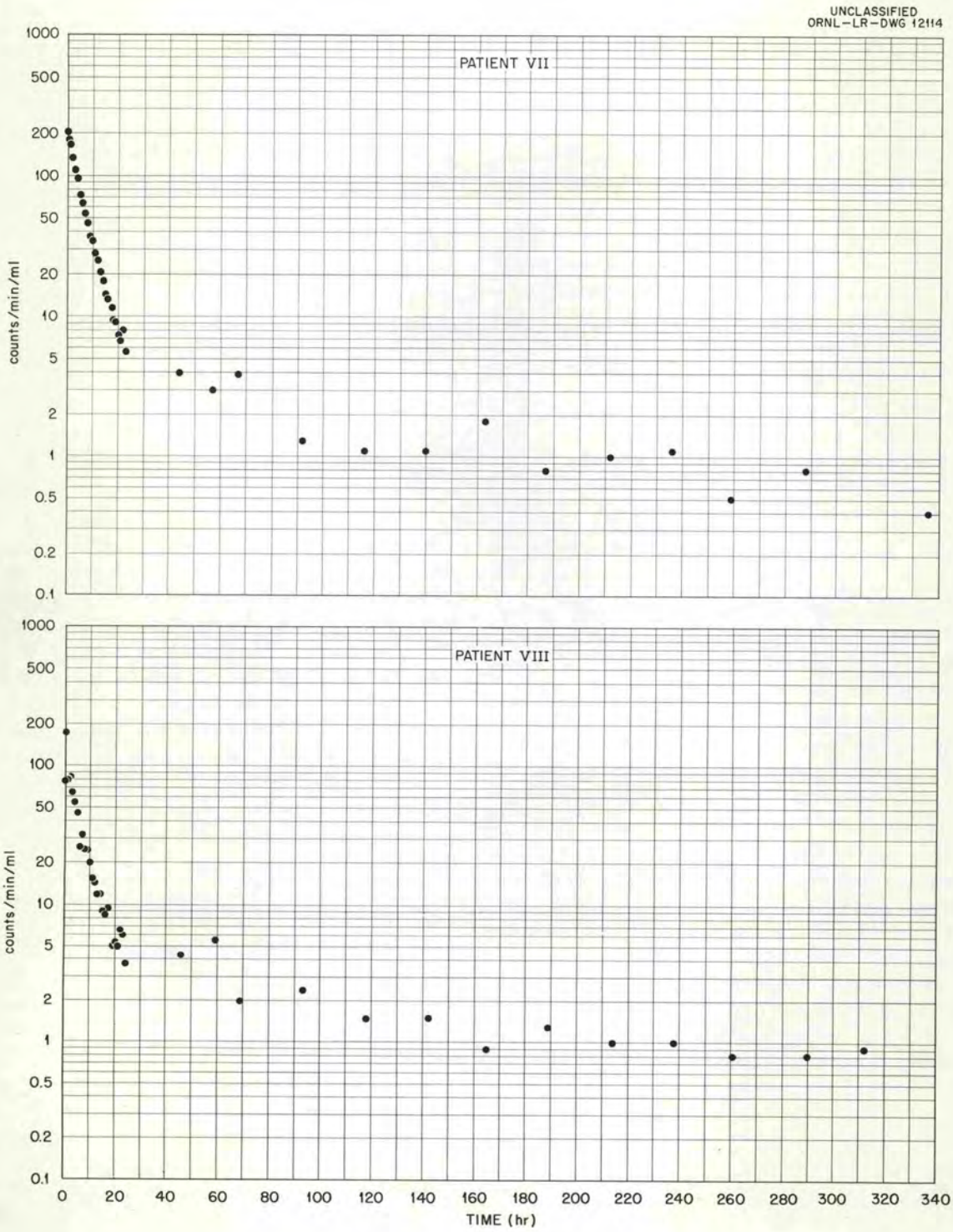

Fig. 4. Disappearance of U(IV) from Blood of Patients Injected Intravenously with UCl_4.

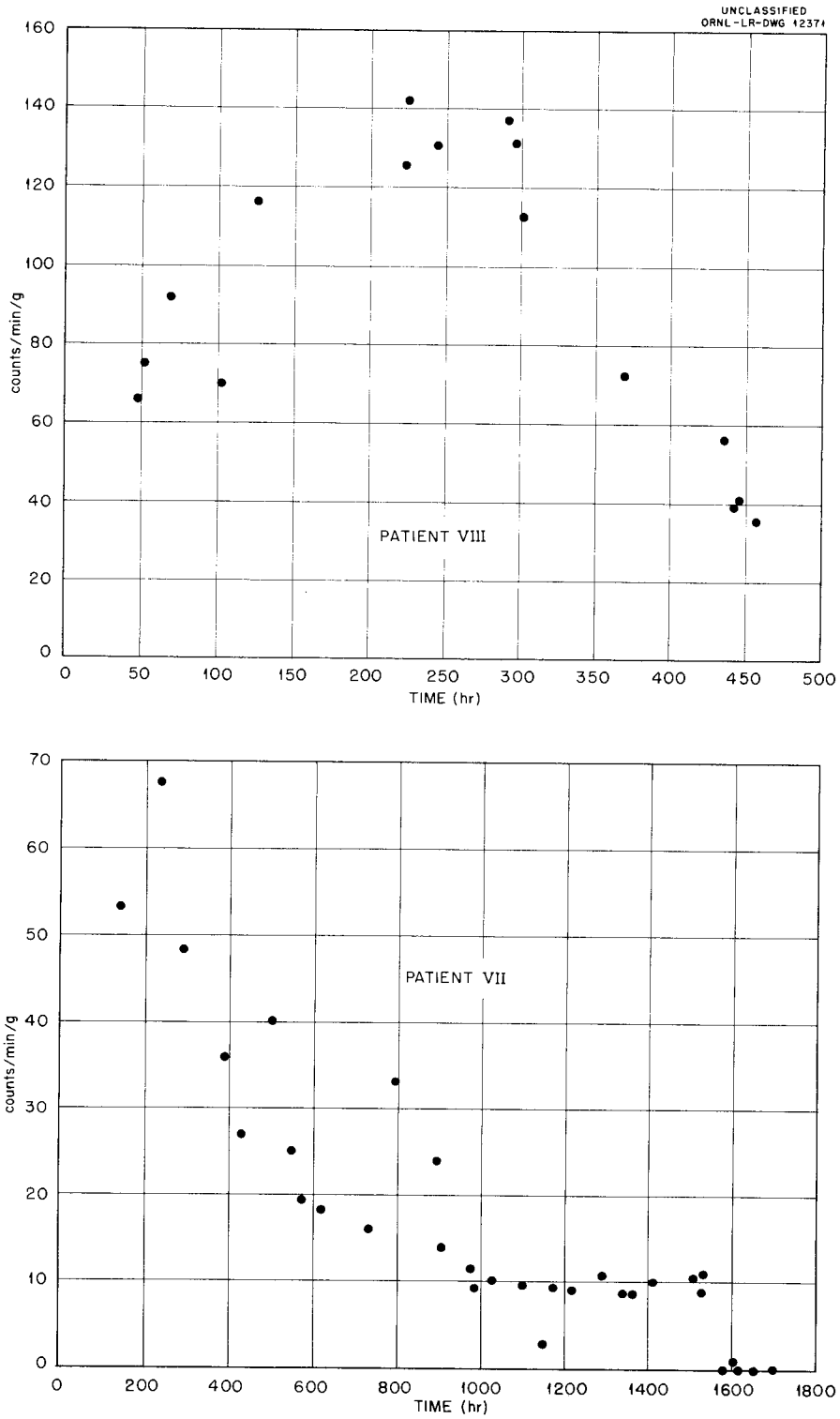

Fig. 5. Excretion of Uranium Via Feces Following Intravenous Administration of UCl_4.

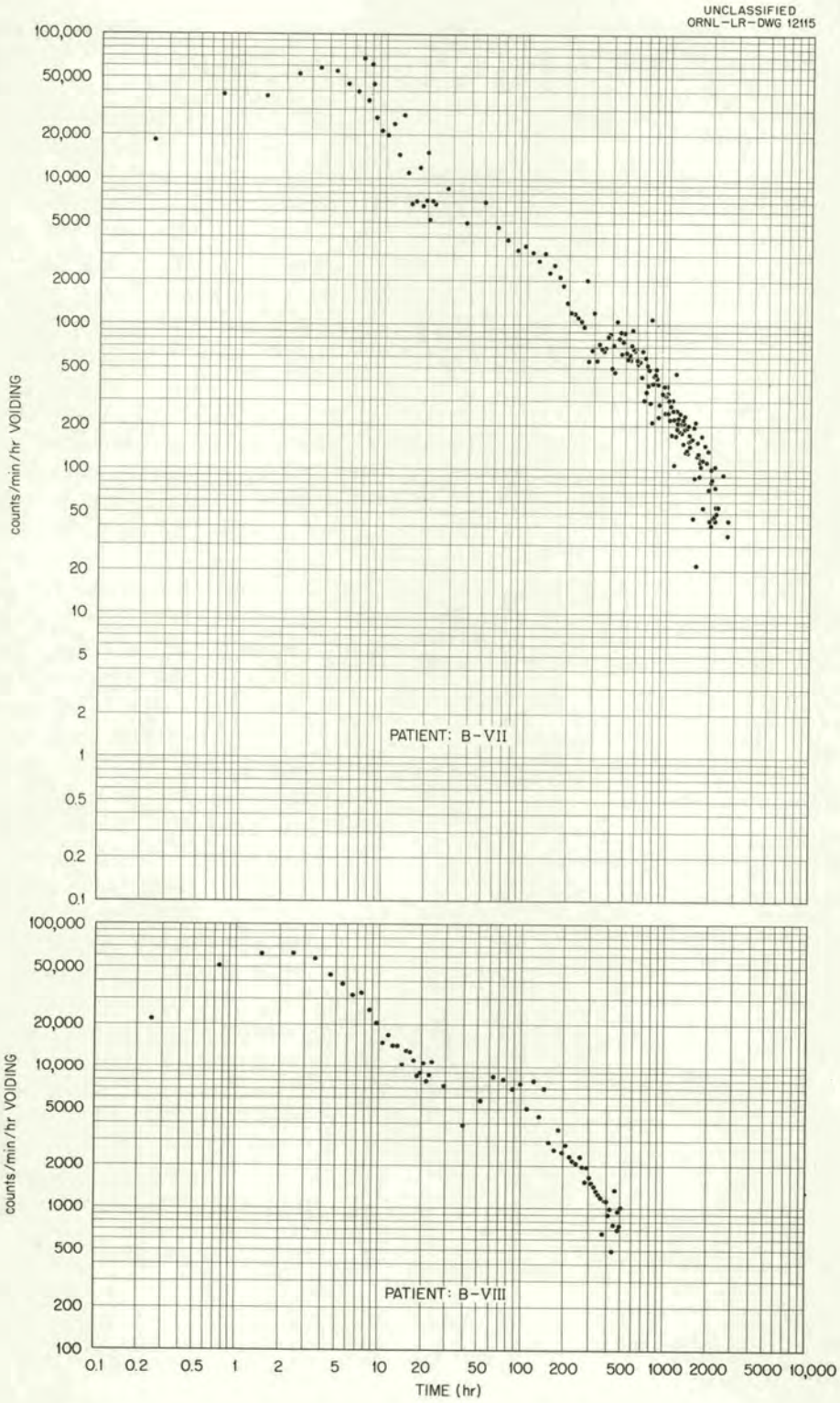

Fig. 6. Urinary Excretion of Uranium Following Intravenous Administration of UCl_4.

strontium in the soil on the uptake of Sr^{90} by the bean plants. There appears to be a gradual decrease in the concentration factor

$$\frac{\text{counts/min per gram of leaf}}{\text{counts/min per gram of soil}}$$

as the per cent of strontium in the cation composition of the soil increases, as indicated by the data in Table 4.

The distribution of the Sr^{90} activity in the various parts of the plant with respect to soil treatment is well illustrated by the data in Table 5. A general decline of activity in the stems, leaves, and pods with increasing amounts of carrier strontium available was noted. The seeds seem to accumulate more of the activity as more carrier strontium and less calcium are available in the soil. In each series the leaves contained more activity than the corresponding stems, pods, or seeds.

TABLE 4. CONCENTRATION OF Sr^{90} IN 12-DAY-OLD BEAN LEAVES ACCORDING TO SATURATION OF SOIL WITH CALCIUM AND STRONTIUM CARRIER

Degree of Soil Saturation (%)		Concentration Factor
Sr	Ca	
10	70	8.19
20	60	6.71
30	50	6.48
40	40	5.38
50	30	3.99
60	20	3.91

TABLE 5. Sr^{90} ACTIVITY IN BEAN PLANT PARTS ACCORDING TO CALCIUM AND STRONTIUM IN THE SOIL

Degree of Saturation of Soil Colloids (%)		Activity (counts/min/mg)			
Sr	Ca	Stems	Leaves	Pods	Seeds
10	70	48.7	60.9	30.4	4.8
20	60	38.3	54.0		5.1
30	50	39.9	53.5	30.5	5.7
40	40	37.6	50.7	25.6	8.1
50	30	33.8	38.0	25.7	9.6
60	20	27.6	35.4	19.2	11.4

Tables 6 and 7 indicate the magnitude of the decline of the Sr^{90} activity of the leaves and stems. It is notable that the decline occurs at all stages of growth. This is in agreement with the theory of isotope dilution.

By increasing the degree of saturation of the soil with carrier strontium, the uptake of this element by all plant parts was enhanced, although the concurrent decrease of calcium in the soil was not always accompanied by a proportionate decrease of the calcium concentration in the plants. The data in Table 8 indicate that only after 36 days of growth do the plants begin to show a definite dependence on the soil calcium. Determination of the magnesium and potassium concentration in the plant parts indicated that these elements had been supplied in adequate amounts and that they were freely available from the soil colloids used in this study.

The growth of the plants did not show evidence of injury from either the activity or high concentration of strontium in the soil. Definite decreases in seed yield became evident as less calcium and more strontium were available in the soils.

It appears reasonable to conclude from the experiments conducted that (1) the uptake of Sr^{90} from natural soils will be concentrated to a higher degree in the leaves than in the other parts of the bean plant, and (2) the concentration factor will be approximately sixfold and that this factor may depend on the total amounts of strontium available in the soil. The amount per unit weight of active strontium absorbed and translocated to leaves declines as more carrier strontium is available in the soil. Uptake of calcium from the soil appears to be almost independent of soil saturation with calcium, at least in the earlier stages of plant growth.

Strontium can replace calcium on the soil colloid to make adequate amounts of potassium and magnesium available for plant growth.

Effects of Gamma Radiation on *Onthophagus texanus* Schaeffer (Coleoptera, Scarabaeidae)

A species of soil-inhabiting beetle, *Onthophagus texanus*, was subjected to gamma radiation from a

Co^{60} source. *Onthophagus* beetles were used because they have a short, continuous life cycle, can be easily handled and sexed, and are readily reared in earth-filled flower pots.

Female beetles, when supplied with day-old cow dung, construct 3 to 7 in. burrows, each with a wad of dung at its terminus. A single egg is placed in each wad; the larva develop within the wad. Since the larvae could not complete development without this food supply furnished by the adult beetles, not only doses which produce sterility but any radiation effect on adult activity must be considered. The dry wads containing the larvae were easily removed from the pots, irradiated,

TABLE 6. CONCENTRATION OF CARRIER* AND RADIOACTIVE STRONTIUM** IN BEAN LEAVES OF DIFFERENT STAGES OF GROWTH

Degree of Saturation of Soil Colloids (%)		Growth Stage							
		12 Days		24 Days		36 Days		48 Days	
Stable Sr	Ca	Sr^{90}	Total Sr	Sr^{90}	Total Sr	Sr^{90}	Total Sr	Sr^{90}	Total Sr
0	80	0.8	0.025	0.7	0.014	0.7	0.023	0.7	0.034
10	70	79.3	0.179	112.2	0.635	53.7	0.439	60.9	0.375
20	60	76.4	0.597	105.7	1.288	65.2	0.927	54.0	0.637
30	50	62.6	1.031	98.4	1.986	64.4	1.394	53.5	1.127
40	40	56.3	1.143	79.2	2.848	48.6	1.796	50.7	1.260
50	30	56.2	1.203	64.6	2.534	53.0	2.160	38.0	1.613
60	20	47.5	1.304	59.1	2.634	52.7	2.405	35.4	1.910

*Total Sr given as per cent dry weight.

**Sr^{90} given as counts/min per mg of dry leaf corrected to 10% geometry. Each value is the average of three determinations on independently grown cultures of five plants each.

TABLE 7. CONCENTRATION OF CARRIER* AND RADIOACTIVE STRONTIUM** IN BEAN STEMS HARVESTED AT DIFFERENT STAGES

Degree of Saturation of Soil Colloids (%)		Growth Stage							
		12 Days		24 Days		36 Days		48 Days	
Stable Sr	Ca	Sr^{90}	Total Sr	Sr^{90}	Total Sr	Sr^{90}	Total Sr	Sr^{90}	Total Sr
0	80	0.6	0.062	1.0	0.011	0.4	0.027	0.9	0.019
10	70	122.9	0.500	69.3	0.354	56.5	0.415	48.7	0.314
20	60	72.3	0.609	69.1	0.935		0.788	38.3	0.547
30	50	71.2	1.018	70.1	1.495	45.7	0.971	38.0	0.884
40	40	57.5	0.953	59.6	1.752	41.1	1.385	37.6	1.064
50	30	53.3	1.113	55.0	1.629	41.6	1.653	33.8	1.251
60	20	51.9	4.89	44.9	1.825	41.5	1.733	27.6	1.324

*Total Sr given as per cent dry weight.

**Sr^{90} given as counts/min per mg of dry stem corrected to 10% geometry. Each value is the average of three determinations on independently grown cultures of five plants each.

TABLE 8. Sr-Ca COMPOSITION OF BEAN PLANTS AT VARIOUS STAGES OF GROWTH ACCORDING TO TREATMENT OF THE SOIL WITH CALCIUM AND STRONTIUM

Degree of Saturation of Soil Colloids (%)		Leaves		Stems		Roots	
Sr	Ca	Total Sr	Ca	Total Sr	Ca	Total Sr	Ca
			12-Day-Old[a]				
0	80	0.035	0.981	0.062	0.916	0.079	0.328
10	70	0.179	0.540	0.500	1.132	0.147	0.325
20	60	0.597	1.160	0.609	1.169	0.230	0.264
30	50	1.031	1.102	1.018	0.941	0.309	0.262
40	40	1.143	0.728	0.953	0.546	0.294	0.229
50	30	1.203	0.577	1.113	0.446	0.416	0.239
60	20	1.304	0.536	4.89	0.284	0.448	0.232
			24-Day-Old[b]				
0	80	0.014	1.447	0.011	0.9842	0.217	0.6259
10	70	0.635	1.583	0.354	0.6531	0.365	0.6118
20	60	1.288	1.692	0.935	0.8981	0.604	0.6117
30	50	1.986	1.342	1.495	0.9850	0.862	0.6619
40	40	2.848	1.587	1.752	0.9184	0.756	0.6066
50	30	2.534	1.514	1.629	1.0023	0.423	0.4310
60	20	2.634	1.352	1.825	0.8192	0.787	0.5224
			36-Day-Old[a]				
0	80	0.023	2.635	0.027	1.618	0.020	0.971
10	70	0.439	2.203	0.415	1.604	0.095	0.910
20	60	0.927	2.385	0.788	1.699	0.176	0.644
30	50	1.394	2.012	0.971	1.008	0.228	0.628
40	40	1.796	1.755	1.385	1.231	0.326	0.723
50	30	2.160	1.720	1.653	1.146	0.416	0.719
60	20	2.405	1.220	1.733	0.962		

Degree of Saturation of Soil Colloids (%)		Leaves		Stems		Pods		Seeds	
Sr	Ca	Total Sr	Ca	Total Sr	Ca	Total Sr	Ca	Total Sr	Ca
				48-Day-Old[a]					
0	80	0.034	2.405	0.019	1.6030	0.004	0.681	0.002	0.084
10	70	0.375	1.783	0.314	1.2054	0.144	0.583	0.014	0.084
20	60	0.637	1.605	0.547	1.2007	0.334	0.551	0.023	0.097
30	50	1.127	1.765	0.884	0.9009	0.354	0.562	0.030	0.115
40	40	1.260	1.495	1.064	0.9001	0.408	0.444	0.056	0.115
50	30	1.613	1.300	1.251	0.8063		0.406	0.066	0.139
60	20	1.910		1.324	0.7037	0.465	0.376	0.073	

[a]Each value is an average of three cultures representing a total of 15 plants. Values given in per cent of dry weight.
[b]In the determination of strontium in the roots, there was some contamination from soil.

and then kept in metal salve boxes, where their development could be observed.

Adult beetles were given a dose of 5000 r at a dose rate of 26 r/sec. Second-stage larvae in the dung wads were given total doses of 2000 and 4000 r at the same dose rate.

The number of dung wads placed at the ends of the burrows by the adults was considered as one criterion of activity, while the lack of eggs within the wads was considered as an indicator of sterility. With doses of 3000 to 5000 r the adult beetles formed fewer egg cells than the controls, and in no case did the treated adults produce fertile eggs. Table 9 summarizes this portion of the work.

The second-stage larvae were divided into three lots of 30 cells each, which were in turn divided into sublots of 10 cells. One lot of 30 cells was left untreated, one lot received a dose of 2000 r, and one lot of 30 received 4000 r. Table 10 summarizes the results. No developmental differences could be noted between the controls and those cells given the 2000-r dose. With 4000 r there was a high mortality and the few beetles reaching the adult stage were badly deformed. The crumpled elytra, shortened antennae with the antennal clubs fused, tarsal segments fused or missing, and the deformed clypeus were a few of the more obvious deformities produced. While radiation-induced deformities have been noted in *Drosophila* and *Habrobracon*, they have not been previously recorded for beetles.

The adults resulting from the treated larvae were placed in rearing pots. The deformed adults from the larvae given the 4000-r dose were too abnormal to burrow and were therefore incapable of reproduction even if they had been fertile. The adults from the 2000-r larval treatments, while normal in appearance, produced few cells and no fertile eggs, as is indicated in Table 11. Whiting and Bostian[6] found that some *Habrobracon* adults

[6] A. R. Whiting and C. H. Bostian, *Genetics* 16, 659–680 (1931).

TABLE 9. REPRODUCTION OF *ONTHOPHAGUS* CONTROLS AND IRRADIATED ADULTS

Number of Pairs	Dose (r)	♂ Life Span (days)	♀ Life Span (days)	Number of Egg Cells Formed	Number of Egg Cells Viable
			Irradiated		
1	5000	19	8	4	0
1	5000	14	16	4	0
3	5000	7, 8, 15	7, 17, 13	0	0
3	5000	9, 14, 14	14, 14, 16	1	0
1	3000	17	21	0	0
3 ♂	♂ – 5000	9, 9, 14			
			Controls		
1 ♀	♀ – 0		14	1	0
1	0	15	25	5	3
2	0	15	18	8	8
2	0	av for	av for	7	6
2	0	males	females	8	7
2	0	15	18	13	12
2	0	15	18	23	22
2	0	15	18	8	8
2	0	15	18	4	4

TABLE 10. DEVELOPMENT OF ADULT *ONTHOPHAGUS* FROM CONTROL AND IRRADIATED SECOND INSTARS

	Number of Cells	♂	♀	Number Unsuccessful	Average Development Time (days)
				Control	
	10	4	2	4	35–51, 39 median
	10	5	2	3	
	10	3	4	3	
Total	30	12	8	10	
				Irradiated	
				2000 r	
	10	1	6	3	35–44, 38 median
	10	4	2	4	
	10	7	0	3	
Total	30	12	8	10	
				4000 r	
	10	1	0	9	42–49, 42 median; all adults deformed
	10	0	2	8	
	10	0	0	10	
Total	30	1	2	27	*

*1 ♂, 3 ♀ dead in cells.

emerging from larvae which had been subjected to doses as low as 730 r failed to reproduce. The number of failures increased as the dose was increased. These investigators suggested that this was not entirely due to sterilization but to lessened vigor, which resulted in early death. In the *Onthophagus* from the 2000-r treatment there was no evidence of shortened life span, but, since they produced considerably fewer cells, it is possible that their vigor was affected as well as (or instead of) their fertility.

Delayed Effects of Gamma Radiation on Tree-Hole Arthropods

A single beech tree hole from the Laboratory environs was completely excavated, and part of the removed substrate was subdivided into 100-g samples. These samples were grouped into three series, each series consisting of eight samples divided into the following doses of gamma radiation from a Co^{60} source: 3×10^3, 8×10^3, 1.5×10^4, 2.5×10^4, 5×10^4, 7.5×10^4, 1×10^5, and 1.25×10^5 r, at a dose rate of 26 r/sec. Five control samples were set up as a part of each series. After irradiation each sample was transferred to a sterile red-clay flower pot covered with cellophane. The pots were stored in chambers where the temperature was kept at 75 ± 3°F and the relative humidity ranged from 65 to 85%. At the end of 30 days a series, consisting of eight experimental and five control samples, was removed and processed through Berlese-type funnels to extract the surviving arthropods. Of the remaining two series, one was processed after 60 days and the other after 90 days. All samples were counted in a gridded evaporating dish under a dissecting microscope. Total counts were made in all cases.

Preliminary analysis of the data indicates differences in response to irradiation under these conditions for Acarina, Collembola, Isopoda, and Chilopoda. In the case of the Acarina and Collembola there is evidence of difference even between species which are morphologically closely

TABLE 11. REPRODUCTION OF *ONTHOPHAGUS* FROM CONTROLS AND ADULTS IRRADIATED AT SECOND INSTAR

Number of Pairs	Dose (r)	♂ Life Span (days)	♀ Life Span (days)	Number of Cells Formed	Number of Cells Viable
		Irradiated			
2	2000	18, 20	14, 14	0	0
2	2000	12, 13	16, 38	3	0
2	2000 (+3000 as adults)	13, 14	16, 18	1	0
1	4000	6	6	0*	
		Control			
1	0	15	25	5	3
2	0	15	18	8	8
2	0	av for	av for	7	6
2	0	males	females	8	7
2	0	15	18	13	12
2	0	15	18	23	22
2	0	15	18	8	8
2	0	15	18	4	4

*Adults unable to burrow.

related. At the higher taxonomic category levels, differences appear to be even more pronounced. Most of the Acarina showed relatively high resistance to radioactivity for the entire period of the experiment, but the Isopoda and Chilopoda were adversely affected (as measured by survival) by much lower doses of radiation. The Collembola, both at the species and family level, showed greater resistance to the irradiation under these conditions than did either the isopods and chilopods but less resistance than did the mites. A more detailed statistical analysis of the data is currently in progress.

Studies of the Uptake of Fission Products by Earthworms

Uptake of Sr^{89} by *Allolobophora caliginosa* (Savigny). – To investigate further the ability of earthworms to concentrate Sr^{89} present in the soil, an experiment was conducted which was similar to the one used for *Eisenia foetida* (Savigny)[7] except that *Allolobophora caliginosa* (Savigny)[8] was used in place of *Eisenia foetida*. *Allolobophora caliginosa* is believed to be the most abundantly represented and most widely distributed of the North American earthworms.[9]

The design of this experiment differed somewhat from the previous experiment.[7] Two soil series were used. In one series the same type of soil as in the previous experiment was used without modification. In the second series the soil was enriched with certain inorganic constituents considered to be of importance in soil fertility. The

[7] S. I. Auerbach *et al.*, *HP Semiann. Prog. Rep. July 31, 1955*, ORNL-1942, p 7.

[8] The authors are indebted to Dr. W. Murchie, Thiel College, Greenville, Penn., for supplying the worms.

[9] F. Smith, *Proc. U. S. Nat. Museum* 52, 157–182 (1917).

analyses of these two soils[10] are given below:

	Soil I	Soil II
Organic matter, %	4.1	4.4
P_2O_5, ppm	29	45
K, ppm	12	28
Mg, ppm	13	13
Ca, ppm	100	160
pH	5.3	6.2
Total hydrogen, meq/100 g	6.0	2.5
Cation exchange capacity, meq/100 g	12	12
Base saturation, %	50	79

Six red-clay flower pots were used for each series. Each series was divided into five experimental pots and one control pot. Each of the five pots was brought up to a different activity level of Sr^{89}. The activities (in microcuries per gram of soil) were as follows: 1.88×10^{-3}, 3.77×10^{-3}, 5.65×10^{-3}, 7.54×10^{-3}, 9.43×10^{-3}. These activities were the same in both series. The isotope was added to the soils in the same manner as before.[7] Six adult worms were added to each pot. The pots were weighed twice a week to determine the water loss, and water was added as needed.

After 30 days the pots were examined for the surviving worms; 69 of an initial 72 specimens were found to have survived. All the specimens were placed between sheets of moistened filter paper for three days while they emptied their intestinal tracts of soil.

Fifty per cent of the individuals from each pot were cut in half. The two halves were analyzed separately to determine any gross difference in the distribution of the radionuclide in the body of the worm. All the remaining worms were then weighed individually and sacrificed. Preparation of the worms for counting and the counting procedures were the same as before.[7]

The radionuclide uptake, as determined from the whole worms in each series, is presented in Table 12, together with the activity of the soil at the time that the worms were removed. The ratio of worm to soil (in $\mu c/g$) is given. The results indicate that although there is some uptake of the fission product Sr by this species of worm there is no concentration under the conditions of this experiment. Furthermore, as shown in the enriched soil series, it is evident that the addition of calcium to the soil served to depress the uptake of Sr^{89}.

In Table 13 these ratios for *A. caliginosa* are compared with those for *E. foetida*. The data indicate that *A. caliginosa*, even when the diluting effect of calcium is present, has a greater affinity for the radionuclide than does *E. foetida*. The reason for this is probably related to the fact that *A. caliginosa* is a true soil-feeding species whereas *E. foetida* prefers humus and other decomposing organic matter both as food and as a niche.

In Table 14 the uptake ratios and the specific activity for the anterior and posterior sections of *A. caliginosa* under both soil conditions are

[10]Soil analyses were made by the Department of Soils, College of Agriculture, University of Missouri, Columbia.

TABLE 12. ANALYSIS OF Sr^{89} ACTIVITY IN EARTHWORM, *ALLOLOBOPHORA CALIGINOSA* (SAVIGNY)

Pot No.	Activity of Soil at End of Experiment ($\mu c/g$)	Number of Individuals	Untreated Soil Series: Activity ($\mu c/g$ of worm)	Untreated Soil Series: Ratio $\left(\frac{\mu c/g \text{ of worm}}{\mu c/g \text{ of soil}}\right)$	Number of Individuals	Enriched Soil Series: Activity ($\mu c/g$ of worm)	Enriched Soil Series: Ratio $\left(\frac{\mu c/g \text{ of worm}}{\mu c/g \text{ of soil}}\right)$
I	1.25×10^{-3}	3	2.39×10^{-4}	0.191	3	0.963×10^{-4}	0.077
II	2.51×10^{-3}	2	3.23×10^{-4}	0.128	3	1.64×10^{-4}	0.065
III	3.76×10^{-3}	3	5.22×10^{-4}	0.138	3	3.37×10^{-4}	0.089
IV	5.02×10^{-3}	3	5.58×10^{-4}	0.111	3	4.63×10^{-4}	0.092
V	6.27×10^{-3}	3	7.16×10^{-4}	0.114	3	4.17×10^{-4}	0.066
Control	0	3	0		3	0	

TABLE 13. COMPARISON OF WORM UPTAKE–SOIL ACTIVITY RATIOS OF Sr^{89} IN THE CASE OF *EISENIA FOETIDA* AND *ALLOLOBOPHORA CALIGINOSA*

Pot No.	*Eisenia foetida*		*Allolobophora caliginosa*		
	Activity of Soil at End of Experiment ($\mu c/g$)	Ratio $\left(\frac{\mu c/g \text{ of worm}}{\mu c/g \text{ of soil}}\right)$	Activity of Soil at End of Experiment ($\mu c/g$)	Untreated Soil Ratio $\left(\frac{\mu c/g \text{ of worm}}{\mu c/g \text{ of soil}}\right)$	Enriched Soil Ratio $\left(\frac{\mu c/g \text{ of worm}}{\mu c/g \text{ of soil}}\right)$
I	0.937×10^{-3}	0.030	1.25×10^{-3}	0.191	0.077
II	1.87×10^{-3}	0.057	2.51×10^{-3}	0.128	0.065
III	2.81×10^{-3}	0.043	3.76×10^{-3}	0.138	0.089
IV	3.75×10^{-3}	0.046	5.02×10^{-3}	0.111	0.092
V	4.69×10^{-3}	0.049	6.27×10^{-3}	0.114	0.066
Control	0	0	0	0	0

TABLE 14. ANALYSIS OF ACTIVITY IN ANTERIOR AND POSTERIOR PORTIONS OF *ALLOLOBOPHORA CALIGINOSA*

Pot No.	Number of Individuals	Anterior Portions ($\mu c/g$ of tissue)	Ratio $\left(\frac{\mu c/g \text{ of tissue}}{\mu c/g \text{ of soil}}\right)$	Posterior Portions ($\mu c/g$ of tissue)	Ratio $\left(\frac{\mu c/g \text{ of tissue}}{\mu c/g \text{ of soil}}\right)$
			Untreated Soil		
I	3	1.90×10^{-4}	0.152	0.89×10^{-4}	0.071
II	3	4.77×10^{-4}	0.190	2.27×10^{-4}	0.090
III	3	8.10×10^{-4}	0.215	3.27×10^{-4}	0.086
IV	3	8.33×10^{-4}	0.166	3.89×10^{-4}	0.077
V	3	10.30×10^{-4}	0.164	2.49×10^{-4}	0.040
Control	3	0	0	0	0
			Enriched Soil		
I	3	1.82×10^{-4}	0.145	0.95×10^{-4}	0.076
II	2	2.35×10^{-4}	0.093	1.16×10^{-4}	0.046
III	3	4.17×10^{-4}	0.111	3.78×10^{-4}	0.100
IV	3	7.07×10^{-4}	0.141	2.69×10^{-4}	0.053
V	3	6.98×10^{-4}	0.111	1.98×10^{-4}	0.031
Control	3	0	0	0	0

presented. In both series at each level of soil activity the anterior portions contained more radionuclide than did the posterior portion. The explanation for this phenomenon may be due to the presence of the calciferous glands in the anterior segments of the worm. Recent work[11] on some other species of earthworms has demonstrated that these glands are concerned with the extraction and storage of calcium. This would account for their affinity for strontium and for the higher activity in the nontreated soil series.

URINALYSIS RESEARCH

L. B. Farabee

Although there are several complicated techniques in general use for the determination of radioactive cesium in biological materials and in water, none of them are entirely satisfactory. There is a need for a simple, reliable procedure. The recently reported[12] precipitation of potassium as its tetraphenylboron salt provides a simple method for the separation of potassium from a wide range of ions associated with it. Potassium and cesium form very insoluble tetraphenylboron compounds in dilute mineral acids, whereas the sodium salt is very soluble.

Preliminary tests with procedures for separating Cs^{137} from biological materials with the use of sodium tetraphenylboron give excellent recovery as well as good separation from the other fission products. However, potassium, which is present in large amounts in such samples, coprecipitates with the cesium and makes the sample rather bulky for counting. Also, K^{40} contributes to the radioactivity of the sample.

In the analysis of muscle tissue of fish as well as in urinalysis the radioactive cesium can be concentrated by a precipitation of the potassium in the sample as potassium cobaltinitrite. The cesium can be separated subsequently from potassium by precipitating cesium silicotungstate. The cesium is finally precipitated as cesium tetraphenylboron.

DISTRIBUTION OF RADIOISOTOPES IN ANIMAL TISSUE

M. J. Cook F. G. Karioris[13]
K. Z. Morgan

It is extremely important to test experimentally the mathematical relation used (in publications by the National Committee on Radiation Protection[14] and the International Commission of Radiological Protection[15]) in employing single-exposure data to determine the MPC of radionuclides in air and water for continuous exposure. A pilot experiment on Co^{60} was computed,[16] and the indication is that the mathematical relations used in the handbooks on internal dose are correct within a factor of 2 for Co^{60}. A study with mice was initiated to check this relationship for other radionuclides.

Each mouse was given a single dose of 10 μc of $Sr^{90} + Y^{90}$ by stomach tube. In groups of 10, the mice were sacrificed at the following intervals: 4 and 24 hr; 3, 5, and 7 days; 2, 3, 4, 5, and 7 weeks. The animals that were sacrificed at the periods of from 4 hr through 2 weeks were dissected into 16 parts. In the 2-week group, only a trace of Sr^{90}-Y^{90} remained in the soft tissue; therefore, the mice sacrificed after 2 weeks are dissected only into soft tissues, femur, and carcass. Other mice will be sacrificed at 3, 6, 12, and 18 months.

As a second part of the experiment mice will be subjected continuously to a fixed concentration of $Sr^{90} + Y^{90}$ in the drinking water. In order to know the exact amount of water containing the radioisotope which the mice drink *ad libitum*, a capillary drinking fountain was designed and is pictured in Fig. 7. The critical factor in this device is the height of the liquid in the drinking pool, which must remain within narrow limits to be available to the animals and to prevent spills. Within less than 24 hr, the mice learn to drink from the fountain. Now that this fountain has been

[11] H. V. Kashyap and M. R. Ranade, *Proc. Zool. Soc. Bengal* 5, No. 1, 1–9 (1952).

[12] G. Wittig and P. Raff, *Ann. Chem., Justus Liebigs* 573, 195 (1951).

[13] Summer research participant from the Physics Department of Marquette University, Milwaukee, Wisconsin.

[14] United States National Bureau of Standards, *Maximum Permissible Amounts of Radioisotopes in the Human Body and Maximum Permissible Concentrations in Air and Water*, Handbook 52 (1953), Superintendent of Documents, Washington 25, D.C.

[15] International Cangress of Radiology, "Recommendations of the International Commissian of Radiological Protectian," *Brit. J. Radiol.* Suppl. 6 (revised Dec. 1, 1954).

[16] M. J. Cook, K. Z. Morgan, and A. G. Barkow, "An Experiment Designed to Test the Validity of the Current Practice of Using Single-Exposure Data to Calculate Maximum Permissible Concentration in Water for Continuous Exposure to Radioisotopes." Accepted for publication in *Am. J. Roentgenol., Radium Therapy Nuclear Med.*

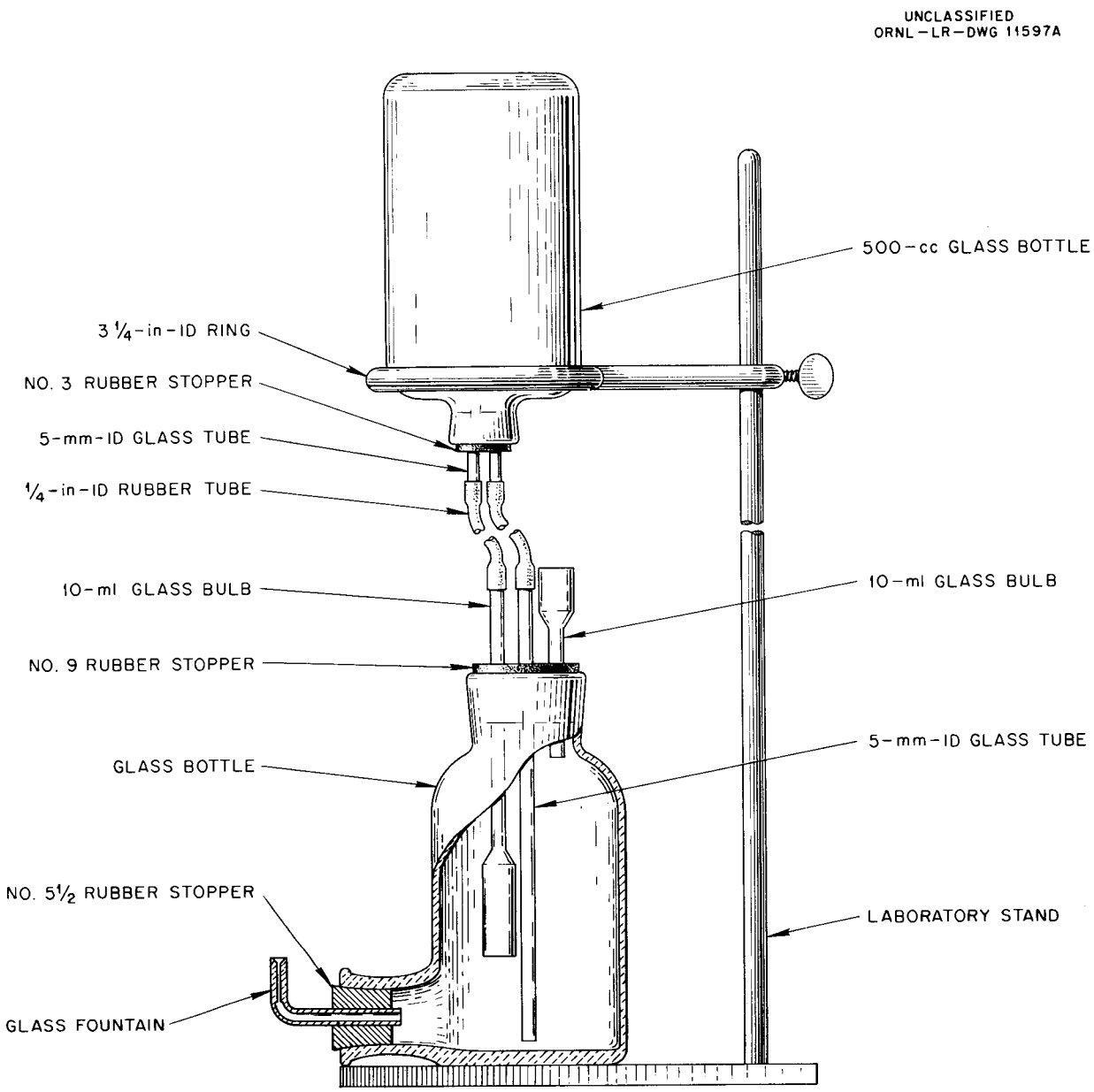

Fig. 7. Measuring Capillary Fountain.

developed and tested, the second part of this experiment is getting under way.

ISOTOPIC DISTRIBUTION IN MAN

Internal Dose

K. Z. Morgan M. J. Cook
M. R. Ford

The tables of maximum permissible concentrations for continuous exposure to radioisotopes[14,15] are being revised. The revision will include new biological data, additional elements, additional isotopes, and additions to the bibliography.

Spectrographic Analysis of Human Tissue

I. H. Tipton D. K. Bowman
M. J. Cook K. K. McDaniel

During the period from July 1, 1955, through December 31, 1955, the collecting of normal human tissue was extended to four more cities in the

United States, making a total of eight cities distributed in seven states. Tissues from 57 adult autopsies, with an average of 26 tissues per autopsy, were received.

In addition to the tissues from adult autopsies the program is being expanded to include analyses of tissues from fetuses, still births, babies, children, and teen-agers. From each city where adult tissues are being received, it is hoped that the following tissues may be received in order to compare the elements found in the tissues of adults with those in the tissues of younger people:

Fetus (6 to 9 months)	2 whole
Birth to 6 months	1 autopsied
3 to 6 years	1 autopsied
14 to 18 years	1 autopsied

Invitations have been extended by pathologists in four additional cities in the United States, and arrangements will be made at a later date to extend the program to these cities.

Perhaps the most difficult tissue to obtain is the eye. Fifteen eyes have been secured from fetuses and still births or from infants whose bodies were left at the hospital for disposal.

The tissues are packed in dry ice and shipped via air express to this laboratory, where they are stored in the deep-freeze unit until time for ashing. From shipment until arrival, the time in all instances has been less than 24 hr.

The tissues are dry-ashed as follows:

1. Tissues are trimmed, weighed, and then washed in ion-exchange water.
2. Tissues are placed in the oven and the temperature is gradually brought to 300°C, where it is held for 20 hr.
3. At the end of 20 hr the tissues are cooled and reweighed in order to obtain the dry weight.
4. Tissues are placed in the oven and the temperature is gradually brought to 450°C, at which temperature the tissues remain for 24 hr or longer if necessary.
5. The tissue ashes are cooled and reweighed.
6. The ash is transferred to a polyethylene bottle and ground for 30 min.

During the past six months 806 tissues have been dry-ashed and sent to the Physics Department of the University of Tennessee, where over 30,000 spectrographic determinations have been made.

The analytical method is essentially the same as that described in earlier reports except that two internal standards are employed: indium for the elements boron, zinc, gallium, silver, cadmium, tin, lead, gold, and bismuth; and palladium for the elements manganese, iron, cobalt, nickel, copper, cesium, strontium, molybdenum, barium, lanthanum, and gold. The upper and lower limits of sensitivity in parts per million in ash and the precision of the method expressed as coefficients of variation in per cent are given in Tables 15 and 16. The coefficients of variation were determined from 16 replicate analyses of a single standard sample.

The improved techniques of collection and ashing make the analyses more meaningful, since there is

TABLE 15. SPECTROGRAPHIC DETERMINATIONS OF DRY-ASHED SOFT TISSUE FOR LIMITS OF SENSITIVITY AND COEFFICIENTS OF VARIATION

Element	Limits of Sensitivity (ppm in ash)		Coefficient of Variation (%)
	Upper	Lower*	
Boron	400	10	
Aluminum	4,000	2	15
Titanium	1,000	10	15
Vanadium	1,000	10	
Chromium	1,000	0.1	10
Manganese	1,000	1	10
Iron	100,000	1,000	
Cobalt	400	5	
Nickel	1,000	10	10
Copper	1,000	25	5
Zinc	10,000	400	5
Gallium	20	1	
Strontium	40	1	15
Molybdenum	1,000	10	10
Silver	400	1	15
Cadmium	5,000	75	4
Tin	1,000	10	20
Cesium	3,000	100	
Barium	400	0.2	20
Lanthanum		100	
Gold	400	20	
Lead	1,000	10	15
Bismuth	400	10	

*Other elements with lower limits include: beryllium (3), arsenic (300), zirconium (30), niobium (100), ruthenium (10), antimony (100), and thallium (10).

TABLE 16. SPECTROGRAPHIC DETERMINATIONS OF DRY-ASHED BONE FOR LIMITS OF SENSITIVITY

Element	Limits of Sensitivity (ppm in ash)	
	Upper	Lower*
Boron		30
Aluminum	100	4
Titanium		40
Vanadium		20
Chromium		5
Manganese	100	2
Iron	4000	100
Cobalt		10
Nickel		30
Copper	100	2
Zinc	3000	700
Gallium		5
Strontium	1000	10
Molybdenum		15
Silver	100	1
Cadmium		200
Tin	400	10
Cesium		400
Barium	200	4
Lanthanum		400
Gold		15
Lead	400	10
Bismuth		20

*Other elements with lower limits include: arsenic (1000), zirconium (400), niobium (150), ruthenium (?), antimony (100), and thallium (20).

considerably less cross-contamination. The elements beryllium, arsenic, zirconium, niobium, ruthenium, antimony, and thallium are sought in every sample. However, except for traces of ruthenium in two spleen samples, none have been detected. Part of the results of the analyses of tissues collected from one city are presented in Table 17, which does not include all the tissues received from the autopsies but only the tissues analyzed spectrographically as of December 31, 1955. All the elements were sought, and a blank space means that nothing was detected within the limits of sensitivity. Table 17 presents data which indicate the specific tissues in which the various elements are found. Gallium was found in three specimens of lung only (average value of 0.03 μg/g) and is not included in the table. Tables are available on request giving the element distribution in each tissue.

TABLE 17. CONCENTRATIONS OF ELEMENTS IN SPECIFIC WET TISSUES

Tissue	Number of Samples: Analyzed	Number of Samples: Containing Element*	Average Value for Samples Containing Element (μg/g)	Number of Samples: Analyzed	Number of Samples: Containing Element*	Average Value for Samples Containing Element (μg/g)
	Aluminum			**Bismuth**		
Adrenal	3	3	0.70	3		
Aorta	12	12	0.87	12	3	0.40
Bladder	13	13	1.1	13		
Bone	23 (5)	13	0.53	23		
Brain	21	21	0.40	21 (1)		<0.15 T
Esophagus	8	8	1.4	8 (1)	1	>>4
Heart	19	19	0.43	19 (1)		<0.10 T
Intestine						
Duodenum	7	7	0.76	7	1	>>4
Jejunum and ileum	20	20	0.80	20 (2)	1	>>4
Large	22	22	1.0	22 (3)	1	0.07
Kidney	24	24	0.67	24	6	1.1
Liver	24	24	0.70	24	3	0.90
Lung	24	24	23	24 (1)		<0.11 T
Muscle	18	18	0.50	18		
Pancreas	21	21	0.70	21 (1)	2	0.36
Prostate	8	8	0.75	8 (2)		<0.13 T
Spleen	22	22	2.2	22	2	0.36
Stomach	20	20	0.53	20 (1)	1	>>4
Thyroid	8	8	1.40	8 (1)		<0.11 T
	Barium			**Boron**		
Adrenal	3	3	0.03	3 (1)	2	0.17
Aorta	12	12	0.11	12	1	0.40
Bladder	13 (1)	10	0.03	13 (1)	1	0.30
Bone	23	23	1	23		
Brain	21	9	0.04	21	3	0.18
Esophagus	8	8	0.04	8		
Heart	19 (2)	15	0.02	19		
Intestine						
Duodenum	7	7	0.03	7	2	0.08
Jejunum and ileum	20	20	0.05	20 (2)	2	0.22
Large	22	22	0.06	22 (4)	1	0.12
Kidney	24 (3)	16	0.06	24 (1)	1	0.16
Liver	24 (2)	2	0.04	24 (5)	3	0.30
Lung	24	24	2.6	24 (3)	2	0.14
Muscle	18 (1)	12	0.02	18		
Pancreas	21 (2)	14	0.06	21 (2)	4	0.17
Prostate	8 (1)	6	0.08	8 (1)	1	0.24
Spleen	22 (1)	14	0.04	22 (1)	1	0.20
Stomach	20	19	0.03	20 (2)	4	0.13
Thyroid	8	8	0.34	8		

*The numbers in parentheses indicate the number of samples with a trace.

TABLE 17 (continued)

Tissue	Number of Samples			Average Value for Samples Containing Element (μg/g)	Number of Samples			Average Value for Samples Containing Element (μg/g)
	Analyzed		Containing Element*		Analyzed		Containing Element*	
	Cadmium				Chromium			
Adrenal	3		2	0.41	3		3	0.08
Aorta	12		1	0.87	12	(2)	4	0.07
Bladder	13				13		5	0.06
Bone	23				23	(1)		<0.8 T
Brain	21				21	(2)	2	0.02
Esophagus	8				8	(1)	5	0.03
Heart	19				19	(1)	8	0.03
Intestine								
Duodenum	7	(2)		<0.60 T	7		2	0.03
Jejunum and ileum	20	(5)	5	0.92	20	(4)	6	0.02
Large	22				22	(2)	11	0.04
Kidney	24		24	31	24	(2)	4	0.04
Liver	24	(1)	22	3.3	24	(7)	4	0.03
Lung	24	(4)	7	1.1	24		23	0.14
Muscle	18				18	(1)	3	0.06
Pancreas	21	(7)	9	1.6	21	(2)	2	0.04
Prostate	8	(1)		<1.0 T	8	(1)	2	0.30
Spleen	22		1	1.3	22	(8)	5	0.05
Stomach	20	(2)		<0.64 T	20	(4)	6	0.03
Thyroid	8	(1)	2	1.9	8	(2)	3	0.06
	Cesium				Cobalt			
Adrenal	3				3		2	0.05
Aorta	12				12		2	0.12
Bladder	13	(1)	1	1.7	13			
Bone	23				23			
Brain	21				21			
Esophagus	8				8			
Heart	19				19		1	0.20
Intestine								
Duodenum	7				7			
Jejunum and ileum	20				20			
Large	22				22		1	0.12
Kidney	24	(2)		1.1 T	24	(1)		<0.11 T
Liver	24				24	(2)	4	0.12
Lung	24		12	3.1	24	(1)	3	0.22
Muscle	18				18			
Pancreas	21				21			
Prostate	8				8			
Spleen	22				22			
Stomach	20				20			
Thyroid	8		1	2.8	8		2	0.26

*The numbers in parentheses indicate the number of samples with a trace.

TABLE 17 (continued)

Tissue	Number of Samples		Average Value for Samples Containing Element (μg/g)	Number of Samples		Average Value for Samples Containing Element (μg/g)
	Analyzed	Containing Element*		Analyzed	Containing Element*	
	Copper			Iron		
Adrenal	3	3	1.1	3	3	28
Aorta	12	12	1.1	12	12	30
Bladder	13	13	1.1	13	13	19
Bone	23	23	0.69	23	23	95
Brain	21	21	4.8	21	21	44
Esophagus	8	8	1.3	8	8	32
Heart	19	19	3.1	19	19	46
Intestine						
Duodenum	7	7	1.5	7	7	48
Jejunum and ileum	20	20	3.0	20	20	32
Large	22	22	1.4	22	22	29
Kidney	24	24	2.9	24	24	76
Liver	24	24	5.7	24	24	170
Lung	24	24	1.4	24	24	210
Muscle	18	18	0.90	18	18	31
Pancreas	21	21	1.8	21	21	43
Prostate	8	8	1.9	8	8	25
Spleen	22	22	1.3	22	22	280
Stomach	20	20	1.5	20	20	24
Thyroid	8	8	1.2	8	8	69
	Gold			Lanthanum		
Adrenal	3	(1) 2	0.24	3		
Aorta	12	(2) 1	0.24	12		
Bladder	13	(1)	<0.16 T	13		
Bone	23			23		
Brain	21			21		
Esophagus	8	(2)	<0.19 T	8		
Heart	19	(1) 1	0.33	19		
Intestine						
Duodenum	7			7		
Jejunum and ileum	20	(1)	<0.18 T	20		
Large	22			22		
Kidney	24	(1)	<0.22 T	24		
Liver	24			24	(1)	<1.2 T
Lung	24			24	(3)	<1.1 T
Muscle	18			18		
Pancreas	21			21		
Prostate	8			8		
Spleen	22			22	(6)	<1.3 T
Stomach	20			20		
Thyroid	8			8		

*The numbers in parentheses indicate the number of samples with a trace.

TABLE 17 (continued)

Tissue	Number of Samples: Analyzed	Number of Samples: Containing Element*		Average Value for Samples Containing Element (μg/g)	Number of Samples: Analyzed	Number of Samples: Containing Element*		Average Value for Samples Containing Element (μg/g)
	Lead				**Molybdenum**			
Adrenal	3		3	0.08	3	(1)	2	0.17
Aorta	12	(1)	11	0.87	12			
Bladder	13	(1)	8	0.23	13			
Bone	23		23	4.2	23			
Brain	21	(5)	4	0.85	21		1	0.30
Esophagus	8	(2)	5	0.09	8			
Heart	19	(7)	4	0.68	19		1	0.30
Intestine								
Duodenum	7		5	0.10	7			
Jejunum and ileum	20		15	0.38	20			
Large	22	(6)	10	0.12	22		1	0.07
Kidney	24		24	0.94	24		24	0.33
Liver	24		24	1.5	24		21	1.1
Lung	24		24	0.63	24			
Muscle	18	(3)	2	0.09	18			
Pancreas	21		21	0.63	21			
Prostate	8	(5)	1	2.6	8		1	0.13
Spleen	22		21	0.38	22			
Stomach	20	(4)	14	0.14	20			
Thyroid	8	(2)	6	0.14	8			
	Manganese				**Nickel**			
Adrenal	3		3	0.15	3		3	0.50
Aorta	12		12	0.10	12		3	0.35
Bladder	13		11	0.10	13	(1)	3	0.29
Bone	23	(1)		<0.35 T	23		1	1.8
Brain	21		21	0.26	21		1	0.15
Esophagus	8		8	0.14	8		1	0.09
Heart	19		19	0.18	19	(1)	3	0.17
Intestine								
Duodenum	7		7	0.3	7	(1)		<0.08 T
Jejunum and ileum	20		20	0.43	20	(2)	4	0.34
Large	22		22	0.23	22	(2)	9	0.18
Kidney	24		24	0.56	24			
Liver	24		24	0.76	24		2	0.26
Lung	24		24	0.19	24		8	0.33
Muscle	18		18	0.06	18			
Pancreas	21		21	0.73	21		1	0.36
Prostate	8		8	0.30	8			
Spleen	22		22	0.13	22			
Stomach	20		20	0.25	20			
Thyroid	8		8	0.26	8		1	0.23

*The numbers in parentheses indicate the number of samples with a trace.

TABLE 17 (continued)

Tissue	Number of Samples: Analyzed		Number of Samples: Containing Element*	Average Value for Samples Containing Element (μg/g)	Number of Samples: Analyzed		Number of Samples: Containing Element*	Average Value for Samples Containing Element (μg/g)
	Silver				Tin			
Adrenal	3		3	0.03	3		3	0.24
Aorta	12	(2)	7	0.06	12	(1)	10	0.30
Bladder	13	(5)	3	0.008	13		11	0.20
Bone	23		1	0.4	23	(1)	1	3
Brain	21	(3)	17	0.03	21	(1)		<0.15 T
Esophagus	8	(1)	6	0.01	8		7	0.22
Heart	19	(7)	8	0.01	19	(2)	11	0.18
Intestine								
Duodenum	7	(3)	4	0.01	7	(1)	5	0.56
Jejunum and ileum	20	(6)	13	0.02	20	(1)	16	0.66
Large	22	(7)	10	0.01	22		21	0.78
Kidney	24	(5)	15	0.02	24	(2)	21	0.27
Liver	24	(7)	17	0.03	24	(1)	23	0.56
Lung	24	(11)	8	0.02	24		24	1.1
Muscle	18	(5)	3	0.02	18	(1)	1	0.12
Pancreas	21	(7)	10	0.02	21	(5)	6	0.20
Prostate	8	(2)	4	0.05	8	(2)	6	0.26
Spleen	22	(9)	5	0.06	22	(4)	15	0.27
Stomach	20	(4)	11	0.02	20		15	0.24
Thyroid	8	(2)	5	0.06	8		7	0.35
	Strontium				Titanium			
Adrenal	3		3	0.03	3		2	0.16
Aorta	12		12	0.20	12	(1)	2	0.48
Bladder	13		13	0.12	13	(1)	3	1.1
Bone	23		23	20	23			
Brain	21		21	0.07	21			
Esophagus	8		8	0.13	8	(2)	1	0.17
Heart	19		19	0.07	19			
Intestine								
Duodenum	7		7	0.12	7		1	0.08
Jejunum and ileum	20		20	0.15	20	(1)	2	0.46
Large	22		22	0.13	22	(1)	4	0.34
Kidney	24		24	0.08	24	(2)	5	0.67
Liver	24		24	0.04	24		2	0.50
Lung	24		24	0.13	24		24	2.8
Muscle	18		18	0.04	18			
Pancreas	21		21	0.08	21	(3)	3	0.36
Prostate	8		7	0.14	8		2	0.41
Spleen	22		22	0.06	22	(1)	4	1.0
Stomach	20		20	0.11	20	(2)		<0.08 T
Thyroid	8		7	0.17	8		4	1.20

*The numbers in parentheses indicate the number of samples with a trace.

TABLE 17 (continued)

Tissue	Number of Samples			Average Value for Samples Containing Element (μg/g)	Number of Samples		Average Value for Samples Containing Element (μg/g)
	Analyzed	Containing Element*			Analyzed	Containing Element*	
	Vanadium				Zinc		
Adrenal	3				3	3	7.8
Aorta	12	(1)		<0.10 T	12	12	16
Bladder	13				13	13	21
Bone	23				23		
Brain	21				21	21	14
Esophagus	8				8	8	23
Heart	19				19	19	29
Intestine							
Duodenum	7				7	7	16
Jejunum and ileum	20	(1)		<0.09 T	20	20	22
Large	22		1	0.34	22	22	19
Kidney	24	(1)		<0.11 T	24	24	48
Liver	24	(2)		<0.12 T	24	24	48
Lung	24	(4)	12	0.27	24	24	17
Muscle	18				18	18	53
Pancreas	21				21	21	31
Prostate	8				8	8	80
Spleen	22	(2)		<0.13 T	22	22	21
Stomach	20				20	20	19
Thyroid	8				8	8	28

*The numbers in parentheses indicate the number of samples with a trace.

SANITARY ENGINEERING RESEARCH

E. G. Struxness R. J. Morton

FIELD INVESTIGATIONS

K. E. Cowser F. M. Empson
W. de Laguna (USGS) H. J. Wyrick

Unlined Experimental Pit[1]

During the drilling of the auger holes around the unlined experimental pit, it was found that the depths of these holes were limited by a shale material at approximately 19 ft below the surface. In order to determine whether this shale would restrict in any unusual fashion the vertical movement of waste solutions in the pit, water-level recorders were installed on an existing core hole (UC43) cased through the shale and on an adjacent auger hole (UI) that terminated at the top of the shale. A continuous record of the water levels for a two-week period was obtained. The water-level fluctuations in these wells were compared with barometer response and with tide effect in another ORNL well. The fluctuations in levels in UC43 and UI do not appear to be tidal but rather to follow barometer changes. The changes in water levels in wells UC43 and UI were 11.5 and 12%, respectively, of the associated changes in barometric pressure. On the basis of this analysis, it would appear that the shale encountered will not create any unusual restrictive effect on potential vertical movements of chemical wastes in the pit.

Probe Development

The circuit of the trailer-mounted well-logging equipment was modified to improve the stability and operating characteristics of the assembly. Halogen-type G-M tubes are now in use in these units. To improve cable feed, a spring-loaded pulley which will apply pressure on the cable as it revolves over the existing feed pulley is being installed in one unit.

A portable deep-well scintillation probe has been obtained from the AEC New York Operations Office and will be tested in operations at ORNL.

Aerosol Entrainment Well

The entrainment-well experiment was originally designed to evaluate the evolution and entrainment of radioactive aerosols in the Hope-type waste-disposal pit. This objective has been altered to obtain more general data on the filtration of aerosols arising from hot and boiling radioactive liquids. The installation is shown in Fig. 8. A second thermocouple is located at the center of the entrainment well, coinciding in this view with the heater conduit. Each thermocouple well contains seven thermocouples spaced equally through the 20-ft depth of the well. The thermocouple wells and the heater conduit are maintained under a positive nitrogen pressure to prevent leakage of water into the system. The thermocouple wells and heater assembly are of welded construction.

In operation, the entrainment well will be maintained under a slight negative pressure by a vacuum pump. Radioactive aerosols, carried by water vapor and some air from the vent, will flow to the condenser and cold trap. The filter test unit installed ahead of the condenser will allow study of the effectiveness of various filter materials. The filter unit may be bypassed for study of the formation of aerosols.

Preliminary tests have been made of entrainment at temperatures below boiling. A dilute solution of $K_2^{42}CO_3$ was heated in the well, and the vapor was condensed. The results are tabulated in Table 18. The extremely low decontamination factors shown here led to the laboratory study of the evolution of K^{42} described in a later section.

Future work will include an evaluation of sand and glass fiber for removal of radioactive aerosols at superficial velocities approaching 0.002 cm/sec and a study of the entrainment of radioactive aerosols from both hot and boiling solutions.

Pilot Pit No. 1

Pilot pit No. 1 is designed as the first step in the field-scale testing of a method for radioactive waste disposal which involves fixing and fusing of the radioactive material in an insoluble ceramic mass. It is proposed to add shale, limestone, and soda ash to high-level-waste solutions. This will form a mass which will be sintered at a temperature of 500 to 900°C by self-heating. Successful laboratory-scale tests were made by the Ceramics Group of the Metallurgy Division. These were

[1] R. J. Morton *et al.*, *HP Semiann. Prog. Rep. Jan. 31, 1955*, ORNL-1860, p 14.

nonradioactive experiments in which electric heat was used.

Pilot pit No. 1 (Fig. 9) will be a concrete tank, 6 ft in diameter and 10 ft deep and composed of precast sections, within a larger tank built of concrete silo blocks; the design has been completed and construction has begun. The tank will be insulated by 18 in. of foam-glass blocks on the

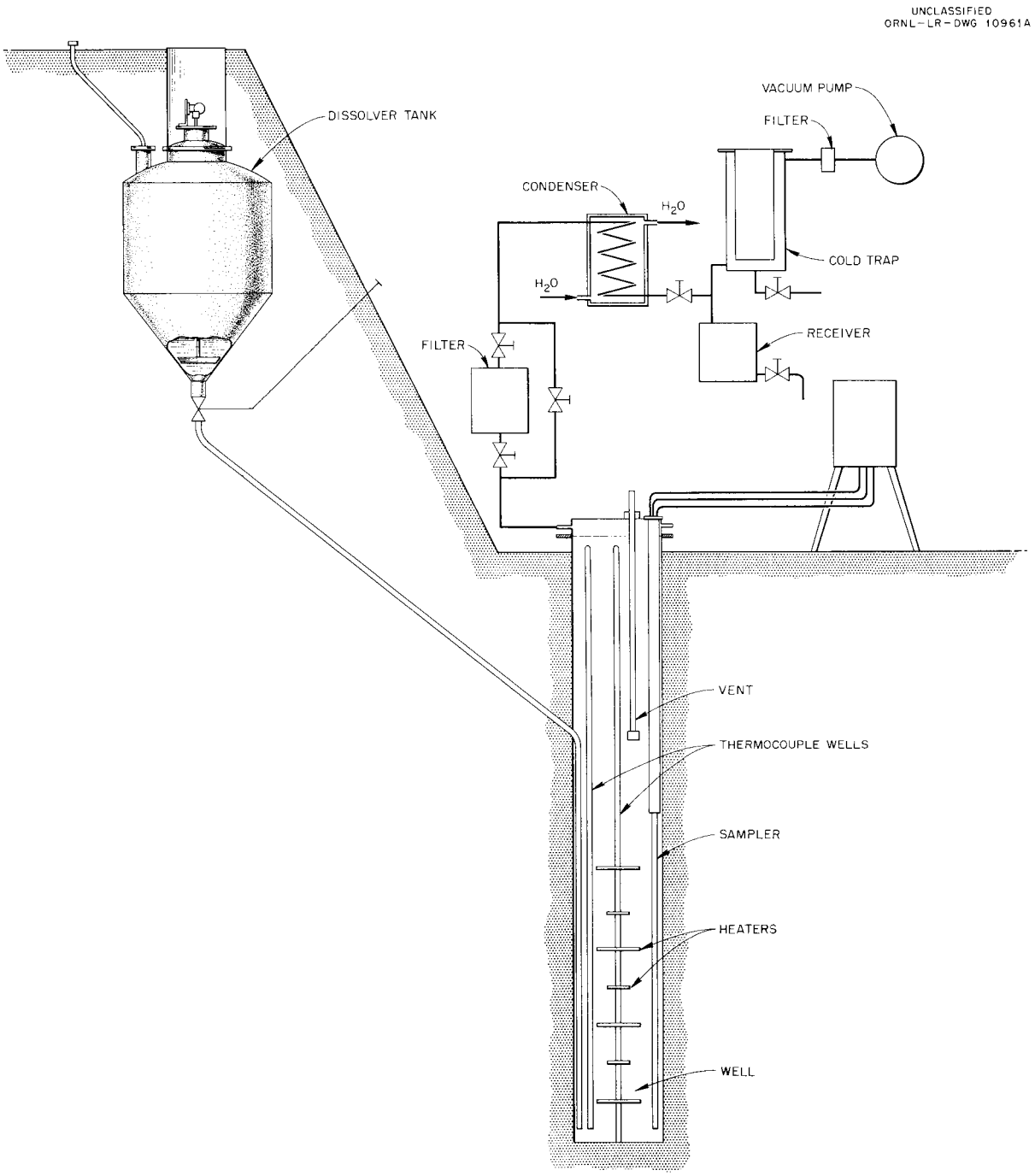

Fig. 8. Schematic Elevation of Dissolver Tank and Entrainment Well.

TABLE 18. ENTRAINMENT BY EVAPORATION-ENTRAINMENT WELL

Well		Condensate Activity (counts/min/ml)	Decontamination Factor
Temperature (°C)	Activity (counts/min/ml)		
90–100	856	1.340	6.39×10^2
86	8514	1.35	6.3×10^3
91	8514	2.47	3.44×10^3
95	8514	63	1.35×10^2

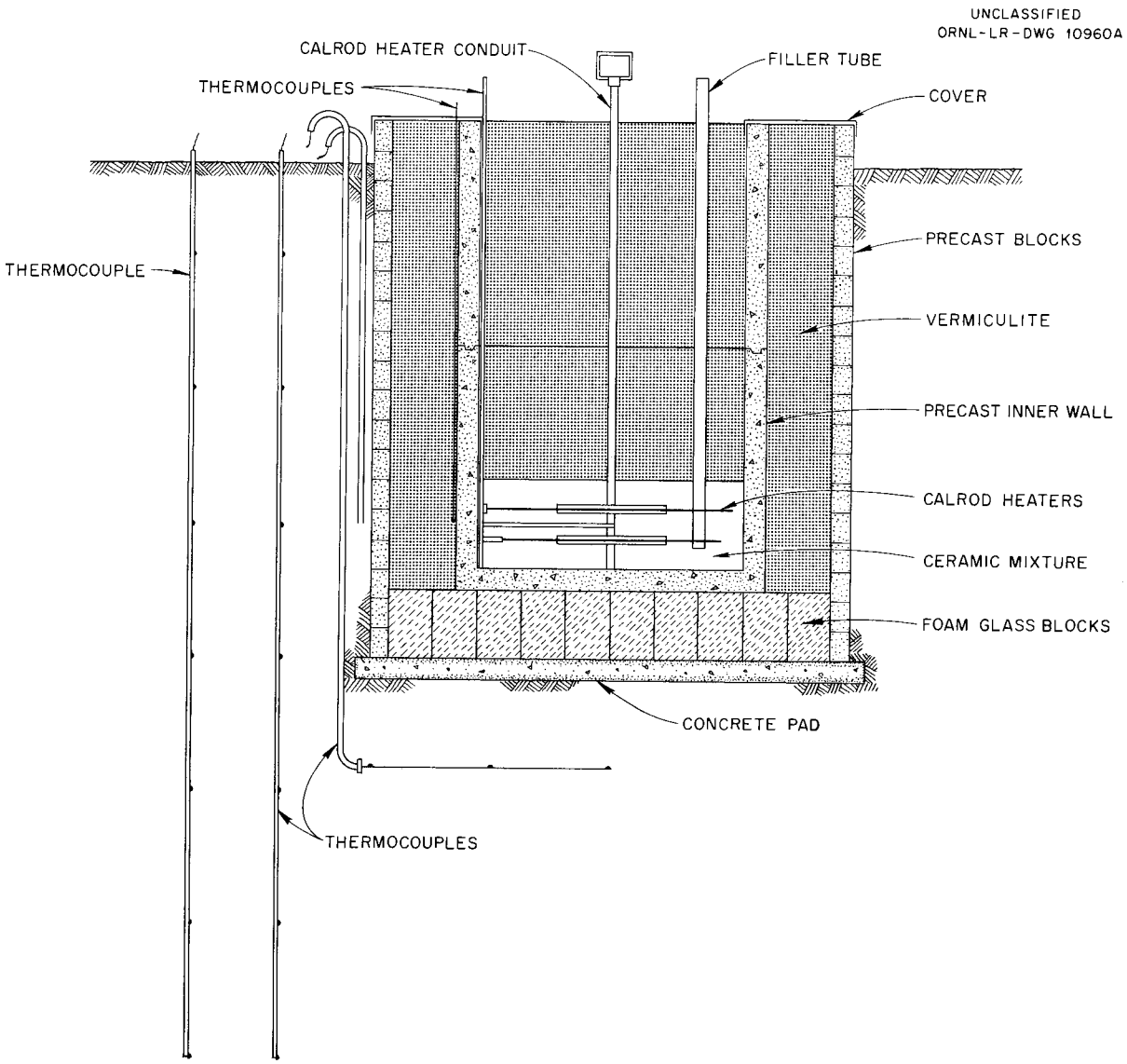

Fig. 9. Pilot Pit No. 1.

bottom and 18 in. of vermiculite on the sides. This insulation is needed for sufficiently high operating temperatures to be obtained. Electric heat, to simulate the self-heating of radioactive waste, will be added through Calrod heaters located near the bottom of the inner tank. Thermocouples will be located on the heaters, in the ceramic mixture, between the tanks, and in the earth outside the outer tank. They will be used to determine temperatures during operation of the pit and to obtain heat transfer data. The entire inner tank assembly can be removed to permit use of the facility for more than one experiment.

In this experiment a mixture of 2405 lb of shale, 720 lb of soda ash, 720 lb of limestone, and 720 gal of simulated acid aluminum nitrate waste solution will be placed in the pit and heated. The water will evaporate first; then nitrogen oxides will be given off. When all the water has evaporated, a bed of vermiculite will be added over the dried ceramic mass to insulate the upper surface for the final sintering of the mass. The first run will not include the use of mixed fission products but will test only the sintering process.

Chemical Waste Storage Pits

To facilitate understanding of the operation of the chemical waste pit system, a more detailed material balance was initiated to include chemical, radiochemical, and liquid components of the wastes. The physical arrangement of the system is shown in Fig. 10. The numbered circles show the location of wells which were drilled to provide geologic and hydrologic information and which are used as observation wells to detect underground movement of wastes. The relative locations of the waste pits, of the discharge pipe through which wastes are pumped to the pits, and of the overflow pipes between pits are as indicated. Wastes are pumped directly to pit 3, and after completion of pumping they are transferred to pit 2 through a valved overflow pipe. Pit 2 may be overflowed to pit 4, which was constructed during November 1955 but has not yet been used.

Liquid Inventory. – Seepage from the pits is of primary interest. However, the total liquid budget of the pits includes additions by waste-pumping and rainfall and losses by evaporation as well as by seepage. Through a cooperative project of the U.S. Weather Bureau, U.S. Geological Survey, and ORNL a study of the evaporation component of the loss has been undertaken at the pit sites. The meteorological data necessary for computing evaporation by the mass-transfer method must include measurements of air and liquid temperature gradients, wind speed gradients, and humidity, for which equipment has been procured and is being installed. Two circular, sunken, 5-ft-dia evaporation pans, one unscreened and containing water and the other screened and containing a simulated waste solution, have been installed to empirically determine rate of evaporation.

A comparison of records taken from continuous-stage recorders in pit 3 and in the unscreened evaporation pan suggests that the evaporation rates from the pit and the pan are much the same. An example of the data showing the comparison is given in Table 19. The seepage estimate corresponds to a daily loss of 1200 gal from pit 3. Less detailed records from pit 2 suggest a daily seepage rate of 3200 gal. These figures are subject to correction as more detailed data are obtained. To improve the accuracy of the recording of the liquid stage in pit 3, the recorder was mounted directly over the stilling well.

Chemical and Radiochemical Inventory. – During 1955, 1,620,000 gal of waste containing 21,340 curies of beta activity was pumped to pit 3. A comparison of gross-beta activity in composite samples of the waste added to pit 3 and of the

TABLE 19. PRELIMINARY ESTIMATE OF EVAPORATION AND SEEPAGE LOSS

Time	Pit Stage Decrease (ft)	Pan Stage Decrease (ft)	Estimated Seepage Loss (ft)
August 19–26	0.165	0.09	0.075
September 2–9	0.165	0.09	0.075
December 27–January 3	0.085	0.015	0.070

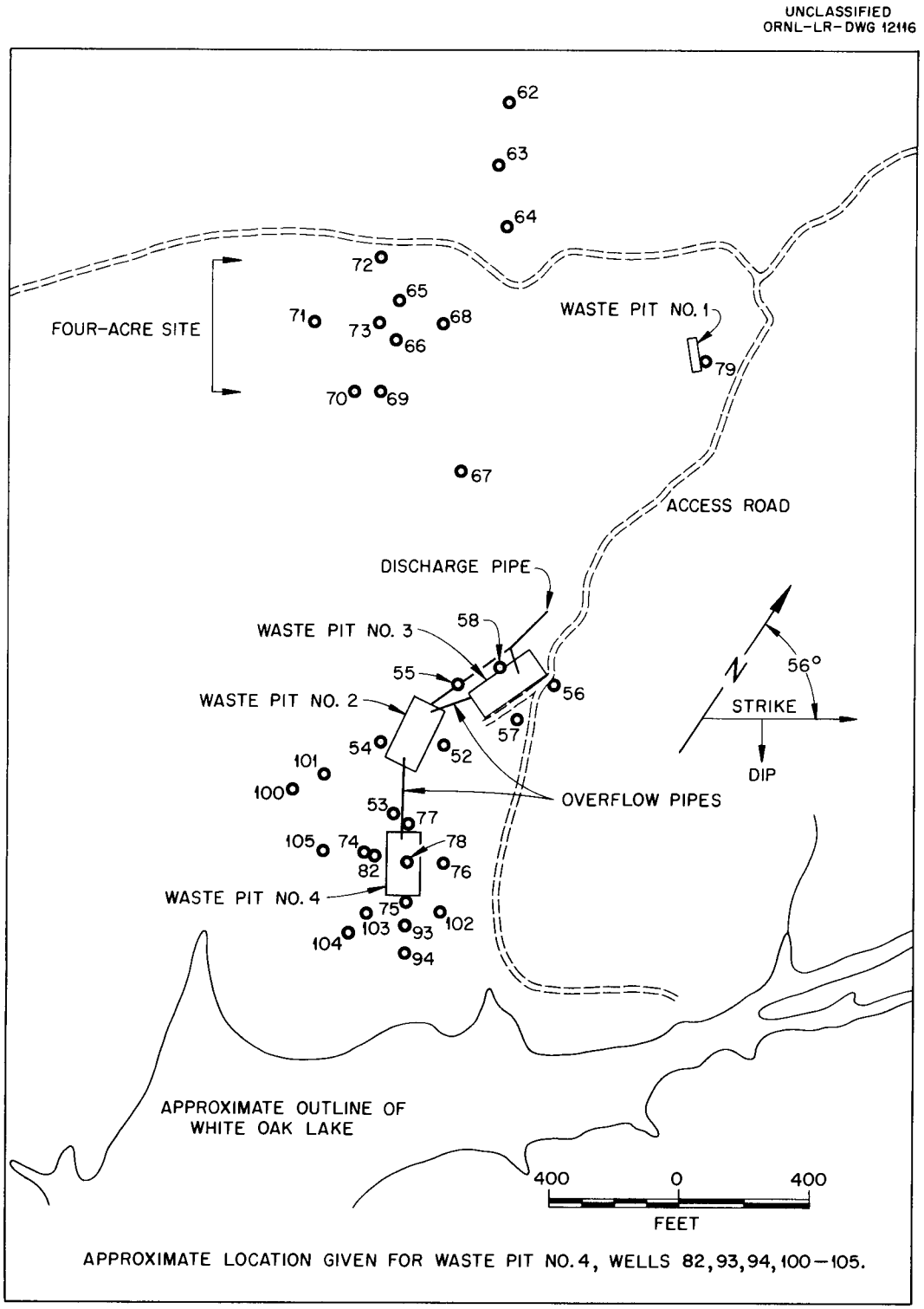

Fig. 10. Waste-Pit Disposal Area.

waste overflowed to pit 2 has shown that the levels of activity were reduced by a factor of approximately 2 as the waste passed through pit 3. Judging by the gross-beta analyses and the volume of waste overflowed, an estimated 2500 curies of beta activity was transferred by overflow to pit 2. The first composite samples were analyzed for the cations Na, Al, and NH_4, the anions Cl, NO_3, and SO_4, the radionuclides Cs^{137}, Ru^{106}, Sr^{90}, and the trivalent rare earths. The above stable elements accounted for 80% of the total solids present and the radionuclides accounted for 90% of the gross-beta activity.

Definition of Underground Contamination. – The study[2] for defining the vertical configuration of waste flow through the soil formations has suggested need for the prevention of direct access of wastes to the observation well. This will assist in interpretation of radiologs by eliminating the influence on probe response of variations in hole diameter, waste stratification, and activity sorption on the side wall of the hole. With assistance of TVA personnel a casing was grouted in place in well No. 82, as shown in Fig. 11. The pattern of waste intercepted by this well will be compared with that of ungrouted well No. 74 to determine the differences of probe response under these varying conditions.

[2] R. J. Morton *et al.*, *HP Semiann. Prog. Rep. July 31, 1955*, ORNL-1942, p 14.

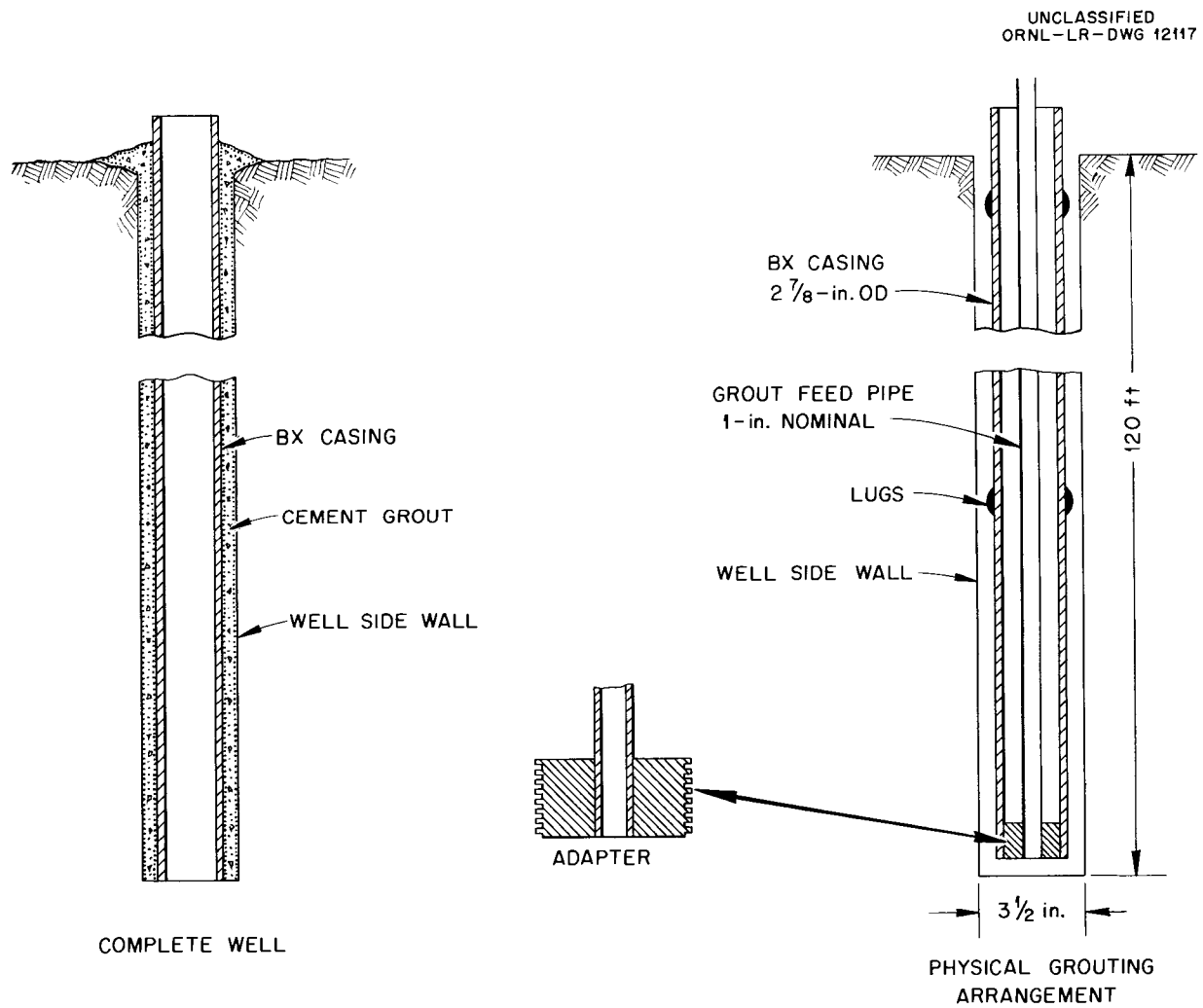

Fig. 11. Details of Grouted Well No. 82.

There has been no observable down-dip movement of radioactive wastes from pit 3 into well 57, which is located so as to detect any such bedding plane influence. Contamination was intercepted by this well after approximately four months of pit operation and was found to extend to a depth of 10 ft below the liquid level in the well.

Wells 100 and 101 were core-drilled in an underground-contaminated area adjacent to pit 2 to delineate the contamination pattern and to allow water-level measurements for use in the preparation of a water-table contour map of the area. From samples collected while wells 100 and 101 were being drilled, it is estimated that 8 and 13 mc of Ru^{106}, respectively, were discharged with the drilling water to a White Oak Lake contributory. This amounts to less than 0.5% of the total activity discharged from the X-10 area to the Clinch River during this same period. The concentration of Ru^{106} in the drilling water exceeded the maximum permissible concentration value of 1×10^{-4} $\mu c/ml$ for approximately 5 hr. The highest concentration of activity encountered was 4×10^{-3} $\mu c/ml$ from well 101, which subsequently has revealed concentrations as high as 6×10^{-2} $\mu c/ml$. All smears of the drilling equipment, taken over surface areas of 100 cm^2, were found to be below 10 $d/min/cm^2$, which is below the allowable surface contamination limit.

To determine the variability of data obtained with the well-sampling equipment employed, duplicate samples were collected from nine different depths in one well and four different depths in another well. The results indicate a precision, as measured by the standard error computed from duplicate samples, of 14.7 counts/min/ml, applicable over a range of counts from 230 to 690 counts/min/ml.

Hydrology and Geology

Four-Acre Site. – A pumping test was conducted by using a tracer solution consisting of 50 lb of $NaNO_3$, 50 lb of NaCl, 100 gal of methanol, and 100 gal of water. The tracer was introduced into well 71, which is located along the strike from the center well 73, which was pumped at a rate of 1 gpm. The tracer first showed up after 70 hr of pumping, or after 4200 gal of water had been pumped. About 8.7% of the chloride had been pumped through after 282 hr, or after about 17,000 gal had been pumped. About an equal proportion of the nitrate also came through, but, since it appeared in a somewhat erratic pattern, the chloride was judged to be the better tracer. From the shape of the arrival curve (quantity of tracer plotted against time of pumping), it was estimated that the average arrival time for the tracer would have been of the order of 1000 hr, or after 60,000 gal had been pumped. Although the test results are incomplete, they confirm to some degree the impression that water movement is largely in the direction of the strike and that the porosity of the formation is low. The big difference between the time of first arrival and the estimated average arrival time clearly implies that some of the movement of liquid in the rock is along fairly direct channels as compared with the paths followed by most of the liquid. A large safety factor must therefore be applied to any rate of travel estimated on the basis of the average hydrologic properties of the shale. Since the tracer can be moved through 200 ft of shale after only 4200 gal has been pumped, waste can make the reverse journey under similar conditions.

Chemical Waste Pit No. 4 Site. – The first group of wells in this area, prior to the construction of the pit, consisted of a central 6-in. churn hole 300 ft deep (well 78) and four core holes 200 ft deep (wells 74, 75, 76, and 77) equally spaced on the circumference of a circle 125 ft in radius. Pumping of well 78 produced markedly different responses in the observation wells. Wells 74 and 76, located along the strike from the central well, showed much the same drawdown pattern. Substitution of the data in the Theis nonequilibrium formula gave a value for the transmissibility of the formation of about 100 gpd/ft, but the validity of the procedure and the meaning of the result are open to question.

Well 75, located down dip, had a much larger drawdown than did the wells along the strike. An anomalous drawdown of this sort in one particular well is subject to several interpretations, among which would be the following:

1. The pumped well may be obtaining more water from the vicinity of this well because the permeability is greater in this direction.
2. The pumped well may be drafting the same amount of water from this direction as from other directions, but the porosity (that is, the water-holding capacity) in this area may be less.
3. The pumped well may draft equal amounts of water from the vicinity of all observation wells,

with a uniform porosity, but there may be an outlying barrier to the movement of ground water (just beyond well 75) which prevents the inflow of water to this particular observation well.

4. The large drawdown may be due to a pressure effect, with the amount of water actually removed being small and even immaterial.

Because the beds originally were thought to dip to the southeast in this area it seemed possible that the large drawdown in this well was a pressure effect. If so, the pressure changes should be more marked in the lower part of well 75, which intercepts beds that are also cut by the pumped well. To test this possibility a packer was set at a depth of 101 ft, just above the deepest large opening as determined by pressure testing. Drawdowns observed in the upper and lower portions of the well, while well 78 was being pumped, showed the more rapid response and larger drawdown in the upper part of the well. This suggests, but does not prove, that the drawdown is due to the more rapid removal of water from this direction.

The response in well 77 during the early part of the pumping test was apparently due to pressure effects. The water level in this well rose about 0.4 ft in the first 8 hr of pumping, and then fell a total of 1½ ft during the next four days. When the pump was shut off, the water level fell about 0.4 ft in the first 8 hr and then recovered in a normal fashion. A reverse response, somewhat similar in its anomaly, was observed in one of the wells in the Four-Acre Site during several pumping tests, although the magnitude and duration of the anomaly were smaller and shorter. Although not yet explained, two facts appear to bear on the condition of the pit 4 site. The first is an abrupt 10-ft difference in the elevation of the water table, which stands higher in well 77 and in the adjacent, older well 53 than it does in the observation wells to the southwest, south, and southeast. This suggests that the movement of the ground water is blocked by a barrier extending northeast-southwest past the northwest end of the pit. The second fact is the geologic structure which came to light when the pit was dug. The beds of shale exposed in the pit are in contorted, small, tight folds. This type of structure ends abruptly at the northwest end of the pit; northwest of this the shale is in uniform beds which dip to the southeast at about 30 to 35 deg. These relations suggest that the folding in the pit area forms a barrier to the movement of ground water, that in some way it is responsible for the anomalous water-level fluctuations in well 77 during test pumping, and that it may be the cause of the large drawdown in well 75. If this folding is a barrier to ground water movement, it may also be the cause of the radioactive seep southwest of pit 2, for this seep appears about on the strike of the structure.

Water Decontamination Study

Ion-exchange materials and processes on a laboratory scale have been used effectively for removing radioactive ions from contaminated water. Therefore a study was undertaken to determine the influence of various factors on resin capacity for hardness and on the per cent removal of Sr^{89}.

In all studies on the hydrogen cycle Amberlite[3] IR-120 was used as the exchange material and Sr^{89} was employed as the radioactive tracer. This tracer was contaminated with about 2% of Sr^{90}-Y^{90}. Oak Ridge tap water was used, and a standard ion-exchange column operating procedure was followed. Graph I of Fig. 12 indicates that there is a decrease in resin capacity when the flow rate is increased. The plot also contains a bar graph of the average per cent removal until breakthrough (the point at which 1 ppm of the tracer appears in the effluent). Increased flow rate only slightly decreases the efficiency of removal of Sr^{89}. Graph II shows the influence of exchange-resin depth or of column length on capacity for and removal of radiostrontium. It can be seen that the breakthrough capacity (in kilograins per cubic foot) becomes greater with increasing length of column.

The total capacity, the total number of exchanging groups in the column, and the breakthrough capacity (number of milliequivalents or kilograins retained until a leakage of 1 ppm is observed) in percentage of the total capacity all increase when the column length is increased.

The influence of resin particle size on hardness capacity and removal of Sr^{89} was investigated by using for comparison the same resin, bed diameter, pH, and rate of flow that were used in the previous experiments. About 60% of the commercial technical grade resin is of 30-mesh size. The range of particle sizes used was U.S. Standard Sieve 20,

[3] Amberlite is the registered trade mark of the Rohm and Haas Co., Philadelphia, Pa.

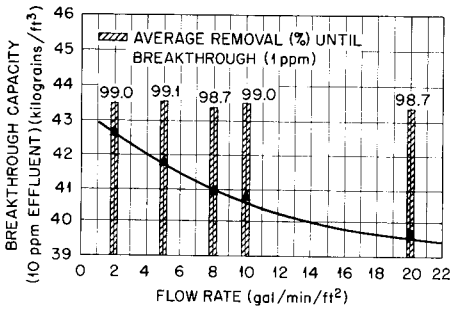

I. FLOW RATE

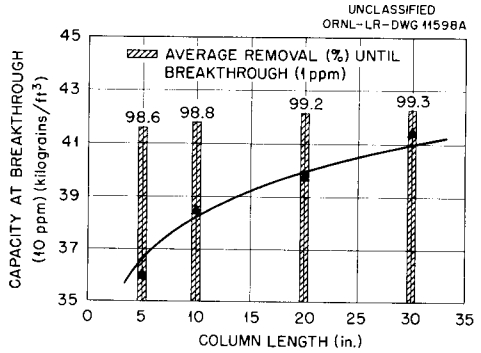

II. COLUMN LENGTH

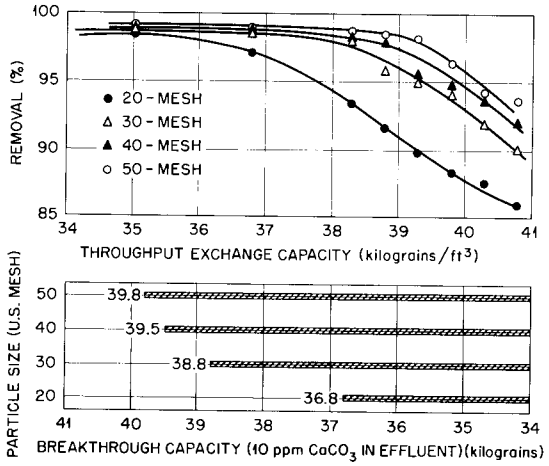

III. RESIN PARTICLE SIZE

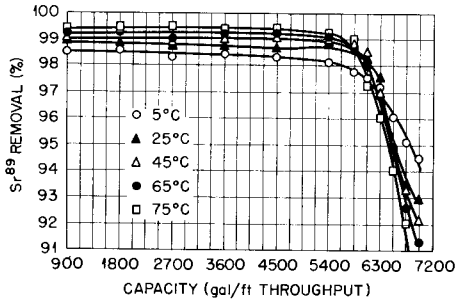

IV. TEMPERATURE OF FEED SOLUTION

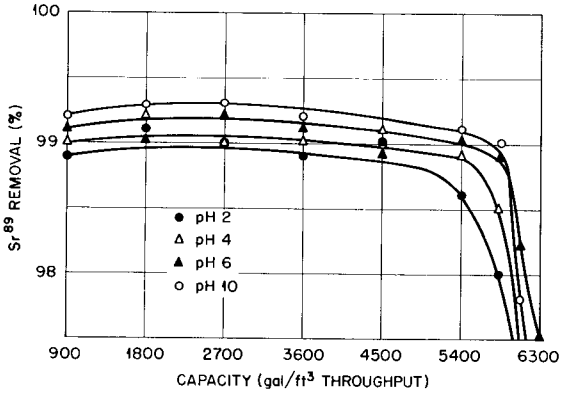

V. ACIDITY OF FEED SOLUTION

Fig. 12. The Influences on Calcium Carbonate Capacity and Sr^{89} Removal.

30, 40, and 50 mesh. Graph III shows that the hardness capacity and the radiostrontium removal increase with decreasing resin particle size.

In the next series of tests the influence of feedwater temperature on the capacity of the ion-exchange resin for calcium carbonate and on the effectiveness of removing Sr^{89} from aqueous solutions was investigated. The tests were made by using the procedure followed in the previous experiments and changing only the temperature of the feed solution. Graph IV on temperature effects indicates that increased temperature of the feed solution resulted in a slightly higher removal of Sr^{89} and a sharper breakthrough of hardness.

The fifth parameter studied in these tests was the effect of hydrogen ion concentration (acidity) of the feed solution on the calcium carbonate capacity and per cent removal of radiostrontium-89. The range of pH values studied was from 2 to 10.

It can be seen from Graph V that within the range of hydrogen ion concentrations studied there is a slight increase in the efficiency of removal of Sr^{89} with increasing pH. The increasing pH of the feed solution also increases the hardness capacity of the resin studied.

These are not the only parameters that should be considered during the operation of an ion-exchange process. The quantitative results reported here are applicable to only the particular cationic resin studied under the test conditions. However, the experimental results are qualitative for the general class of resins of this type.

CHEMISTRY AND SOILS ENGINEERING

C. P. Straub (USPHS)
B. Kahn (USPHS)
A. Rudnick (USPHS)
E. R. Eastwood
M. I. Goldman (USPHS)
H. L. Krieger (USPHS)
W. J. Lacy (ERDL)
M/Sgt. R. R. Rollins (ERDL)

Chemical Laboratory Studies

In April 1955 Hahn and Straub[4] published procedures for the identification of radiostrontium and radiobarium in natural waters. The development of methods for identifying radioisotopes present at low concentrations has continued, and procedures for cesium, yttrium, zirconium, niobium, and the lanthanide fission products are being evaluated. Cesium may be concentrated and separated from mixed fission products by means of phosphomolybdate or cobaltinitrite precipitation techniques. A bismuth phosphate procedure for the separation and identification of zirconium and niobium is under study, and a solvent extraction procedure is being tried for the separation of low concentrations of yttrium and the lanthanide fission products. These procedures are followed by standard radiochemical separation, which gives further purification.

Some preliminary findings in the use of solvent extraction procedures for the separation of the fission products from an acid aluminum nitrate waste solution are summarized in Table 20. Cesium

[4] R. B. Hahn and C. P. Straub, *J. Am. Water Works Assoc.* 47:4, 335–340 (1955).

TABLE 20. EXTRACTION OF FISSION PRODUCTS FROM 50-ml ACID $Al(NO_3)_3$ SOLUTION INTO FOUR CONSECUTIVE 5-ml PORTIONS OF ORGANIC SOLUTIONS

Radionuclide	Solvents Used	Cumulative Activity Extracted (%)			
		1st Pass	2nd Pass	3rd Pass	4th Pass
Sr^{90}	100% TBP*	6.3	7.6	13.7	15.2
Y^{90}	100% TBP	96.8	97.5	99.0	99.6
Ru^{106}	100% TBP (9 months old)	79.9	89.3	94.7	96.0
Ru^{106}	100% TBP (new solution)	66.7	75.3	77.1	79.4
Ce^{144}	100% TBP	94.7	99.6	99.98	99.99
Zr^{95}	0.5 *M* TTA** in benzene	95.5	96.0	96.0	97.6
Total Zr^{95}-Nb^{95}	0.5 *M* TTA in benzene	91.1	93.9	95.1	95.9
Cs^{137}	TTA or TBP	0	0	0	0

*TBP – tributylphosphate. **TTA – thenoyltrifluoroacetone.

and strontium are not removed by solvent extraction following four passes of either thenoyltrifluoroacetone (TTA) or tributylphosphate (TBP).

Soils and Engineering Studies

Typical results of passing an aqueous solution containing fission radionuclides through a column of Conasauga shale are shown in Fig. 13. These values were obtained with the solution adjusted to a pH of 2.3. It will be seen that the strontium moves most rapidly through the soil mass; that is, it is adsorbed more slowly than the other indicated ions. The effect of pH of the solution on removal of cesium by Conasauga shale is shown in Fig. 14. As the pH is increased from 1.5 to 5.0 the amount of soil required per milliliter of waste solution decreases.

The effect of an acid aluminum nitrate waste and of a neutralized sodium aluminate waste on a Tennessee ball-clay liner material has been under investigation for several months. The changes taking place may be noted from an examination of Figs. 15 and 16. Figure 15 indicates the appearance of the liner material as set in a model flume on November 10, the start of the test, and Fig. 16 shows the appearance of the liner material on December 21. Continued observation since November 10 has indicated spalling of the clay liner in contact with the acid medium and a discrete cracking of the clay liner in contact with the alkaline medium. Crystallization at the leakage

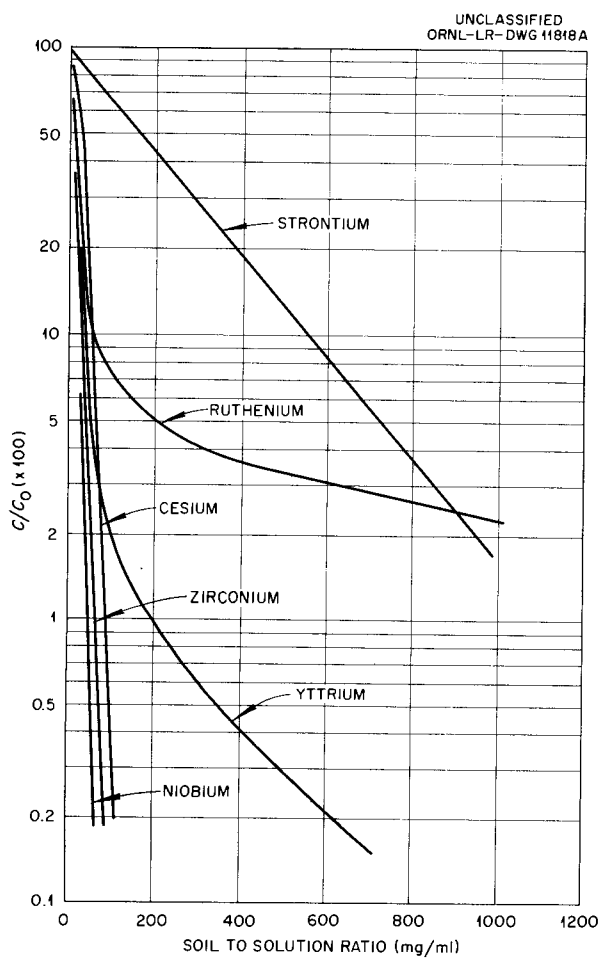

Fig. 13. Removal by Conasauga Shale of Specific Radionuclides from an Aqueous Solution (pH 2.3) Containing Mixed Fission Products.

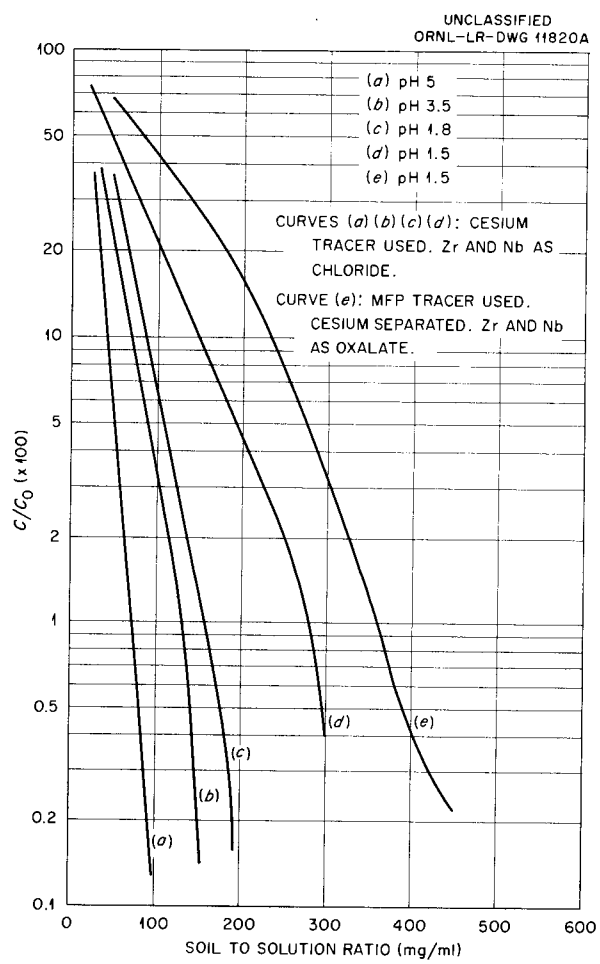

Fig. 14. Effect of pH on Uptake of Cesium from Aqueous MFP Solution by Conasauga Shale.

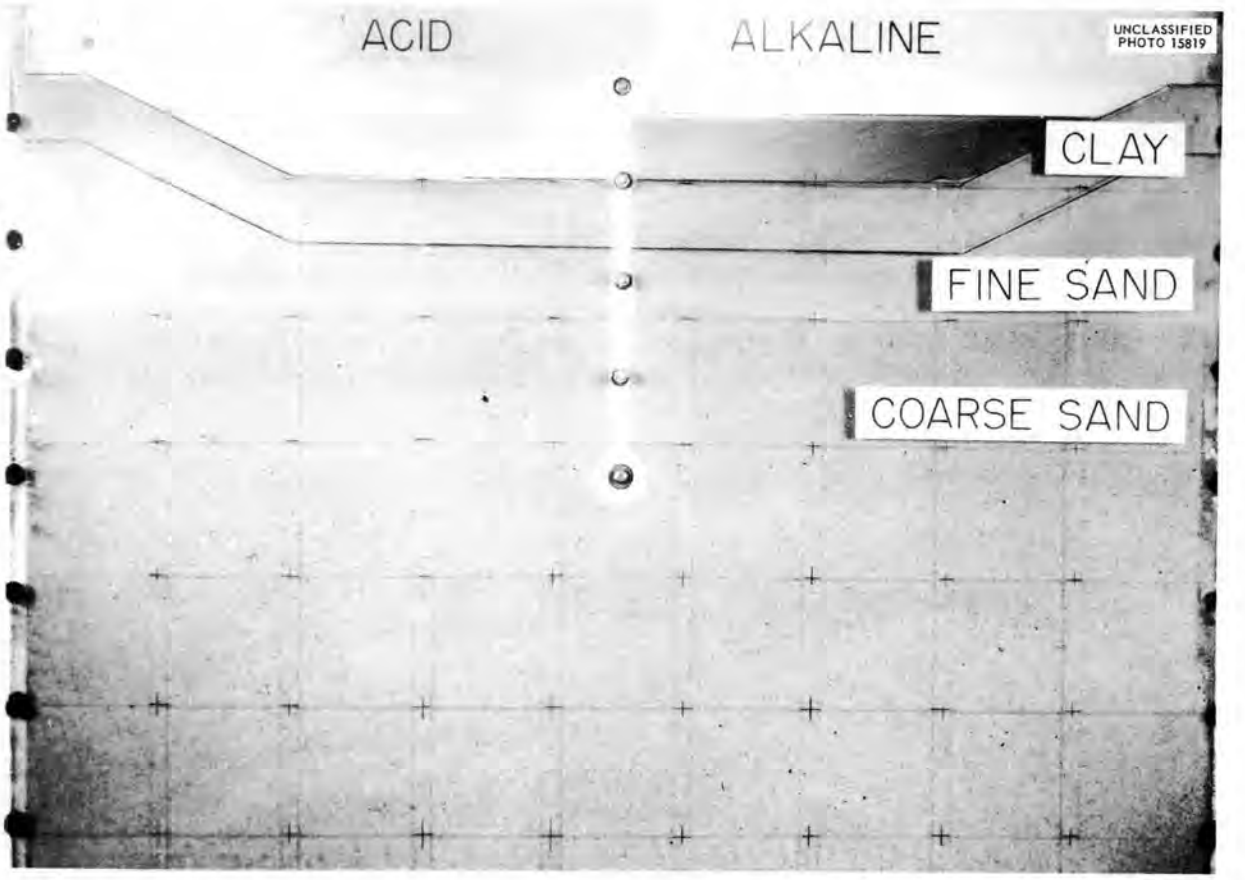

Fig. 15. Appearance of Liner at Beginning of Test – November 10, 1955.

sites and the presence of dye tracer in the underlying sand are further indications of the deterioration of the clay liner in contact with the alkaline wastes. The studies are being continued to determine the significance of the above observations upon the permeability of the liner material and upon its useful life.

AIRBORNE-RADIOACTIVITY STUDIES

J. W. Thomas
F. M. Empson
R. E. Yoder
F. W. Sanders

Evolution of K^{42} from Hot and Boiling Solutions

In a study of the evolution of K^{42} from hot and boiling solutions, air was bubbled through a solution of $K_2^{42}CO_3$ at room temperature with the use of both fritted-disk and open-end bubblers. The decontamination factor is defined as the activity per milliliter of K_2CO_3 solution divided by the activity per milliliter of air. The concentration of K_2CO_3 and the air flow rate were varied through the ranges indicated in Table 21.

The data in Table 21 indicate that increased K_2CO_3 concentration, increased bubble size, and decreased flow rate result in a higher decontamination factor.

Preliminary tests at the aerosol entrainment well indicated that K^{42} was being evolved at a temperature below the boiling temperature of the solution. To get confirmation of these results, dry filtered air was blown across the surface of a hot $K_2^{42}CO_3$ solution in a flask and then passed through a Liebig condenser to remove the entrained material. The flow rate of air used was 4 liters/min. For some runs the solution was acidified with HCl. The decontamination factors, which in this case were defined as the activity per milliliter of K_2CO_3 solution divided by the activity per milliliter of condensate, are listed below. The data indicate

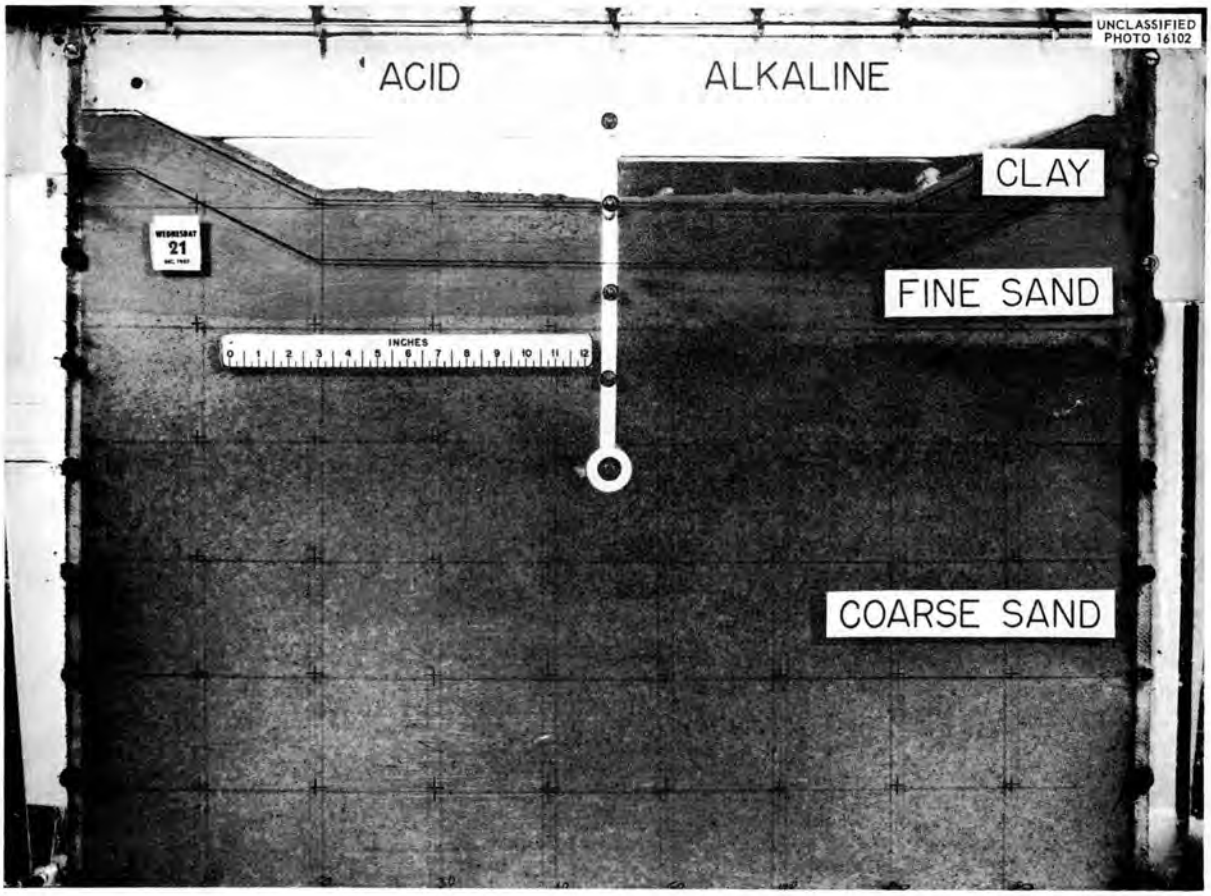

Fig. 16. Appearance of Clay Liner after Six-week Contact with Either Acid Aluminum Nitrate or Sodium Aluminate Solutions.

that lower pH or higher temperature results in a lower decontamination factor.

Temperature (°C)	Decontamination Factor	
	Basic Solution	Acid Solution
90	2.0×10^7	2.6×10^6
98		4.9×10^5
Boiling	3.1×10^5	3.6×10^4

Sand Filters

The main objective of the sand-filter work is to study the removal of aerosols generated in pits containing high-level radioactive wastes. The gas

TABLE 21. RELATION OF CONCENTRATION AND FLOW RATE TO DECONTAMINATION

K_2CO_3 Concentration (mg/ml)	Flow Rate (ml/min)	Decontamination Factor
Fritted-Disk Bubbler		
0.006	500	0.98×10^7
800	500	5.9×10^7
165	150	3.7×10^7
165	4000	0.38×10^7
Open-End Bubbler		
165	500	5.0×10^9
165	4000	3.0×10^9

velocity in the filter is expected[5] to be 0.002 cm/sec. The lowest gas velocity through sand filters attained so far in the laboratory has been 0.054 cm/sec.

Two types of sand have been studied: Pennsylvania sand, used for sand blasting, and the Clinch River sand. The grains of these two sands showed variations in filtration which were probably due to different grain shapes. The Pennsylvania sand was separated into fractions collected on screens numbered 12, 16, 20, and 30. The Clinch River sand was collected on screens numbered 20, 30, 35, 40, and 50. A number 8 screen was the largest sieve used. The sieved sand was placed in columns 5½ in. in diameter; the columns varied in height, by incremental factors of 2, from 1½ to 12 in.

The aerosol penetrations through the sand column are determined as a function of gas velocity, particle radius, and sand grain size. Figure 17 shows data taken on both types of sand under comparable conditions. The size of the sand grain (Dg = grain diameter) is determined by taking the mean value of the openings of the collecting and preceding screen.

[5]R. A. Charpie *et al.*, ORNL-1638 (Jan. 21, 1954). (Secret)

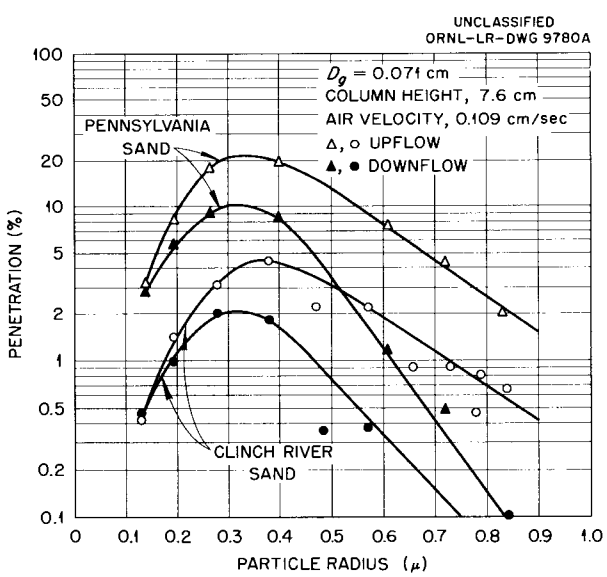

Fig. 17. Aerosol Penetration of Pennsylvania and Clinch River Sands.

The Pennsylvania sand gives penetrations as much as five times greater, at the size for maximum penetration, than the Clinch River sand. The void fraction, or the ratio of the interstitial volume to total volume, is approximately the same for both sands: 0.41 for the Pennsylvania sand and 0.385 for the Clinch River sand. Microscopic examination of the sand grains showed the Pennsylvania sand to have a smooth surface, even though it is an angular sand with a prismatic shape. The Clinch River sand was not so angular but had a much rougher or porous surface. The data indicated that the rougher the collecting sand grain, the greater its efficiency as an aerosol filter.

Figure 18 was plotted from the Clinch River sand data for the largest sand grain fraction, Dg = 0.161 cm, and the smallest sand grain fraction, Dg = 0.036 cm. The advantage of using a small-grained sand is clearly indicated. At the aerosol size for maximum penetration, 0.109 cm/sec, the largest sand grain fraction gives penetrations 100 times greater than the smallest sand grain fraction at the same velocity.

The expression for the filtration of aerosols by sands initially takes the form of the equation

$$C = C_0 e^{-Kz} ,$$

where

C = effluent concentration of aerosol from the filter,
C_0 = influent concentration of aerosol to the filter,
K = attenuation function,
z = column height.

Recent data indicate that the value of K as presented in a previous report[6] should be modified. These data indicate that the accuracy can be expressed to ±15% if

$$K = \frac{10^{-3}}{Dg} (1 - \alpha)\frac{l}{r}\left(1 + \frac{0.087}{r}\right) \times (2.09\, V^{-0.57} + 22\, V^{-0.78}\, r^3) ,$$

where α is the void fraction and V is the superficial velocity.

[6]E. G. Struxness *et al.*, *HP Semiann. Prog. Rep. July 31, 1955*, ORNL-1942, p 19.

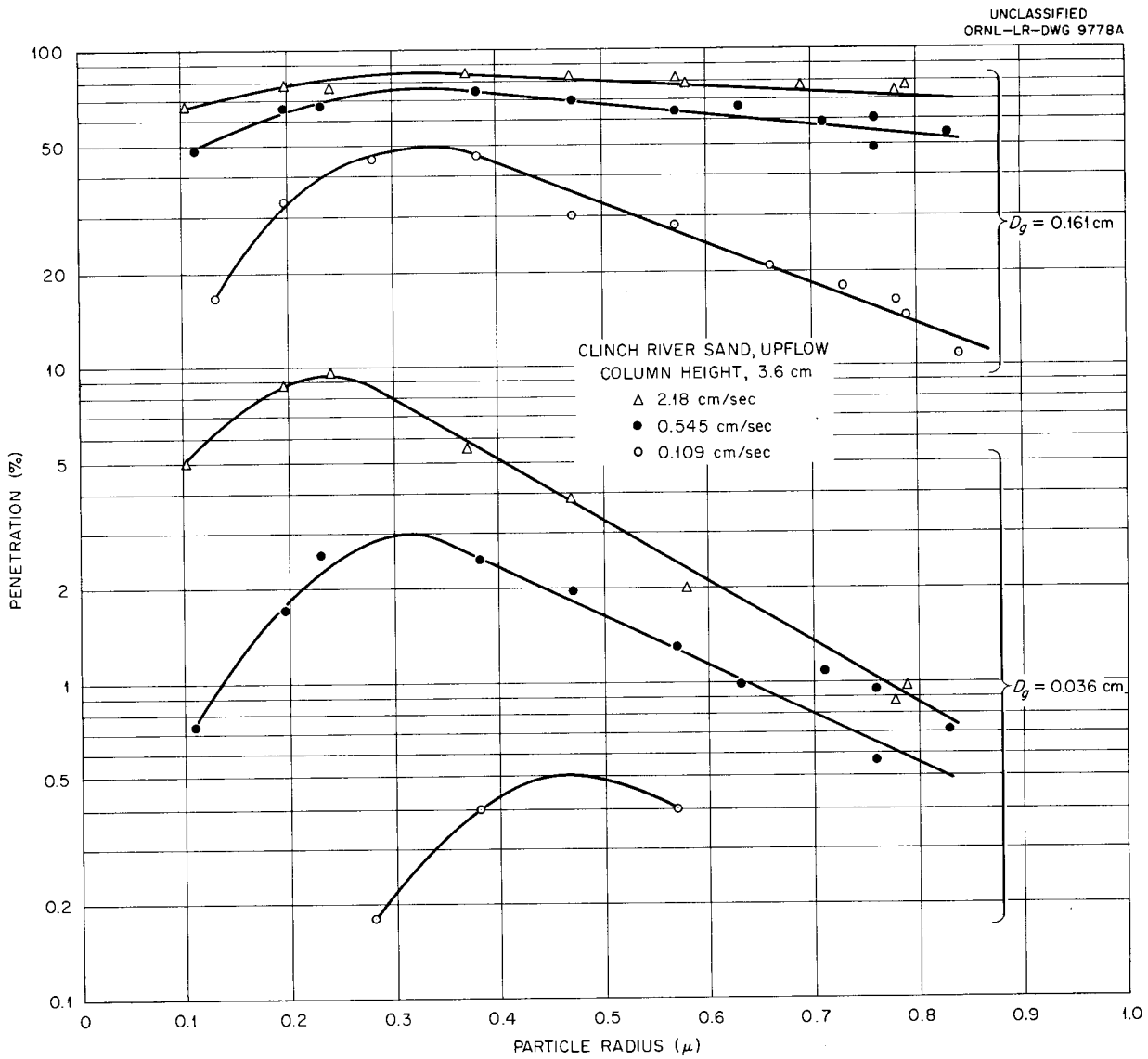

Fig. 18. Penetration of Aerosol Through Largest and Smallest Grain Fractions of Clinch River Sand.

Packed Bead Method of Particle Size Estimation

More recent data on the lead shot column indicate that the calibration curves as presented previously[7] are slightly incorrect. In the 0.2- to 0.4-μ-radius range the curves have been redrawn (see Fig. 19), giving sharper peaks, thus providing a more accurate determination of particle size.

[7] J. W. Thomas *et al.*, *HP Semiann. Prog. Rep. Jan. 31, 1955*, ORNL-1860, p 20–21.

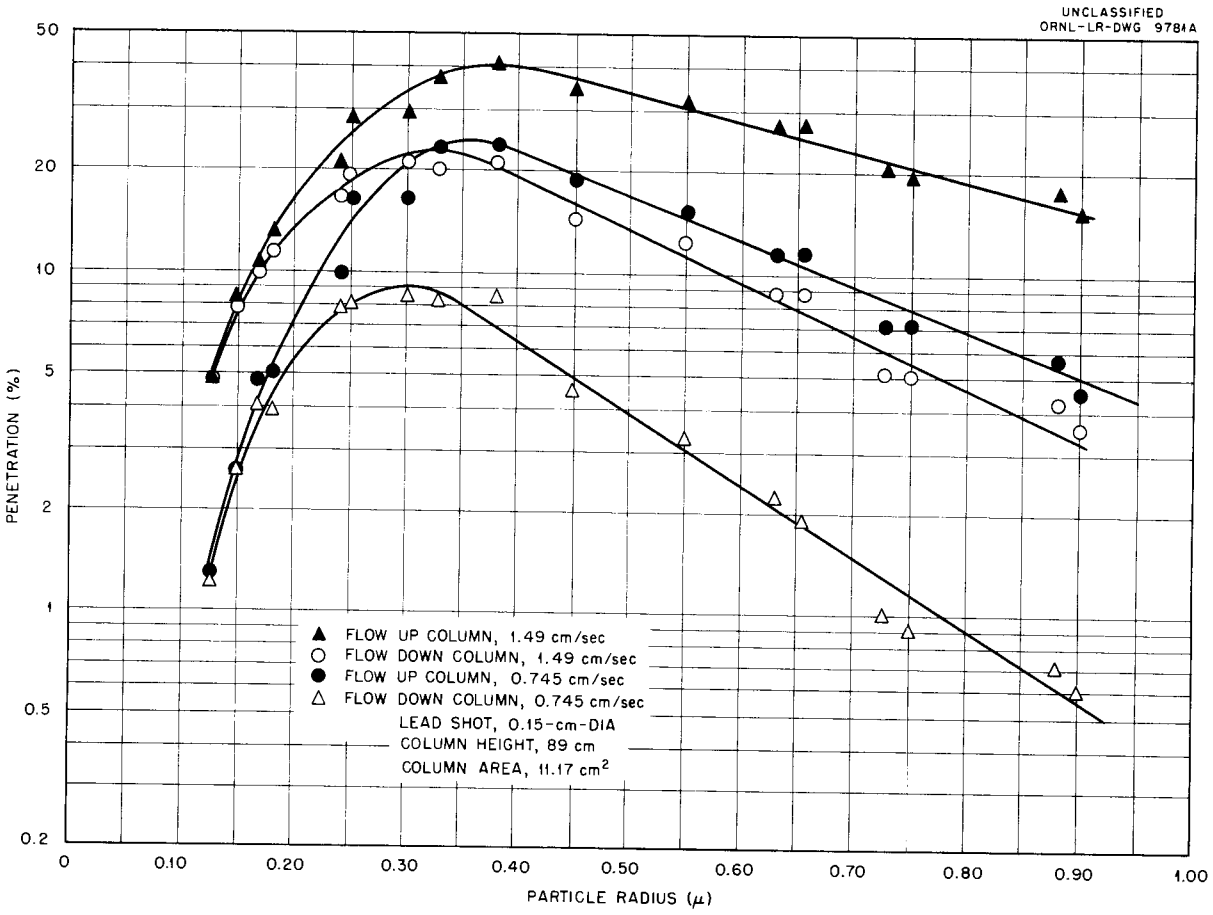

Fig. 19. Aerosol Penetration Through Lead Shot Column.

RADIATION DOSIMETRY

G. S. Hurst R. H. Ritchie

EXPERIMENTAL PHYSICS OF DOSIMETRY

R. D. Birkhoff, C. C. Sartain, F. N. Huffman[1], T. E. Bortner, B. G. Saunders, R. M. Johnson[1], J. S. Cheka, W. G. Stone, H. J. Moe[1], H. H. Hubbell, H. P. Yockey, T. B. Smiley[1]

Physics of Tissue Damage Studies

Because of the enormous complexity of human tissue, studies of the fundamental effects of radiation on inorganic and simple organic materials have been initiated. Advances in the knowledge of the effects of radiation on matter of less complexity will enable this laboratory to select more complex samples for future study.

The low-temperature irradiation facility in the LITR has been given a trial run. Minor flaws in the measuring circuit are being corrected so that properties of matter may be observed continuously and recorded while the samples are undergoing irradiation at low temperatures where any lattice defects are frozen in place. Migration of defects will be observed during the slow warmup to room temperature.

Single crystals of quartz cut for fundamental thickness shear have been irradiated by Co^{60} gamma rays with doses up to 5×10^8 r. Both resonant and antiresonant frequencies decreased about 1 cps per million roentgens.

The resonant and antiresonant equivalent resistances decreased sharply at a dose of 1.2×10^8 r and remained approximately constant to about 4.5×10^8 r. At approximately 4.5×10^8 r the resistance approximately doubled. There has been no observable change in the static capacitance. The crystal piezoelectric activity appears to be unaffected.

Single crystals of Rochelle salt, ammonium dihydrogen phosphate, potassium dihydrogen phosphate, and several other piezoelectric materials have been supplied by the Clevite Research Center.[2] The behavior of the piezo and elastic constants as a function of neutron dose will be studied.

A study is being made of the application of information theory to health physics and radiobiology. Radiation damage, recovery, and natural aging have been considered from the point of view of this theory. An equation relating dose, dose rate, and life span has been derived. This formula can be put in the same form as an empirical equation studied by Blair.[3] A paper on this subject has been submitted to *Radiation Research*.

Application of Information Theory to the Physics of Tissue Damage

Recent advances in knowledge of the structure of deoxyribonucleic acid (DNA) and in the theory of communications make promising an attempt to develop a mathematical theory of those biological events governed by genetic specificity. Watson and Crick[4] have given a structure for DNA and suggest that the genetic specificity is stored as a message coded in a four-letter alphabet along a helical chain of deoxynucleotides. Protein synthesis is thought to be associated with DNA, possibly through the medium of ribonucleic acid (RNA). Regardless of the details of the process, it is believed that protein receives its specificity from DNA. Therefore, if errors occur in the genetical code, script proteins lose their specificity and their function. Some errors may be tolerated, but when too many are introduced the cell dies.

In the application of communication theory to health physics and radiobiology these errors are thought to be introduced by a radiation field and by natural aging. By use of these ideas and some ideas from the theory of chemical rate processes, it is possible to develop expressions for the specificity lost from the genetical code script. The communication theory developed by Shannon and Weaver[5] makes it possible to assign a measure

[1] AEC Fellow in Radiological Physics.

[2] 540 E. 105th St., Cleveland, Ohio.

[3] H. A. Blair, *A Formulation of the Injury, Life Span, Dose Relations for Ionizing Radiations. I. Application to the Mouse*, UR-206 (May 13, 1952); *II. Application to the Guinea Pig, Rat, and Dog*, UR-207 (July 3, 1952); *The Shortening of Life Span by Injected Radium, Polonium, and Plutonium*, UR-274 (Sept. 8, 1953); *Recovery from Radiation Injury in Mice and Its Effect on LD_{50} for Durations of Exposure Up to Several Weeks*, UR-312 (Feb. 10, 1954); and J. N. Stannard, H. A. Blair, and R. C. Baxter, *The Effects of a Maintained Body Burden of Polonium in the Rat. III. Mortality, Life Span, and Growth*, UR-395 (June 6, 1955).

[4] J. D. Watson and F. H. C. Crick, *Nature* 171, 964–967 (1953).

[5] C. E. Shannon and W. Weaver, *Mathematical Theory of Communications*, Univ. of Ill. Press, Urbana, 1949.

to the ability of DNA to transmit specificity to proteins. This measure minus the measure of the specificity lost due to radiation effects and aging gives a measure of the ability of the damaged DNA to transfer specificity. The equation expressing this measure of ability has the same form as an empirical equation used by Blair[3] to represent the data in certain radiation exposure experiments. The experimental justification of the present theory rests on this fact at this time.

This work has a very practical application in that it may be possible to calculate the probable damage resulting from a given dose schedule.

Ionization Produced by Recoil Atoms

The previously reported[6] work on W, the average energy required to produce an ion pair, for recoil atoms resulting from the decay of thorium C and thorium C′ has been extended and improved. A new alpha recoil counter has been designed by R. K. Abele[7] and assembled by K. A. Miller.[7]

The major improvements on the earlier efforts are as follows:

1. use of a stronger ThB source, giving improved counting statistics;
2. addition of a 20-channel analyzer;
3. replacement of the A-1 amplifier by DD-2 amplifiers, giving better resolution at the higher counting rates;
4. use of a new counter design, giving calibration pulses and recoil pulses of about the same order of magnitude, thus extending the range of usable pressures;
5. collimation of the recoil atoms so as to decrease the effect of columnar recombination.

In the previously reported experiment, columnar recombination was possible for the recoil tracks but not for the calibration alpha tracks. In this experiment the situation is reversed. The difference in values could be fully accounted for by assuming 8% loss of ions by recombination when the track is perpendicular to the counter wire.

As shown in Fig. 20, the present design consists of three cylindrical proportional counters whose axes are parallel and lie in the same plane. All pulse-height measurements are made in the center counter, which contains the source material. The two outside counters serve only to single out by coincidence circuitry the specific decay events in which there is interest.

The source of recoil atoms is Pb^{212}(ThB) collected in an electric field from a Th^{228} source.

[6] G. S. Hurst *et al.*, *HP Semiann. Prog. Rep. Jan. 31, 1954*, ORNL-1684, p 8.

[7] Instrument Department, Instrumentation and Controls Division.

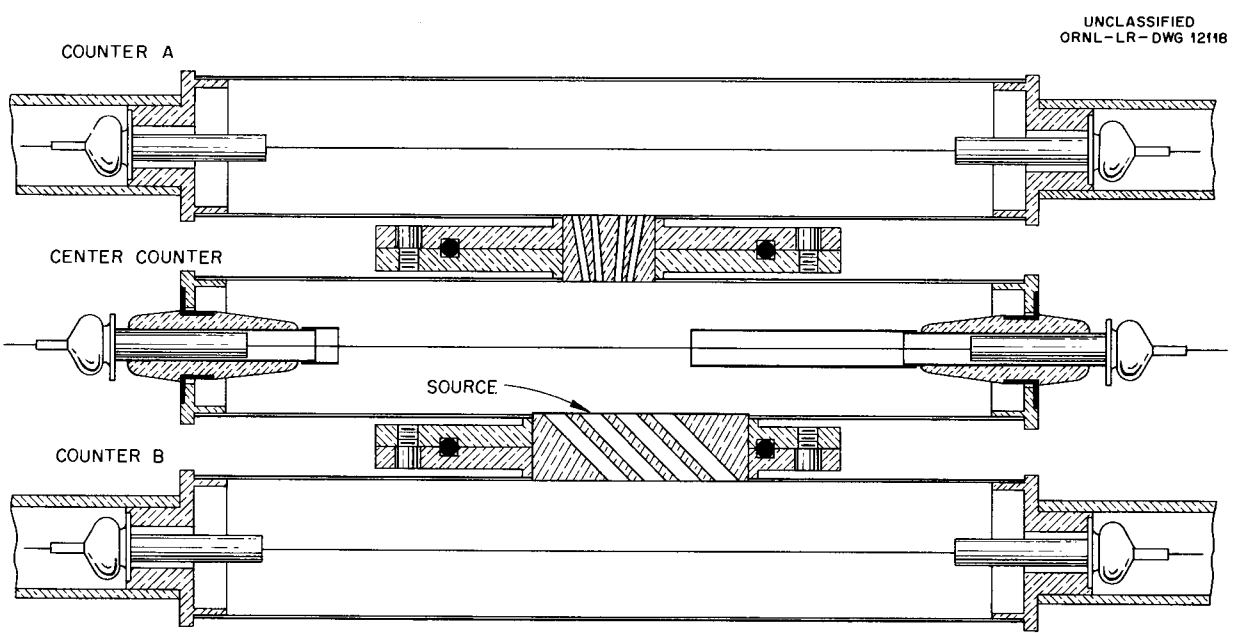

Fig. 20. Alpha Recoil Counter.

The ThB is collected on the inner face of a thin mica window sealed into the wall of the center counter at the mid-point. The half life of Pb^{212} is 10.5 hr; so a very active source is obtained with a deposit having an average thickness which is very small compared with a single molecular layer. The mica window holding the deposited source and the opposite window, also in the wall of the center counter, were made conducting, opaque, and of such a thickness that recoil particles cannot pass through but alpha particles can pass through readily. The gas pressure used in the counters is such that recoil particles are stopped in less than 1 in. but are not stopped in less than 0.1 in.

For calibration the center counter and counter A are connected to the circuit shown in Fig. 21. By the use of coincidence pulses from counter A to gate the signals from the center counter which reach the 20-channel analyzer, effective collimation of the alpha particles is accomplished. By observing the resulting pulse-height distribution on the 20-channel analyzer and using the data of Hirshfelder and Magee,[8] the number of ion pairs corresponding to the observed pulse heights can be calculated, since the energies of the alpha particles from the ThC and ThC′, the gas pressure, and the W values for alpha particles in the gases are known. In methane at pressures above 4 cm Hg the peaks due to the alphas from ThC and ThC′ are well resolved, as illustrated in Fig. 22.

To study the pulses caused by the recoil atoms, the center counter is not disturbed but counter B is connected in place of counter A in the circuit shown in Fig. 21. In this operation alpha particles entering counter B correspond to recoil particles traveling diagonally across the center counter. The pulses in counter B gate the pulses reaching the 20-channel analyzer from the center counter and produce a pulse-height distribution that represents the spectrum caused by the recoil atoms from ThC and ThC′. It has been possible to resolve these two peaks in methane at gas pressures as low as 1 cm Hg.

From the calibration data and the known energies of the recoil atoms the value of W for the recoil atoms is calculated. Results have been obtained for methane at a pressure of 4.75 cm Hg and for hydrogen at a pressure of 4.86 cm Hg. The value of W in units of electron volts per ion pair for the ThC recoil atom is found to be 121 for methane and 82 for hydrogen. The value of W for the ThC′ recoil atoms is found to be 99.5 for methane and 63 for hydrogen.

It is planned to extend these measurements to carbon dioxide, argon, ethylene, and cyclopropane as well as to other pressures of methane and hydrogen.

[8] J. O. Hirschfelder and J. L. Magee, *Phys. Rev.* 73, 207 (1948).

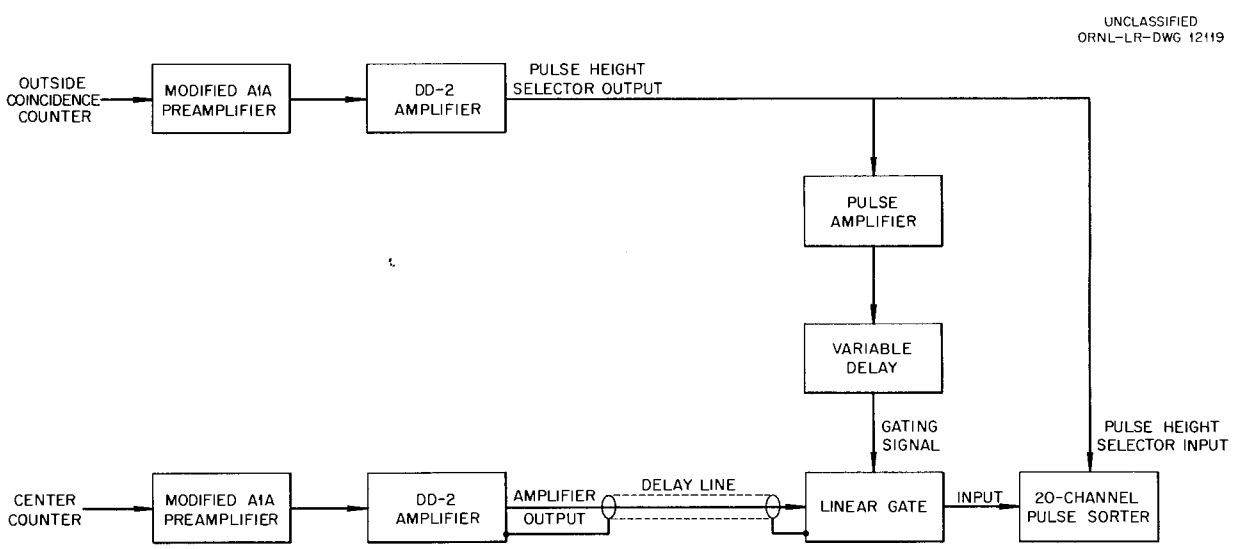

Fig. 21. Schematic Diagram of Circuit for Both Recoils and Calibrating Alphas.

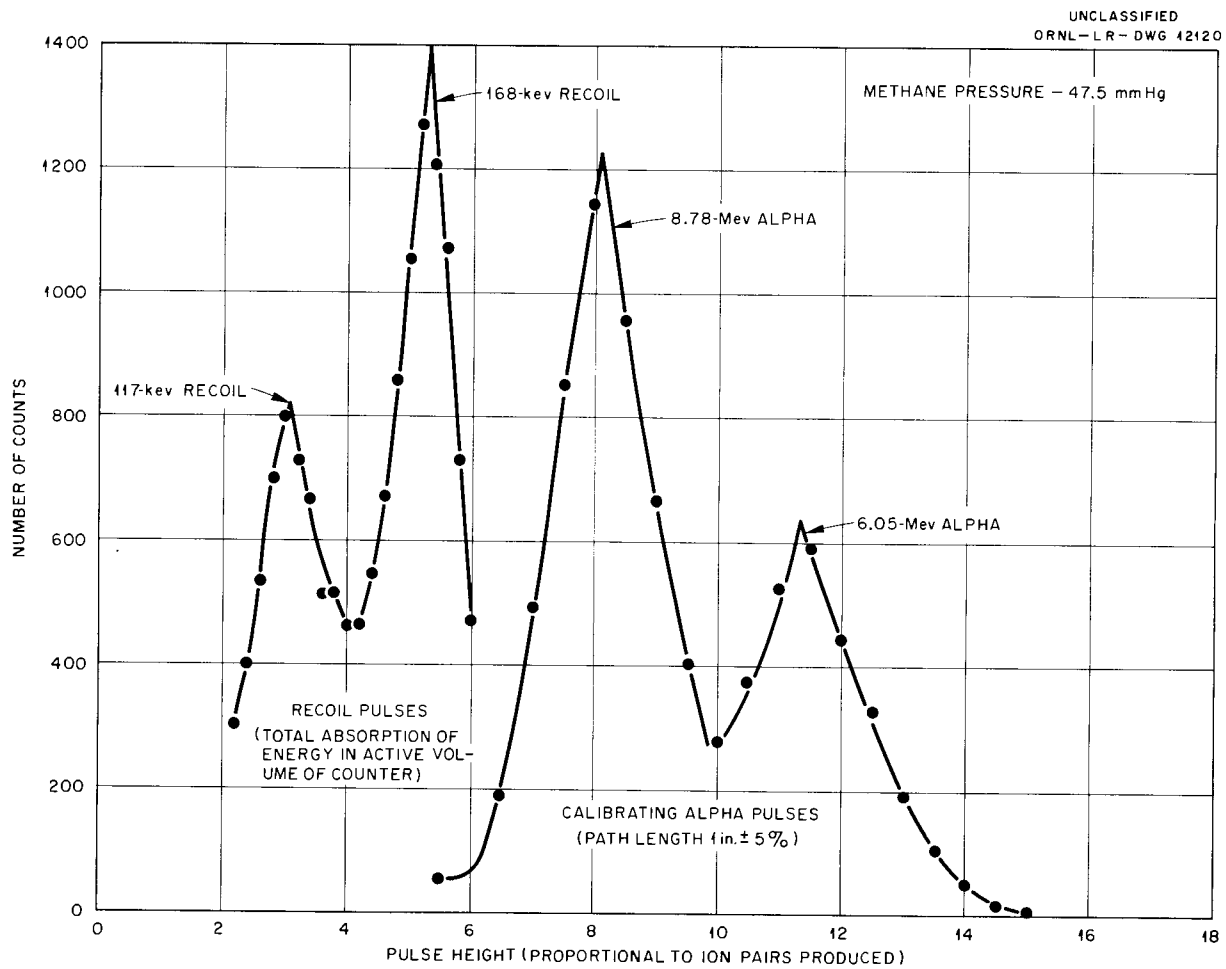

Fig. 22. Peaks of Alpha Particles from ThC and ThC′.

Attachment Coefficient and Drift Velocity of Electrons

The apparatus in Fig. 23 was designed for measuring the effect of attaching gases in ionization chambers and proportional counters on the electron pulse height. A collimated alpha source released free electrons by ionization, all at the same distance from the collector plate in the lower chamber. Some of the electrons are captured before collection, and thus, if the pulse amplifier has a time constant t_1 which is comparable to electron transport time τ_0, the pulse height permits measurements of the probability of electron attachment per centimeter of travel in the field direction and per millimeter of pressure of the attaching gas. The output pulse height from the linear amplifier also depends on the time τ_0; the latter is measured in the upper part of the chamber by the two proportional counters.

Pulse Height. – The pulse height due to free electrons is measured by means of an A-1 linear amplifier (with $t_1 = 15$ μsec) and a single-channel pulse analyzer with a motor-driven base line.

Figure 24 shows the decrease in pulse height as a function of the electric field and the amount of the attaching gas – in this case, oxygen in nitrogen. Figure 25 shows in the same manner the effect of oxygen in methane. Under the above conditions, tube mechanism for electron capture is the straightforward attachment process $O_2 + e^- \rightarrow O_2^-$.

Electron Drift Rate. – Figures 26 through 30 show the electron drift rate as a function of the

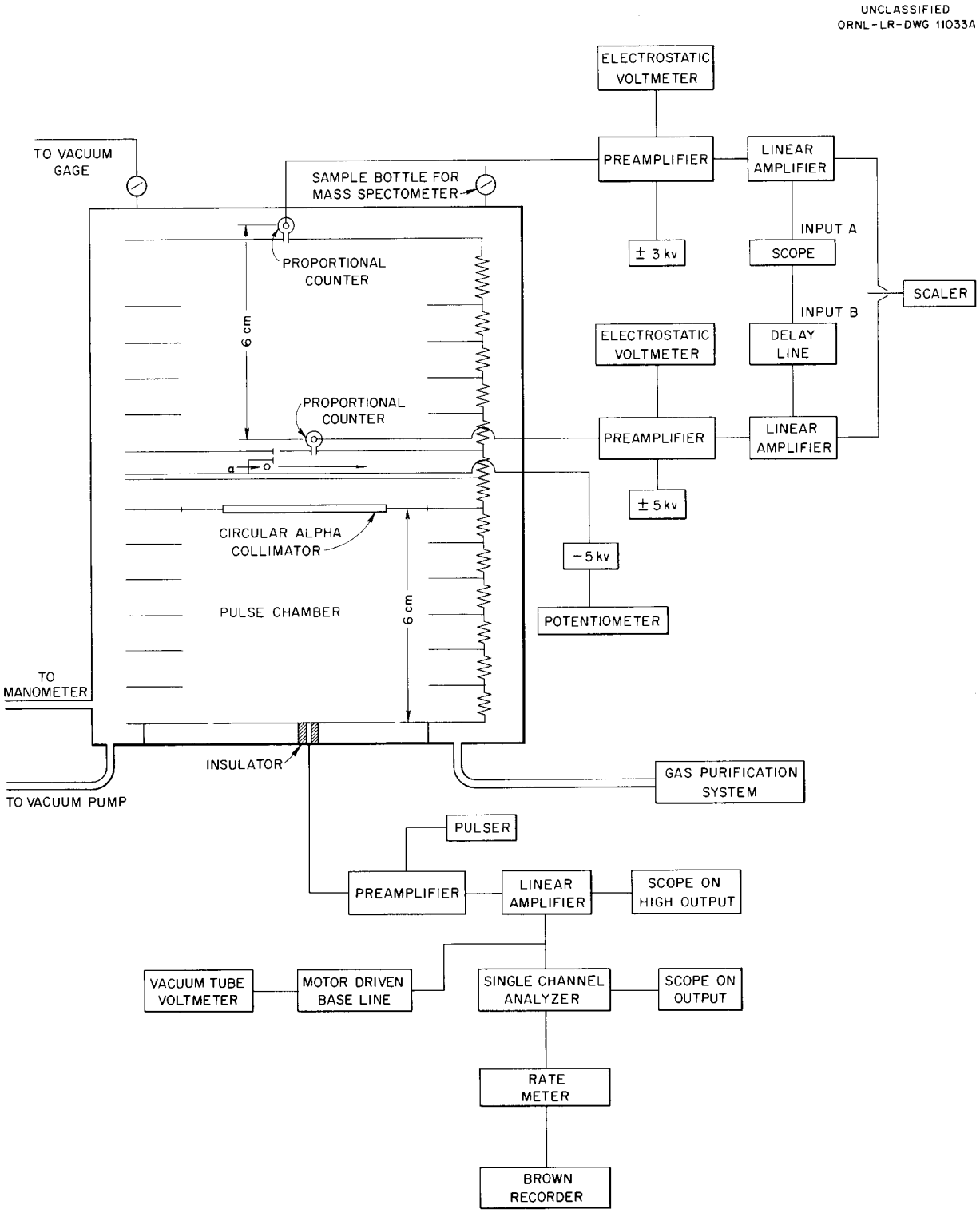

Fig. 23. Electron Attachment and Drift Rate Apparatus.

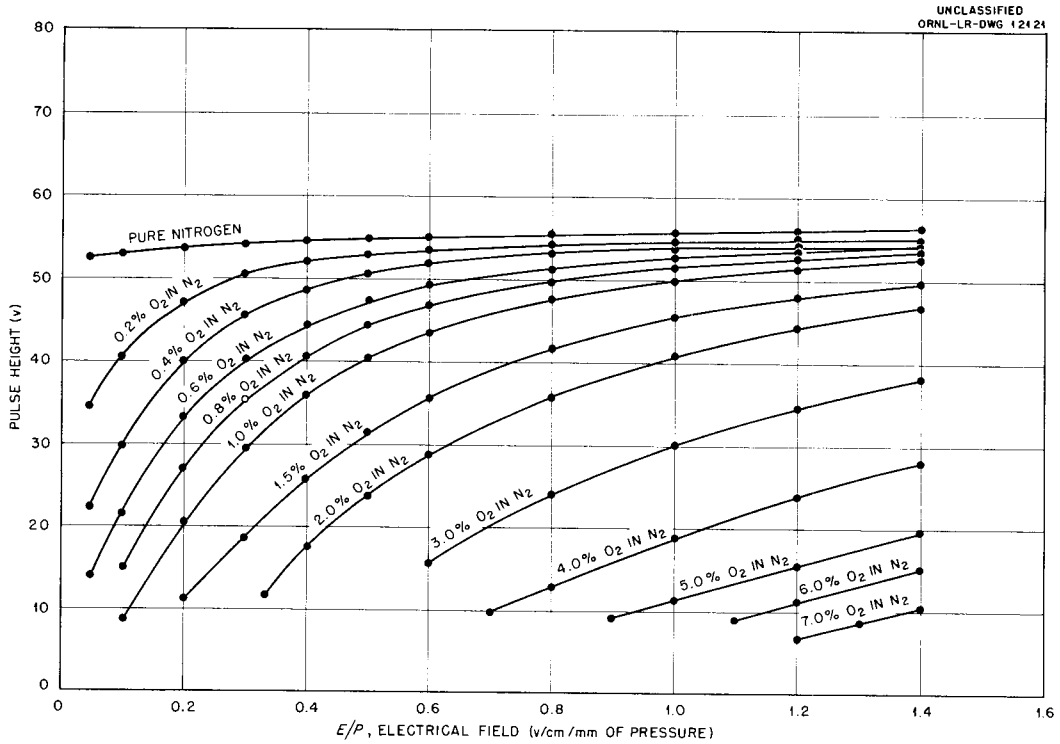

Fig. 24. Pulse Height vs the Electrical Field in Pure Nitrogen and in Nitrogen-Oxygen Mixtures at 40 cm Total Pressure.

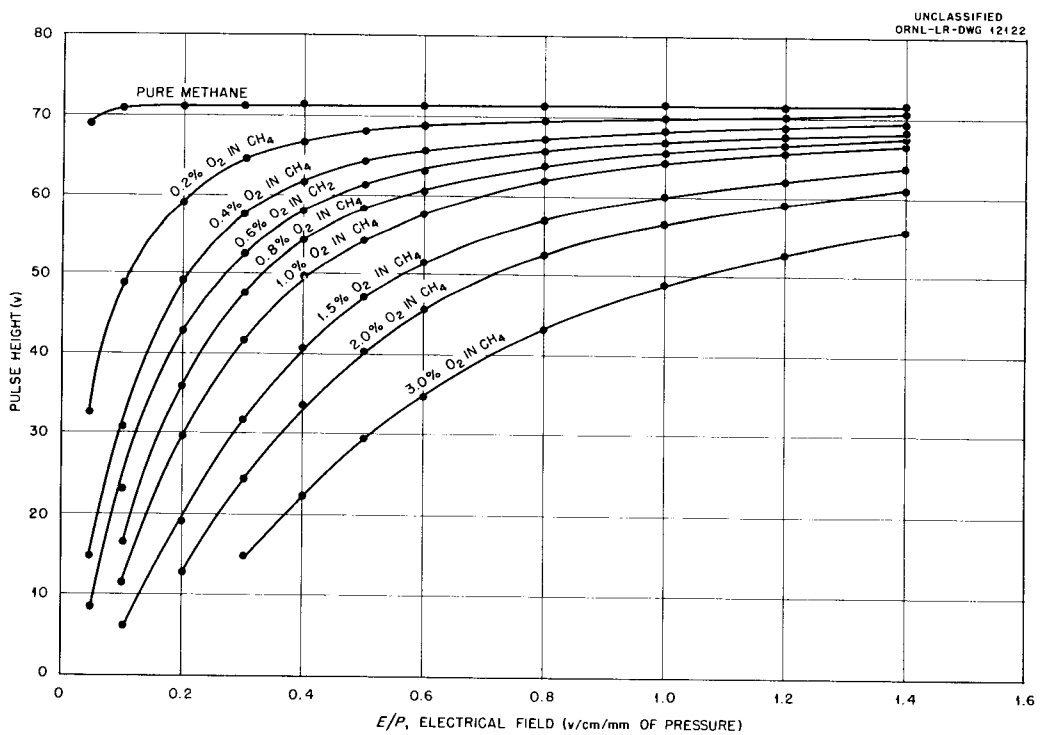

Fig. 25. Pulse Height vs the Electrical Field in Pure Methane and in Methane-Oxygen Mixtures at 40 cm Total Pressure.

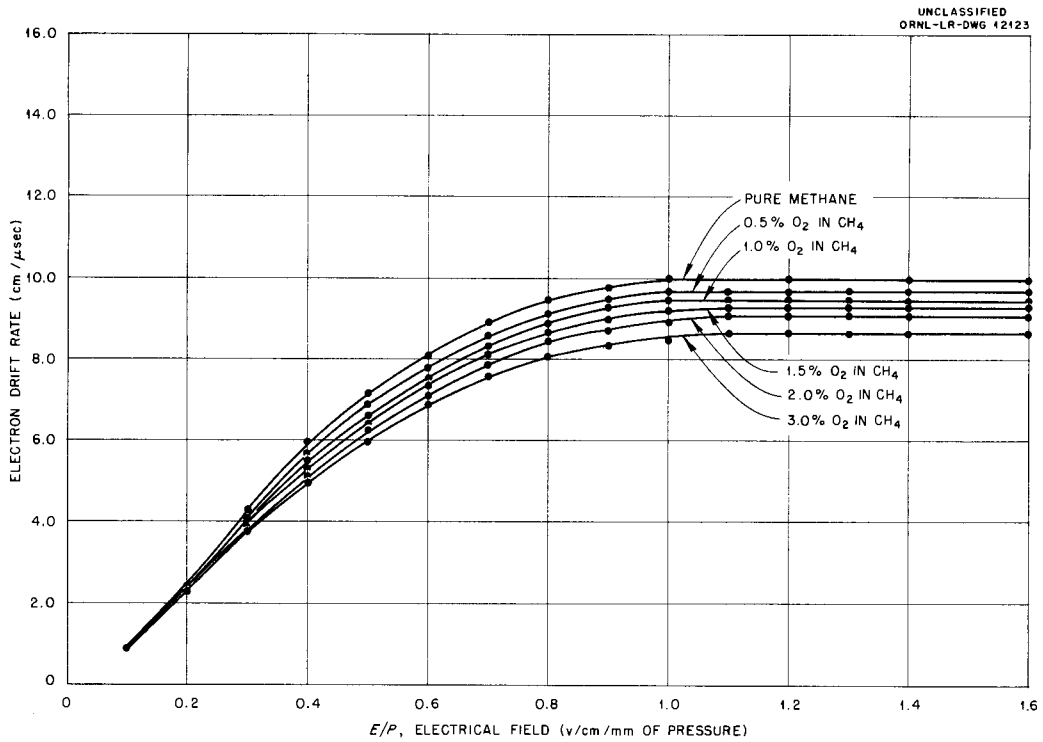

Fig. 26. Electron Drift Rate vs the Electrical Field in Pure Methane and in Methane-Oxygen Mixtures at 40 cm Total Pressure.

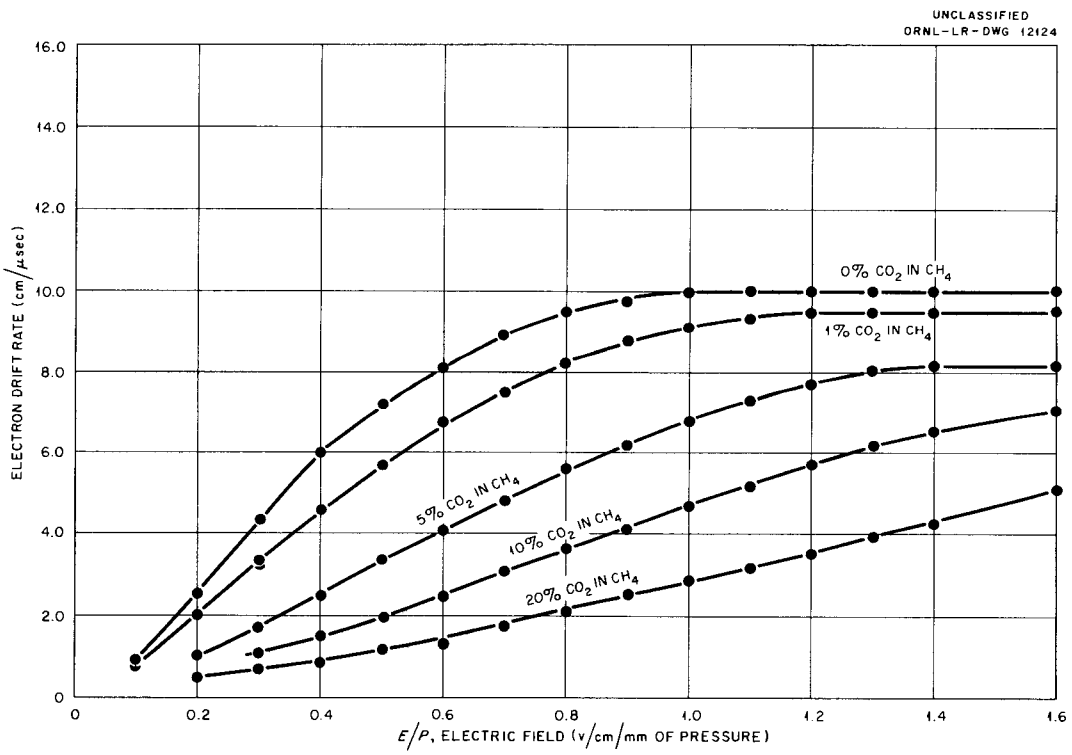

Fig. 27. Electron Drift Rate vs the Electrical Field in Mixtures of Methane and Carbon Dioxide. Pressure 40 cm Hg.

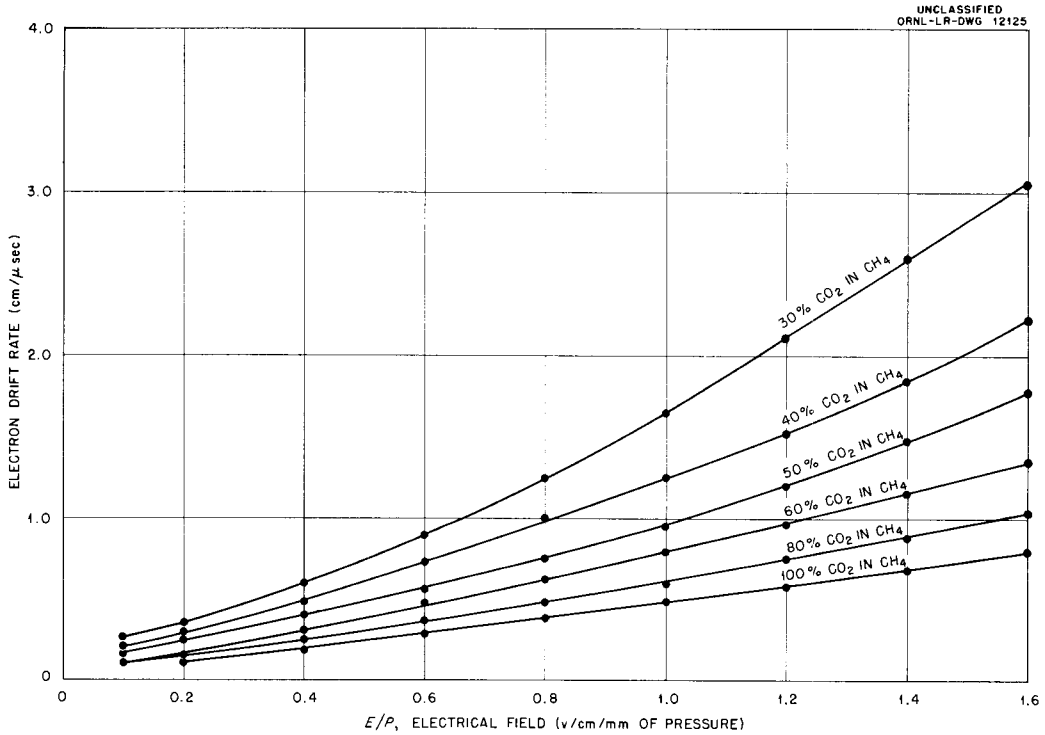

Fig. 28. Electron Drift Rate vs the Electrical Field in Mixtures of Methane and Carbon Dioxide. Pressure 40 cm Hg.

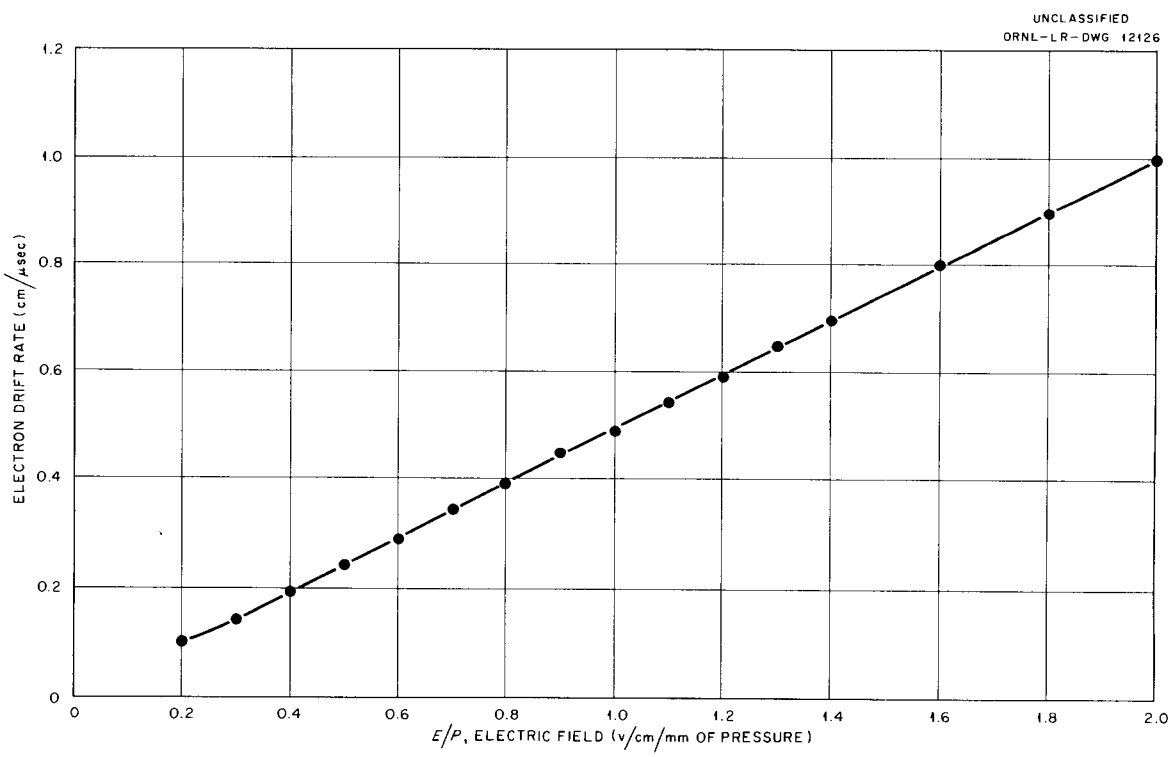

Fig. 29. Electron Drift Rate vs the Electrical Field in Pure Carbon Dioxide at 40 cm Total Pressure.

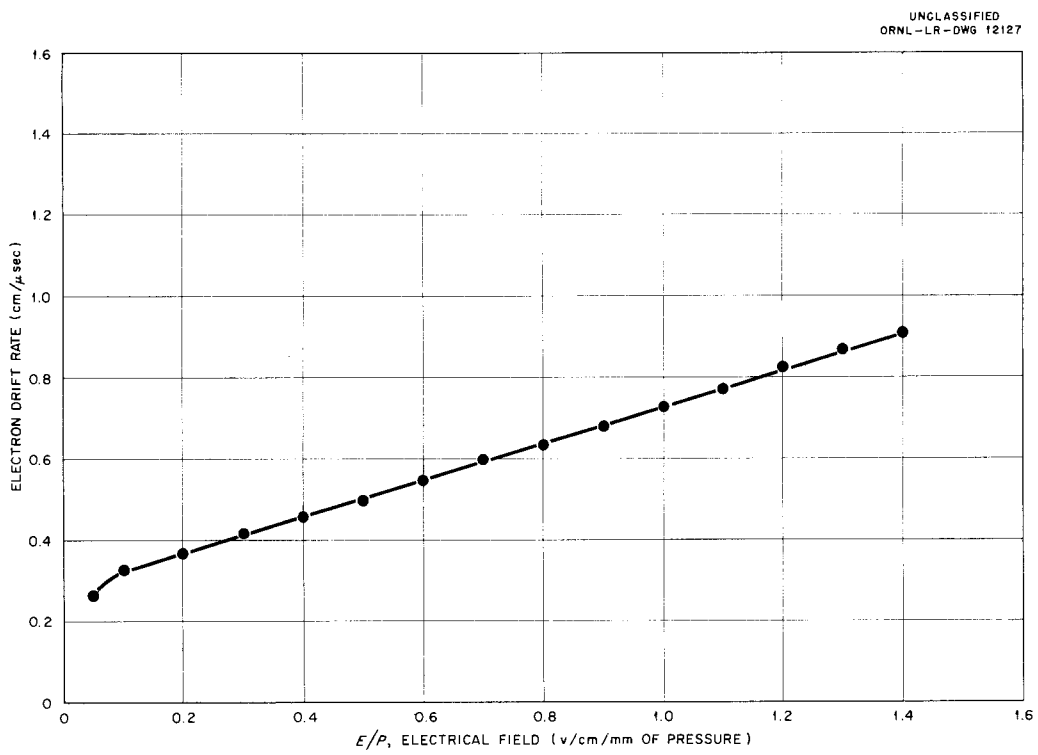

Fig. 30. Electron Drift Rate vs the Electrical Field in Pure Nitrogen at 40 cm Total Pressure.

electrical field for several gases and the effect that oxygen has on the drift rate. In Fig. 24 it is seen that rather small percentages of oxygen decrease the pulse height, but it was found that up to 3% of oxygen in nitrogen had no measurable effect on the drift rate. As can be seen in Fig. 26, the effect of small percentages of oxygen in methane does have some effect on the rate of drift of the electrons. Electron drift rates were measured for mixtures of methane and carbon dioxide, Figs. 27 and 28. Figures 29 and 30 show, respectively, the drift rates in carbon dioxide and nitrogen.

In the case of CH_4 the two signals from the counters are very close together (0.6 μsec), and hence slight changes due to addition of O_2 are difficult to detect. Because of this a variable delay line, containing a booster amplifier, was placed between the first tube and one of the two inputs on the Tektronix 535 scope. The second tube output is connected to the second input of the scope. By inverting one of the signals and adding time delay, the tips of the two signals can be matched, thus giving a null method of reading a time interval. The data in Fig. 26 were taken in this manner.

Attachment Coefficient. – From measurements of the pulse heights and the electron drift velocity, the attachment coefficient α per centimeter of travel in the field direction and per millimeter of attaching gas can be determined from the following equations:

$$V'_\tau = \frac{\text{constant}}{(\tau_0 - t_1 f)} \left[\left(e^{(\tau_0 - t_1 f)/t_1} - 1 \right) \tau' - e^{(\tau_0 - t_1 f)/t_1} \left(\tau_0 - \frac{t_1 \tau_0}{\tau_0 - t_1 f} \right) - \frac{t_1 \tau_0}{\tau_0 - t_1 f} \right] e^{-\tau'/t_1} ,$$

$$\tau' = t_1 \frac{\left[e^{(\tau_0 - t_1 f)/t_1} \left(1 + \frac{\tau_0}{t_1} - \frac{\tau_0}{\tau_0 - t_1 f} \right) + \left(\frac{\tau_0}{\tau_0 - t_1 f} - 1 \right) \right]}{\left[e^{(\tau_0 - t_1 f)/t_1} - 1 \right]} ,$$

$$f = \alpha d f_1 P ,$$

where

t_1 = the time constant for an amplifier having a response $V(t) = (t/t_1)e^{-t/t_1}$ when a step function of unit height is fed into the amplifier,

V'_τ = the maximum pulse height,

d = the distance, cm, from the alpha source to the collector plate,

f_1 = the mole fraction of the attaching gas,

P = the total gas pressure, mm Hg,

τ_0 = the time required for electrons to drift the distance d.

The coefficient α for O_2 in N_2 and O_2 in CH_4 appears to depend on f_1 as well as on P for ranges of f_1 from 0.002 to 0.03 and on P from 350 to 1000 mm. Extensive determination of total pressure and partial pressure dependence is in progress.

Accelerator

The studies of the distribution of dose with depth in a solid bombarded with an electron beam have been continued. Extensive revision of existing apparatus has been found necessary in order that an experiment can be performed which may be interpreted with the aid of the Spencer[9] theory. The problem has been one of providing a means for introducing a parallel beam into a solid which extends to infinity in both directions from the plane of incidence. Ionization in a parallel-plate gas-filled ion chamber should then be measured at various distances from both sides of the source plane. The design has been worked out and measurements are in progress. It has been found necessary to construct a differential pumping system for the ion chamber.

The ion source to be used in making measurements of the ionization of gases by heavy particles has been completed.

Beta Spectrometer

The measurements of electron straggling in thin foils have been discontinued because of interesting recent developments in electron diffusion theory which currently are awaiting experimental verification. Recent discussions with L. V. Spencer and U. Fano at the National Bureau of Standards have pointed to the feasibility of measuring the energy distribution of the electron flux in a medium resulting when radioactive sources are embedded in the medium or when the medium is bombarded with x rays or neutrons. In the material a vacuum cavity with a small hole leading to the outside can be used to supply a sample of the flux, which then may be analyzed by a beta spectrometer. The results should check the Spencer-Fano[10] theory in the region above a few kev where electron collision cross sections are known adequately. Theoretical calculations have been carried out for sources of P^{32}, Tl^{204}, and S^{35} distributed in water or bakelite, and the flux spectra have been obtained. Experiments with P^{32} in bakelite are currently going on, using the beta plaque material available locally.

A paper[11] describing the beta spectrometer has appeared recently in the literature.

X-Ray Exposure Facility

The need for an accurate beta-ray dosimeter for personnel has led to the building and calibrating of several different versions of the pencil type currently in use in this and other laboratories. Modifications include a perforated version of the usual plastic model, aluminum and magnesium screen-covered variations, and "no-wall" types with 7 and 1 mg/cm^2 conducting films defining the sensitive volume. Calibration has been accomplished by inserting the pencil into a cavity in a beta-radioactive liquid where the dosage is accurately known from a measurement of the specific activity of the liquid. The response of the chambers may be predicted from a knowledge of the Spencer-Attix[12] theory of cavity ionization. The response is found to be a sensitive function of the thickness of the foil used to define the volume. For instance a 7 mg/cm^2 foil absorbs about half the dose in a cavity in a P^{32} solution. All pencils are designed so that the response to x and gamma rays remains the same as in the conventional model. Further work is progressing with several different beta-emitting isotopes, and it is hoped that the design for practical field models will be available soon.

[9] L. V. Spencer, *Phys. Rev.* 98, 1597 (1955).

[10] L. V. Spencer and U. Fano, *Phys. Rev.* 93, 1172 (1954).

[11] R. D. Birkhoff *et al.*, *Rev. Sci. Instr.* 26, 959 (1955).

[12] L. V. Spencer and F. H. Attix, *Radiation Research* 3, 239 (1955).

Ionization in Acetylene Mixtures by Pu^{239} Alpha Particles

The ionization produced by Pu^{239} alpha particles in acetylene mixed with helium, neon, argon, carbon dioxide, and nitrogen has been determined. The results yielded W values (average energy used in producing an ion pair) for the mixtures. Huber, Baldinger, and Haeberli[13] introduced the formula

$$\frac{1}{W_m} = \left(\frac{1}{W_1} - \frac{1}{W_2}\right) Z + \frac{1}{W_2} ,$$

where $Z = S_1P_1/(S_1P_1 + S_2P_2)$, W_m is the W for a gas mixture having two components at pressures P_1 and P_2 and molecular stopping powers S_1 and S_2 with W values for the pure gases equal to W_1 and W_2, respectively. This formula is based on the assumption that the presence of a second gas does not contribute to the ionization of the first.

It has been found[14] that for certain combinations of gases, a general formula

$$\frac{1}{W_m} = \left(\frac{1}{W_1} - \frac{1}{W_2}\right) Z + \frac{1}{W_2} ,$$

where $Z = P_1/(P_1 + aP_2)$, in which a is an empirical constant, does hold whereas the equation for the special case given above does not. The purpose of this work was to determine whether acetylene and the group of gases studied would be among those mixtures for which this more general formula held and if so, to determine the empirical constant a. The mixtures shown below gave a good fit to the second equation.

Mixture	S_2/S_1	a
N_2-C_2H_2	1.768	0.267
A-C_2H_2	0.577	3.550
CO_2-C_2H_2	1.321	0.927
He-C_2H_2	0.312	0.058

The a values are compared with S_2/S_1, which is the value of a whenever the general formula is reduced to the special case. The results for the mixture of neon plus acetylene could not be fitted to either equation.

[13] P. Huber, E. Baldinger, and W. Haeberli, *Helv. Phys. Acta* 23, Suppl. III, 85 (1950).

[14] T. E. Bortner and G. S. Hurst, *Phys. Rev.* 93, 1236–1241 (1954).

THEORETICAL PHYSICS OF DOSIMETRY

J. Neufeld R. H. Ritchie W. S. Snyder

Number of Vacancies Created by Corpuscular Radiation[15]

In the previous work[16] on disordering of solids by neutron radiation summarized in the last semiannual report,[17] the number of displacements has been computed under the assumption that a displacement occurs when the struck atom receives energy y larger than α. In this work the number of vacancies is calculated by taking into account replacements that occur when $y > \alpha$ and $x - y < \alpha$, where x is the energy of the striking atom before collision. Then the mean number of vacancies is determined by $g(x) = 1$ for $0 < x < 2\alpha$ and by

$$g(x) = \int_0^{x-\alpha} dy\, K(x, y)\, g(x - y) + \int_\alpha^x dy\, K(x, y)\, g(y - \alpha)$$

for $x > 2\alpha$, where $K(x,y)$ is the scattering kernel. The above equation yields $g(x) \sim x/3\alpha$ for hard-sphere scattering.

Effect of Boundaries on Energy Loss of Charged Particles Passing Through Thin Foils

Recent work[18] on the determination of the mean free path for discrete energy loss of electrons in thin metal foils compares experimental results with theoretical predictions of the energy loss. The transient electrodynamic disturbance created by the passage of an electron through the boundaries of thin foils gives rise to an energy loss which may be comparable with that predicted by conventional energy loss formulas which do not include this transient effect. A formula has been derived for this "transient" energy loss in the case of a relativistic charged particle incident on a foil having a dielectric constant $\epsilon(\omega)$. It is shown that for conduction electrons this transient effect may be neglected only if the foil thickness is much greater than v/Ω, where v is the velocity of the

[15] J. Neufeld and W. S. Snyder, *Phys. Rev.* 99, 1326 (1955).

[16] W. S. Snyder and J. Neufeld, *Phys. Rev.* 97, 1636–1646 (1955).

[17] J. Neufeld, R. H. Ritchie, and W. S. Snyder, *HP Semiann. Prog. Rep. July 31, 1955*, ORNL-1942, p 22.

[18] A. W. Blackstock, R. H. Ritchie, and R. D. Birkhoff, *Phys. Rev.* 100, 1078 (1955).

particle and Ω is the "plasma" resonance frequency. Since v/Ω is of the order of hundreds of angstroms for 100-kev electrons in certain metals, measurements of the kind described by Blackstock, Ritchie, and Birkhoff[18] may show this effect. A more complete account of this work will be submitted for publication.

Asymptotic Solutions of the Heat Conduction Equation in Cylindrical Geometry

The formal solutions of many problems involving transient heat conduction in infinite internally bounded cylindrical solids may be obtained by the standard Laplace transform method. Such solutions are of importance in many physical applications such as heat flow, gas flow through porous media, slowing down of neutrons, and other diffusion phenomena. Asymptotic series representing these solutions for large values of the "time" parameter have been derived. They are expressed in terms of functions related to the derivatives of the reciprocal gamma function, and it has been shown that they are asymptotic in the sense of Poincaré's definition. These results have been applied to selected physical problems in heat conduction. They include cases in which (1) a cylindrical surface is maintained at constant temperature in a medium which is initially at a lower temperature, (2) a constant flow occurs over a surface, and (3) a constant cylindrical shell source exists in the medium. Application is also made to a problem in the flow of gas through porous media. A paper describing this work will be submitted to the *Journal of Applied Physics*.

DOSIMETRY APPLICATIONS

F. J. Davis — J. M. Garner
P. W. Reinhardt — J. A. Auxier
J. A. Harter — E. B. Wagner
H. E. Gilbert[19]

Neutron-Threshold-Detector Program

A method has been described for measuring the spectrum of fast neutrons with a series of foil detectors.[20] The detectors consist of Au and Au plus Cd for determining the thermal flux, Pu^{239} shielded with B^{10} for determining the total fast flux, Np^{237} for determining the total flux above 0.75 Mev, U^{238} for determining the total flux above 1.5 Mev, and S^{32} for determining the total flux above 2.5 Mev. From these data the spectrum of fast neutrons can be constructed reasonably well for spectra similar to the fission spectrum. The amount of induced activity in the detecting elements is determined with scintillation counters, which are calibrated by irradiation of suitable foils with thermal neutrons.

Fast-neutron tissue dose can be calculated from the measured spectrum. Since the foil method of measuring spectra works well for high intensity bursts of neutrons, dosimetry may be accomplished under conditions where other methods, such as the ionization chamber and proportional counter, would lead to questionable data.

The trailer containing the counting equipment necessary for determining the sample activation has been maintained in operation for two reasons:

1. It has been maintained as standby equipment for the emergency monitoring program that has been set up in the Applied Health Physics Group.[21] In case of a neutron accident the threshold-detecting elements are recovered and counted on the scintillation counters as quickly as possible. In this way a measure can be determined of the tissue dose that personnel would have received had they been in the area of the accident.

2. The equipment has been used for comparison with similar equipment that was constructed and installed in a trailer by the Army Chemical Corps.

Very close agreement between the two systems was obtained.

A report entitled "Threshold Detectors – Tissue Dose Determination" has been submitted to *Review of Scientific Instruments* and accepted for publication in either the March or April 1956 issue.

Fast-Neutron Spectrometer

Neutron spectrometers of the proton-recoil type generally collimate the proton recoils in such a way that only those in one direction are utilized. The present spectrometer is designed to accept protons scattered in a wide angle, thereby greatly increasing the efficiency. The principle of this spectrometer is to shape a chamber to the envelope of the range of the proton recoils from neutrons. At a given gas pressure P, neutrons of energy E_0 will produce recoil protons which just reach the

[19] AEC Fellow in Radiological Physics.

[20] G. S. Hurst *et al.*, ORNL-1671 (March 30, 1954). (Secret)

[21] F. T. Howard and W. H. Sullivan, ORNL-1955 (Nov. 7, 1955). (Secret)

envelope regardless of their scattering angle θ. The range of the protons can be expressed as

$$R = \frac{k\,E_\theta{}^n}{P} ,$$

where R is the proton range, k and n are constants for the gas, and E_θ is the proton energy scattered at an angle θ. Since $E_\theta = E_0 \cos^2 \theta$, the following relation results:

$$R = \frac{k\,E_0{}^n \cos^{2n} \theta}{P} .$$

For the gas xenon the constant n is very close to the value $3/2$ for energies above 100 kev; therefore, the envelope equation is

$$R = \frac{k\,E_0{}^{3/2}}{P} \cos^3 \theta = D \cos^3 \theta ,$$

where $(k\,E_0{}^{3/2})/P$ is the constant D. If the wall of this egg-shaped chamber is covered with a scintillator to detect the protons and if the output signal is gated to accept only the small pulses caused by protons which just reach the scintillator, then only the protons scattered by neutrons of one energy are counted even if the target is irradiated by neutrons of more than one energy. If then the detector count rate is plotted as a function of the pressure, the neutron energy spectrum can be obtained. More specifically, the wall must be shaped so that all protons, regardless of angle, arrive at the scintillator with energy E_1, where $E_1 = E_B + \Delta E$. The bias energy required to operate above tube noise is E_B, and ΔE is the energy width of the single-channel analyzer. Thus if protons arrive with energy greater than E_1 or less than E_B, they will not be recorded.

The present design under construction uses a 5-in. 6364 photomultiplier tube and a CsI(Tl) scintillator coupled to a conventional single-channel analyzer.

Improved Fast-Neutron Dosimeter

Further improvements in the performance and ease of operation of the "standard" fast-neutron dosimeter, Q-1696, have been made, and the new version,[22] designated as Model II, is shown in Fig. 31.

[22]Designed by R. K. Abele of the Instrumentation and Controls Division, ORNL.

UNCLASSIFIED
PHOTO 15925

Fig. 31. "Standard" Fast-Neutron Dosimeter, Model II.

For convenience of operation the gas-filling tubes and valves, the electrical connectors, and the solenoid for actuating the alpha-source shutter were all moved to one end of the counter. The brass field tubes were replaced by polyethylene tubes coated lightly with Aquadag, making the chamber a more nearly perfect Bragg-Gray cavity and improving the directional response. The response is uniform to within 5% for neutrons

incident on the end of the chamber at angles from 0 to greater than 100 deg.

Cyclopropane, C_3H_6, has been studied as a possible counting gas, and preliminary data indicate that it has considerable merit; in particular, the operating potential is significantly lower. Since it has the same hydrogen-carbon ratio as ethylene but one more atom of each per molecule, the same sensitivity is obtained at two-thirds the pressure. The decreased pressure further lowers the operating potential.

The rate and quantity of in-gassing and out-gassing of cyclopropane in polyethylene are greater than for ethylene in polyethylene, indicating that it is important to leave the counter connected to the gas-filling system until equilibrium has been reached at the desired pressure.

After equilibrium had been attained, the resolution and gas amplification of the counters remained stable during a period of three weeks. The counters are still under study.

The pulse-height distributions for ethylene and for cyclopropane using plutonium alpha particles are shown as functions of electrode potential and of the gain of the electronic system in Fig. 32.

Neutron-Insensitive Gamma Dosimeter

In radiation fields composed of gamma rays and fast neutrons, it is desirable to make measurements of each component such that the presence of one does not, at the point considered, contribute to the measurement of the other. One of the most pressing problems in radiation dosimetry is the accurate measurement of the gamma radiation in the presence of high fluxes of fast neutrons.

An examination has been made of the potentialities and limitations of the C-CO_2 ionization chamber,[23] which is used extensively in shielding measurements. The predominant mechanisms by which ionization is indirectly produced in this type of chamber by fast neutrons are elastic neutron-

[23] L. H. Ballweg and J. L. Meem, *A Standard Gamma Ray Ionization Chamber for Shielding Measurements*, ORNL-1028 (July 9, 1951).

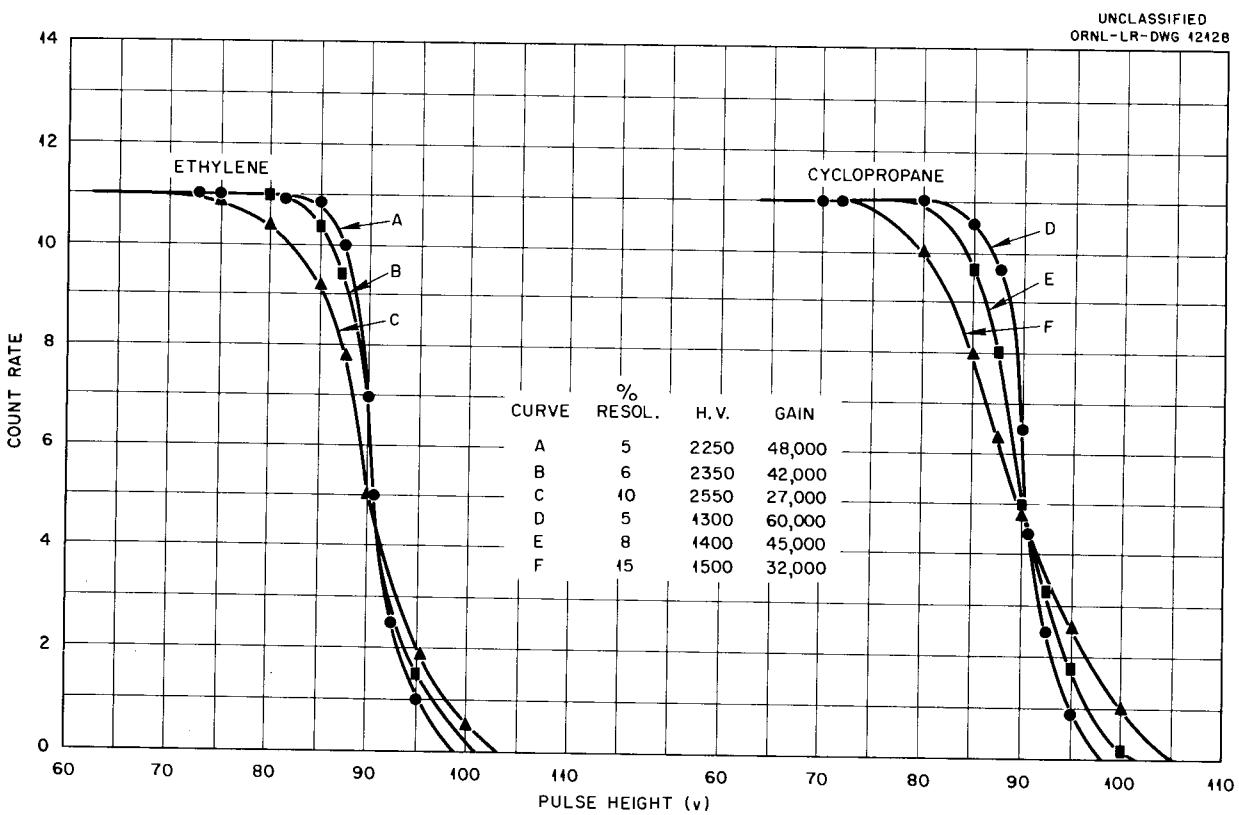

Fig. 32. Resolution as a Function of Electronic Gain and Electrode Voltage.

carbon atom and neutron-oxygen atom collisions resulting in heavy ion recoils and inelastic neutron scattering by the chamber walls and surrounding media.

The ionization current was plotted as a function of collector voltage from 0 to 1500 v for the 900-cc chamber. (The chamber is normally operated at about 200 v.) The curves are shown for Co^{60} gamma radiation and Po-Be fast neutrons (Fig. 33). For gamma radiation, saturation commenced at relatively low voltages, but, when fast neutrons were incident on the chamber, the collection current never reached saturation.

An attempt was made to ascertain whether nonsaturation of the neutron curve could be attributed to columnar recombination. The application of the Jaffe theory of columnar recombination[24] as outlined by Zanstra[25] was followed.

The difference between curve A minus curve B (Fig. 33) was found to satisfy the Jaffe theory and therefore is attributed to columnar ionization by heavy ions.

From curves A and B it is noted that the Po-Be source gives a dose rate, from the gamma rays produced by and associated with the source, equivalent to 25% of the dose rate caused by the fast

[24] G. Jaffe, *Ann. Physik* **42**, 303 (1913).
[25] H. Zanstra, *Physica* **2**, 817 (1935).

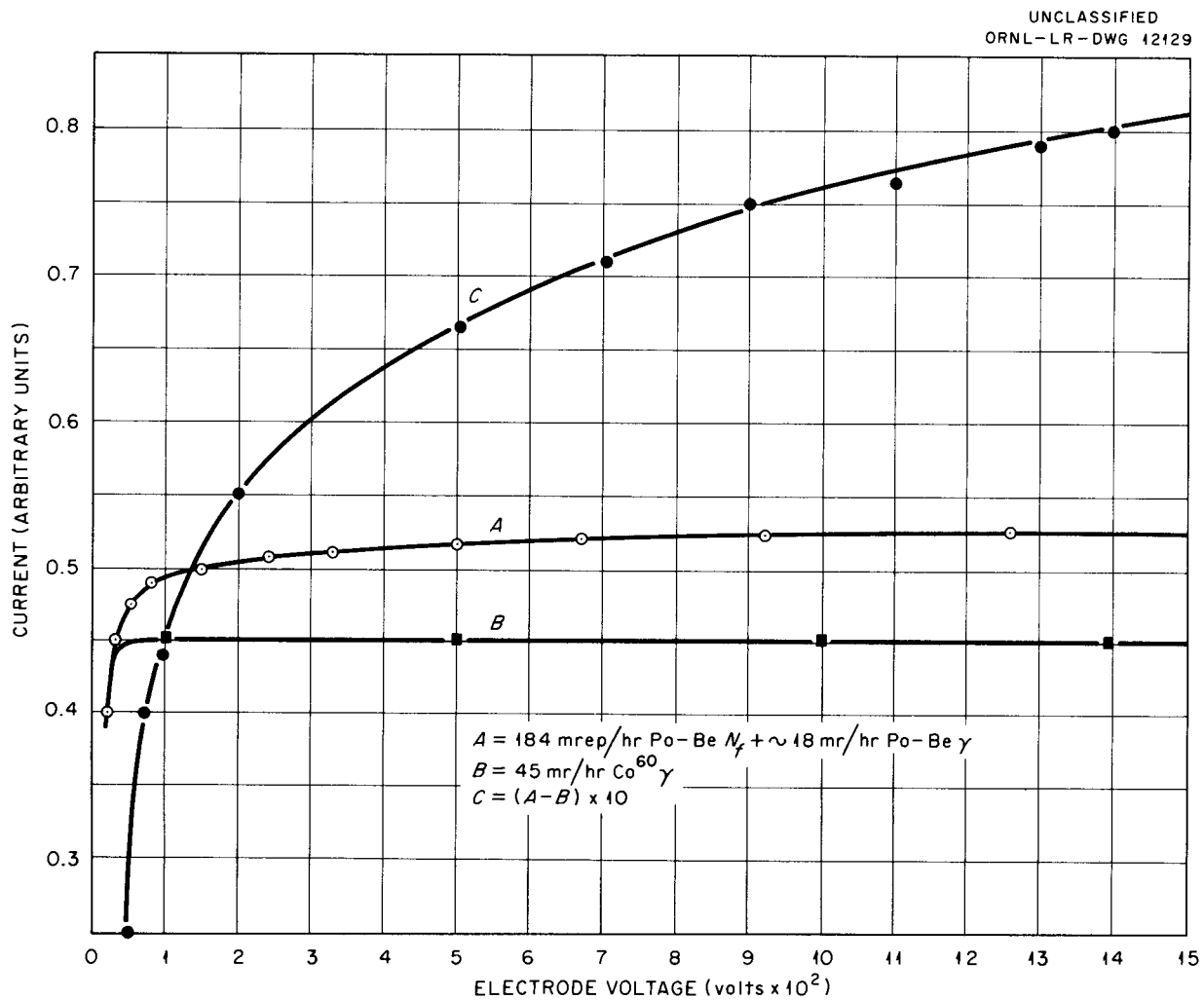

Fig. 33. Chamber Current as a Function of Voltage for Fast Neutrons and Gamma Rays.

neutrons. When a gamma dose of 10% of the neutron dose rate of the Po-Be source was assumed and subtracted from the curve, there was still a response equal to a gamma dose rate of approximately 15% of the neutron dose rate. Some of this was certainly the result of hydrogen capture of thermalized neutrons in the Lucite cover which makes the chamber water- and gas-tight. An aluminum cover $^3/_{16}$ in. thick was substituted for the Lucite, and the gamma response decreased from 15 to about 10%. It seems probable that this part of the neutron response is due to hydrogen capture and to inelastic scattering by the carbon and with surrounding materials.

Therefore, in a mixed field of fast neutrons and gamma radiation, the true gamma dose rate is less than the indicated dose rate by an amount which is a function of true dose rate, relative n_f/γ dose rate ratio, and electrode voltage. Table 22 lists some approximate values for the neutron contribution to the response as compared with the gamma response for dose rates not in excess of a few hundred mrep/hr and at an operating potential of 200 v.

TABLE 22. Po-Be NEUTRON CONTRIBUTION TO IONIZATION

900-cc Chamber, 200-v Electrode Potential

γ/n_f Dose	Gamma Dose Added by n_f Response (%)		Total Error in γ Dose (%)
	By Columnar Ions	By n_f Inelastic Scatter and n_t Capture	
1/10	30	140	170
1/1	3	14	17
10/1	0.3	1.4	1.7

The dependence of these corrections on energy has yet to be determined. When the chamber is used to measure gamma dose rates in such a medium as water, the inelastic scattering contribution would not be subtracted, assuming the composition of chamber housing and surrounding medium to be about the same.

If the isotropic scatter of fast neutrons in CO_2 is assumed, the energy absorbed by recoil oxygen and carbon atoms may be calculated. If curve C (Fig. 33) is extrapolated to infinite voltage in accordance with the Jaffe theory, the total ionization by heavy ions is found. Dividing the calculated value of absorbed energy by the total ionization resulting from heavy ions gives a W value of about 80 ev per ion pair.

A C-CO_2 chamber with parallel plates and guard ring is currently being used in a more comprehensive study of ion recombination.

A New Fast-Neutron Pulse Integrator

The present fast-neutron dosimetry using the binary pulse integrator, while quite satisfactory for laboratory type research, is not well adapted to applications requiring a small, compact instrument, as in applied health physics work and certain radiobiological experiments. One approach to the problem is to scale down the physical size of the present instrument.

The second approach, illustrated in Fig. 34, utilizes a National Union LBS-1 line-beam-switch tube for the pulse amplitude discriminator or pulse sorter. The LBS-1 is similar to a conventional cathode-ray tube in that it contains an electron gun assembly and one pair of deflection plates, but it has ten output anodes which replace the phosphor-coated screen. The number of output anodes swept by the electron beam and the number of resultant output pulses from the paralleled anodes are proportional to the amplitude of the input pulses to the deflection plate. There have been applications of this type of tube to pulse analyzers but not, to the knowledge of this group, to a pulse amplitude integration circuit.[26]

The output pulses from the LBS-1 tube are counted with conventional scaling circuits which are preceded by a fast prescaler utilizing a Haydu DC-1R decade counter tube. The fast prescaler is necessary since the output pulses from LBS-1 are spaced less than 1 μsec apart.

This integrator circuit, at present under development, shows promise of being more compact, simpler to adjust and operate, and more easily adapted for use as a pulse analyzer by switching each of the LBS-1 output anodes to an individual scaler.

[26] W. E. Glenn, *Nucleonics* 9 (6), 24–28 (1951).

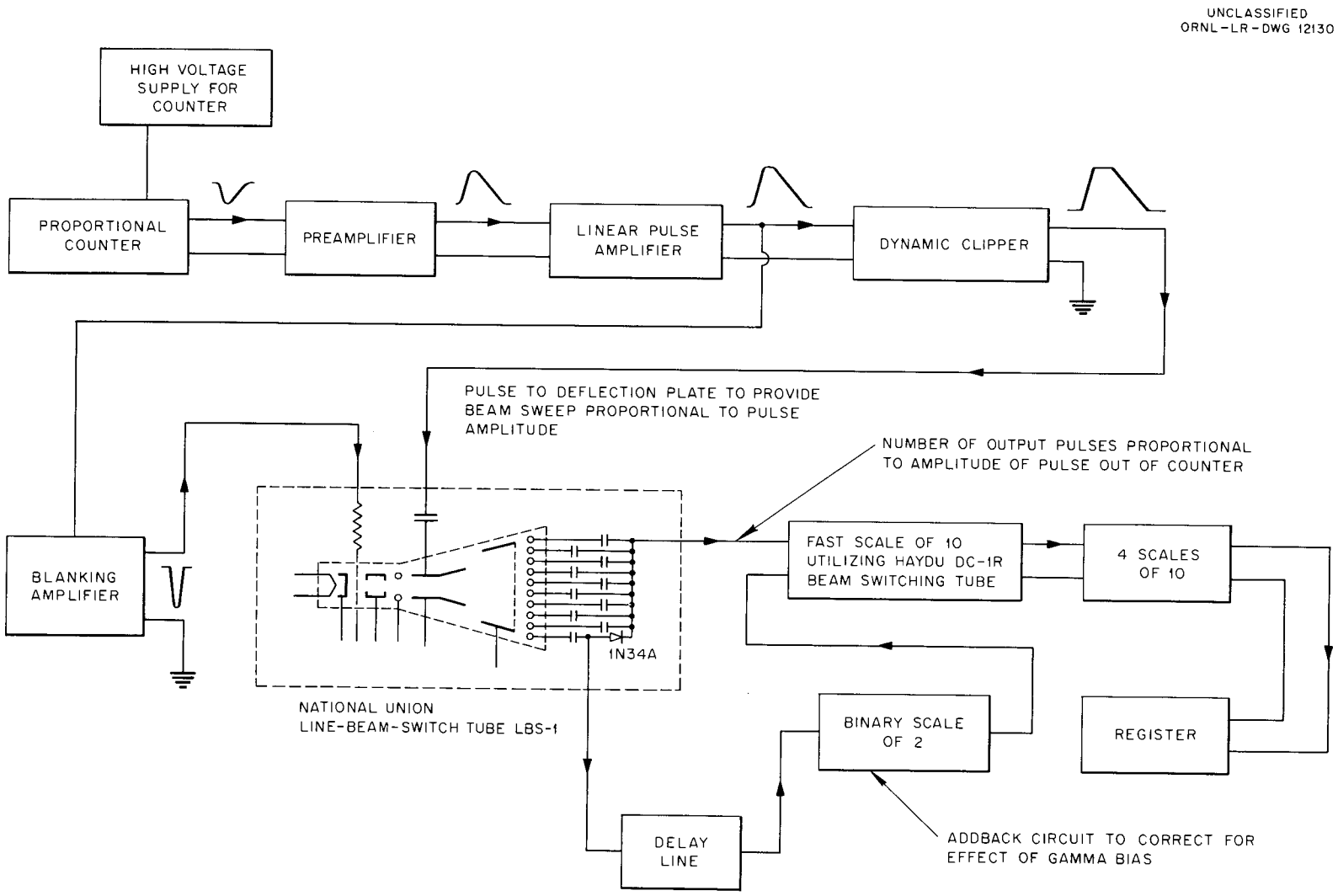

Fig. 34. Block Diagram of New Integrator.

EDUCATION, TRAINING, AND CONSULTATION

E. E. Anderson M. F. Fair

AEC FELLOWSHIP PROGRAM

The AEC Fellows in Radiological Physics for the 1955–1956 program were enrolled at Vanderbilt University in September, and the records for the fall quarter show that 60% of the Fellows have earned an average of B or better.

Of the nine Fellows of the 1954–1955 group who were granted extensions of their Fellowship, five remained at ORNL working on a research problem in the Health Physics Division; the remaining four returned to Vanderbilt.

INTERNATIONAL COURSE IN HEALTH PHYSICS

E. E. Anderson and M. F. Fair conducted a five-week course in Health Physics in Stockholm, Sweden (November 14 through December 16). This course, the first of its kind to be offered in Europe, was conducted at the Institute of Radiophysics of the Karolinska Hospital under the joint sponsorship of the European Division of the World Health Organization, the Swedish Government, and the U.S. Atomic Energy Commission.

Students in the course were from ten European countries – Belgium, Denmark, France, Germany, Iceland, Italy, the Netherlands, Norway, Sweden, and Switzerland. The course was designed for supervisors and instructors in radiation protection.

OTHER ACTIVITIES

Discussions on Health Physics were held with two groups of Maintenance personnel.

One member of the section participated in a Civil Defense Training Course held for the Civil Defense leaders of the State of Virginia at Richmond.

One member of the Nautilus crew, assigned to radiation-protection duties on the submarine, was here for three days of discussion with the Education and Training Section on special personnel monitoring problems.

One member of the section is conducting a course (2 hours per week for 4½ months) in Apprentice Mathematics for the Training Division.

The section organized a five-week laboratory course for six special students of the Reactor Technology School.

A series of seminars was held for the Veterinarians' Course and the Basic Isotopes Course of the Special Training Division of the Oak Ridge Institute of Nuclear Studies.

One laboratory experiment on Health Physics instrumentation was conducted for the Oak Ridge School of Reactor Technology.

PUBLICATIONS

H. H. Abee, *Particle Activity Determination by Autoradiography*, ORNL CF-55-12-121 (Dec. 29, 1955).

R. D. Birkhoff, A. W. Smith, H. H. Hubbell, Jr., and J. S. Cheka, "High Resolution Automatic Beta Spectrometer," *Rev. Sci. Instr.* **26**, 959 (1955).

A. W. Blackstock, R. H. Ritchie, and R. D. Birkhoff, "Mean Free Path for Discrete Electron Energy Losses in Metallic Foils," *Phys. Rev.* **100**, 1078 (1955).

T. E. Bortner and H. K. Richards, *Ionization Chamber Measurement of Backscatter and Absorption of Beta Particles*, ORNL CF-55-8-104 (Sept. 1, 1955).

J. W. Cure, III, *Neutron Scattering*, ORNL-2013 (Dec. 9, 1955).

G. S. Hurst, W. A. Mills, F. P. Conte, and A. C. Upton, "Principles and Techniques of Mixed Radiation Dosimetry – Application to Acute Lethality Studies of Mice with the Cyclotron," *Radiation Research* **4**, 49 (1956).

B. Kahn, *Procedures for the Analysis of Some Radionuclides Adsorbed on Soil*, ORNL-1951 (Sept. 28, 1955).

H. L. Krieger, B. Kahn, and C. P. Straub, *The Removal of Fission Products from an Acid Aluminum Nitrate Solution by Co-precipitation Methods*, ORNL-1966 (Sept. 28, 1955).

W. S. Lyon and B. Kahn, "Decay of Sc^{47}," *Phys. Rev.* **99**, 728 (1955).

K. Z. Morgan, "The Application of External and Internal Radiation Exposure Limits," *American Industrial Hygiene Association Quarterly* **16**, 307 (1955).

R. J. Morton, "President's Column," Tenn. Valley Section, Am. Soc. Civil Engrs., *Tennessee Valley Engineer* **16**, Nos. 1–12 (1955).

R. J. Morton, "Public Health Implications of Peacetime Nuclear Reactor Development," Proc. Amherst Health Conf., Amherst, Mass., June 15–17, 1955, Part II, *Commonhealth* **3**, 11–14 (1955). (Summary of paper presented June 17, 1955.)

R. J. Morton, "The Role of the Sanitary Engineer in the Nuclear Energy Program," *Proc. Am. Soc. Civil Engrs.* **81**, Paper No. 749 (1955).

R. J. Morton, "Waste Disposal Problems," *Proceedings of the Second AEC Sanitary Engineering Conference, Baltimore, Maryland, April 15–16, 1954*, WASH-275, p 320–329.

J. Neufeld and R. H. Ritchie, "Density Effect in Ionization Energy Loss of Charged Particles," *Phys. Rev.* **99**, 1125 (1955).

J. Neufeld and W. S. Snyder, "Number of Vacancies Created by Heavy Corpuscular Radiation," *Phys. Rev.* **99**, 1326 (1955).

H. K. Richards, *Detection and Telemetering of Ionizing Radiation by Frequency Variation*, ORNL CF-55-9-122 (Sept. 30, 1955).

B. G. Saunders, *Cloud Chamber for Counting Condensation Nuclei in Aerosols*, ORNL-1957 (Oct. 6, 1955).

C. P. Straub, "Limitations of Water Treatment Methods for Removing Radioactive Contaminants," *Public Health Report* **70**(9), 897–904 (1955).

C. P. Straub, "Progress Review of Accomplishments at ORNL Since September 1952," *Proceedings of the Second AEC Sanitary Engineering Conference, Baltimore, Maryland, April 15–16, 1954*, WASH-275, p 175–187.

C. P. Straub, The Column "Nuclear Notes" in *Civil Engineering*:

XII. "Statistics of Nuclear Measurements," **25**(7), 90 (1955) (Paper prepared by B. Kahn).
XIII. "Preparation of Samples for Assay," **25**(8), 82 (1955) (Paper prepared by B. Kahn).
XIV. "Identification of Radioisotopes by Relative Counting Techniques," **25**(9), 86 (1955) (Paper prepared by M. I. Goldman).
XV. "Introduction to Shielding," **25**(11), 86 (1955) (Paper prepared by R. H. Ritchie).
XVI. "Human Tolerance to Radiation," **25**(12), 86 (1955) (Paper prepared by R. H. Ritchie).
XVII. "Attenuation of Photons in Matter," **26**(1), 90 (1955) (Paper prepared by R. H. Ritchie).

C. P. Straub and E. G. Struxness, *The Impact of Radioactive Waste Disposal on Chemical Processing*, ORNL CF-55-8-97 (Aug. 15, 1955).

PAPERS

H. H. Abee, *Disposal of Radioactive Contaminated Waste Material and Equipment,* Sanitary Engineering Conference, December 7, 1955, Cincinnati, Ohio.

S. I. Auerbach and M. Engelmann, *Effects of Gamma Radiation on the Biology and Ecology of Arthropods. A. Preliminary Studies on Certain Tree-Hole Arthropod Populations,* Third Annual Meeting of the Entomological Society of America, November 28, 1955, Cincinnati, Ohio.

T. E. Bortner, *Ionization of Pure Gases and Mixtures of Gases by 5 Mev Alpha Particles,* Radiological Society of North America, December 11–16, 1955, Chicago, Illinois.

F. J. Davis, *Aerial Radiation Surveys for Uranium Prospecting,* Society of Exploration Geophysicists, October 6, 1955, Denver, Colorado.

H. F. Howden, *Effects of Gamma Radiation on the Biology of* Onthophagus texanus *Schaeffer,* Third Annual Meeting of the Entomological Society of America, November 28, 1955, Cincinnati, Ohio.

K. Z. Morgan, W. S. Snyder, and M. R. Ford, *Maximum Permissible Concentration of Radioisotopes in Air and Water for Short Period Exposure,* International Conference on the Peaceful Uses of Atomic Energy, August 8–20, 1955, Geneva, Switzerland.

K. Z. Morgan, *Maximum Permissible Concentration of Radionuclides in Air and Water,* Nuclear Engineering and Science Congress, December 16, 1955, Cleveland, Ohio.

K. Z. Morgan, *Organization of Professional Health Physicists,* Health Physics Conference, Ohio State University, June 13–15, 1955, Columbus, Ohio.

R. J. Morton and E. G. Struxness, *Ground Disposal of Radioactive Wastes,* American Public Health Association, November 16, 1955, Kansas City, Missouri.

LECTURES

S. I. Auerbach, *Radiation of Arthropods as Part of the ORNL Ecology Program,* Zoology Department Seminar, University of Tennessee, November 8, 1955, Knoxville, Tennessee.

R. D. Birkhoff, *Energy Measurements of 0.1 Mev Particles by Stopping Potential Techniques,* Traveling Lecture Program, Vanderbilt University, November 10, 1955, Nashville, Tennessee.

M. I. Goldman, *Environmental Radiocontamination and Waste Disposal,* Armed Forces Veterinary Officers Course, Oak Ridge Institute of Nuclear Studies, September 19, October 3, 17, 31 and November 14 and 28, 1955.

K. Z. Morgan, *Control of Radiation by the Health Physicist,* Bethesda Medical School, October 4, 1955, Bethesda, Maryland.

K. Z. Morgan, *Maximum Permissible Levels of Exposure and Ionization,* University of North Carolina, Chapel Hill, North Carolina, December 8, 1955.

R. J. Morton, *Experience at ORNL with Pit Disposal of Liquid Radioactive Wastes,* Conference on Disposal of Radioactive Waste Products, September 10, 1955, Princeton University, Graduate College, Princeton, New Jersey.

R. J. Morton and C. P. Straub, *Removal of Radionuclides from Water by Water Treatment Processes,* Nuclear Engineering and Science Congress, December 16, 1955, Cleveland, Ohio.

C. P. Straub, *Emergency Maximum Permissible Concentration Values for Water,* Nuclear Engineering and Science Congress, December 16, 1955, Cleveland, Ohio.

C. P. Straub, *Problems of Radioactive Waste Disposal*, Joint Meeting Florida Section American Water Works Association and Federation of Sewage and Industrial Waste Association, November 9, 1955, Orlando, Florida.

C. P. Straub (Discussion Leader), *Environmental Problems of the Atomic Energy Industry – High Level Wastes*, Seminar on the Sanitary Engineering Aspects of the Atomic Energy Industry, December 6–9, 1955, Cincinnati, Ohio.

E. G. Struxness, *The ORNL Concept of Pit Disposal for Reactor Process Wastes*, Conference on Disposal of Radioactive Waste Products, Princeton University, Graduate College, September 11, 1955, Princeton, New Jersey.

H. P. Yockey, *An Application of Information Theory to the Physics of Tissue Damage*, Seminar on Information Theory conducted by Henry Quastler at Argonne National Laboratory, January 17, 1956, Lemont, Illinois.